Reverse genetics reveals the critical role of sporozoite specific genes *SSPELD* and *SCOT-3* in *Plasmodium berghei* Liver stage development

A thesis submitted to University of Hyderabad
for the award of Degree of
DOCTOR OF PHILOSOPHY

By

Faisal Mohammed Abduh Al-Nihmi

09LAPH08

Department of Animal Biology
School of Life Sciences
University of Hyderabad
Hyderabad- 500 046
August 2015

University of Hyderabad

(A central University established in 1974 by an Act of Parliament)

Department of Animal Biology
School of Life Sciences
University of Hyderabad
Hyderabad-500 046

DECLARATION

I, **Faisal Mohammed Abduh Al-Nihmi** hereby declare that the thesis entitled **"Reverse genetics reveals the critical role of sporozoite specific genes *SSPELD* and *SCOT-3* in *Plasmodium berghei* Liver stage development"** submitted by me under the guidance and supervision of Dr. Kota Arun Kumar is an original and independent research work. I also declare that it has not been submitted previously in part or in full to this University or any other University or Institution for the award of any degree or diploma.

Name : **Faisal Mohammed Abduh Al-Nihmi**

Reg. No : **09LAPH08**

Signature :

Date :

University of Hyderabad

(A central University established in 1974 by an Act of Parliament)

Department of Animal Biology
School of Life Sciences
University of Hyderabad
Hyderabad-500 046

CERTIFICATE

This is to certify that the thesis entitled **"Reverse genetics reveals the critical role of sporozoite specific genes *SSPELD* and *SCOT-3* in *Plasmodium berghei* Liver stage development"** is a record of bonafide work done by Mr. Faisal Mohammed Abduh Al-Nihmi, for the Ph.D. programme in the Department of Animal Biology, University of Hyderabad, under my guidance and supervision. The thesis has not been submitted previously in part or full to this or any other University or Institution for the award of any degree or diploma.

Dr. Kota Arun Kumar **Head of the Department**

(Supervisor)

Dean of the School

Acknowledgements

I express my gratitude to my supervisor Dr. Kota Arun Kumar for his constant guidance, encouragement and support throughout my doctoral research.

I thank the current Head of Animal Biology Department, Prof. P. Jagan Mohan Rao and former heads Prof. B. Senthil Kumaran, Prof. Manjula Sritharan and Prof. S. Dayananda for extending departmental facilities.

I thank Prof. P. Reddanna, Dean, School of Life Sciences, and former Deans, Prof. R.P. Sharma, Prof. Aparna Dutta Gupta, Prof. M. Ramanadham and Prof. Raghavendra for allowing me to use the School facilities.

I thank my Doctoral Committee members Dr. Naresh Babu Sepuri and Dr. Arunashree for their valuable suggestions.

I am thankful to the collaborator of my Ph D supervisor- Dr. Satish Mishra, Senior Scientist, Division of Parasitology, CSIR-CDRI for sharing the parasite reagents, plasmid constructs and other crucial reagents like antibodies and fine chemicals.

I thank Mastan for training me with mosquito breeding techniques at the insectary also for initially providing me with mosquitoes for setting up my own colony.

I extend my thanks to my labmates Jyothi, Maruthi, Surendra, Ravi, Mastan, Rameswar, Sandeep and Dipti for all their help during my stay in the laboratory.

I would like to thank all the lab members of Prof. Aparna Dutta Gupta, Dr. Naresh Babu Sepuri and Dr. Suresh Yenugu for allowing me to use their laboratory facilities.

I thank Narasimha and Yadagiri for their assistance in the lab.

The help and cooperation of the non-teaching staff -Mr. Ankeenedu, and Ms. Jyothi is highly acknowledged for their timely assistance at the Department of Animal Biology.

I acknowledge the financial support of DBT, CSIR, ICMR, UGC, PURSE, DBT-CREEB and DST-FIST to the Department and School of Life Sciences.

Finally I thank my parents, my wife and children for all the moral support and Almighty for giving me the strength to face all challenging situations leading to successful completion of my PhD.

Dedicated to
my Parents,
Wife
&
Children

Table of Contents

Abbreviations

AMA	Apical membrane antigen
BSA	Bovine serum albumin
cDNA	Complementary DNA
CDPK	Calcium dependent protein kinase
CS	Circumsporozoite
DAPI	4', 6' diamidino-2 phenyl indole
DHFR	Dihydrofolate reductase
DMEM	Dulbecco's modified Eagle's medium
DNA	Deoxy ribonucleic acid
DOZI	Development of zygote inhibited
EBA	Erythrocyte binding antigen
EBL	Erythrocyte binding like
ECP	Egress cysteine protease
EEF	Exo erythrocytic form
EMP	Erythrocyte Membrane Protein
ePK	Eukaryotic protein kinase
EST	Expressed sequence tag
FBS	Fetal bovine serum
FRT	Flippase recognition target site
FP	Forward primer
GAP	Genetically attenuated parasite
GAP	Glideosome associated protein
GFP	Green fluorescent protein

GSK	Glycogen synthase kinase
HEPES	4-(2-hydroxyethyl)-1-piperazineethanesulfonic acid
HSPG	Heparin sulfate proteoglycan
IMC	Inner membrane complex
iRBC	Infected red blood cell
ITN	Insecticide treated net
KO	Knockout
LB broth	Luria-Bertani broth
MAP/MAPK	Mitogen activated protein kinase
mRNA	Messenger RNA
MTIP	Myosin tail interacting protein
NEK	NIMA related kinase
Ng	nanogram
NIMA	Never in mitosis *Aspergillus*
OD	Optical density
ORF	Open reading frame
P. falciparum	*Plasmodium falciparum*
P. malariae	*Plasmodium malariae*
P.knowlesii	*Plasmodium knowlesii*
P.ovale	*Plasmodium ovale*
P.vivax	*Plasmodium vivax*
PBS	Phosphate buffer saline
PEXEL	*Plasmodium* export element
PK	Protein kinase

PKG	cGMP dependent protein kinase/ protein kinaseG
PUF	Pumilio and fem3 transcription binding factor
PV	Parasitophorous vacuole
PVM	Parasitophorous vacuolar membrane
RBC	Red blood cell
RH	Relative humidity
RNA	Ribonucleic acid
RP	Reverse primer
RPMI	Roswel Park Memorial Institute medium
SAGE	Serial analysis of gene expression
SAP	Sporozoite asparagine rich protein
SCOT	Sporozoite Conserved Orthologous Transcripts
SERA	Serine repeat antigen
SIAP	Sporozoite invasion associated protein
SPECT	Sporozoite protein essential for cell traversal
SRPK	Serine arginine rich protein kinase
SSH	Suppression subtractive hybridization
SSP	Sporozoite surface protein
SSPELD	Sporozoite Surface Protein Essential for Liver stage Development
SUB1	Subtilisin like protease
TBS	Tris buffer saline
TRAP	Thrombospondin related anonymous protein
TRSP	Thrombospondin related sporozoite protein
TSR	Thrombospondin related

UIS	Up regulated in infected salivary glands
UOS	Upregulated in oocyst sporozoites
VTS	Vacuolar translocation signal
WT	Wild type
XA	Xanthurinic acid
mg	Microgram
μL	Microliter
μM	Micrometer

CHAPTER 1

Review of Literature

1.1 Introduction

Malaria is an infectious mosquito borne disease known since 2700 BC. The causative agent of malaria is *Plasmodium*, a protozoan protist that has a digenetic life cycle altering between a vertebrate host and female Anopheline mosquito. In humans, *Plasmodium vivax (P. vivax)*, *Plasmodium ovale (P. ovale)*, *Plasmodium malariae (P. malariae)*, *Plasmodium falciparum (P. falciparum)* and *Plasmodium knowlesii (P. knowlesii)* are reported to be the causative agents of malaria. Among these human species, *P. falciparum* is responsible for the majority of malaria deaths globally followed by *P. vivax*, *P. ovale* and *P. malariae*. *P. falciparum* causes a severe form of malaria in the brain, a condition referred to as cerebral malaria which leads to death in majority of the reported malaria cases. Among 200 million estimated cases reported annually, over half a million people die from malaria each year [1]. Although the vast majority of malaria cases occur in sub-Saharan Africa, the disease is a public health concern in more than 109 countries world wide including India and about 45 countries in Africa (Fig 1) [2]. The disease affects mainly children and pregnant women in majority of the cases. Malaria has a major negative affect on economic development of the country and causes poverty [3]. The visible symptoms of malaria include fever, fatigue, chills, vomiting and headache ultimately leading to coma and death if it is not treated properly.

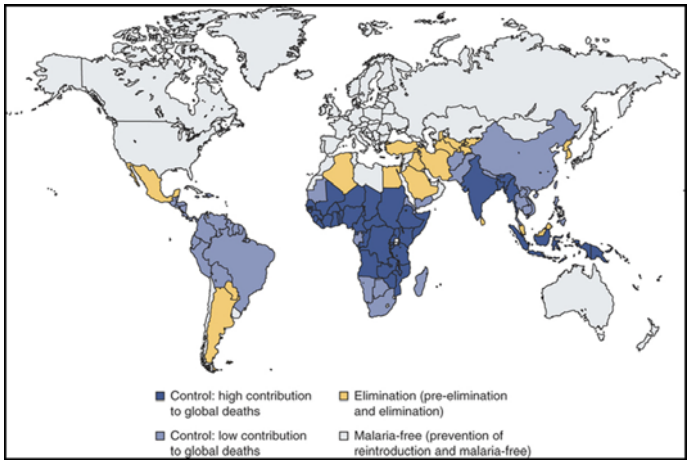

Fig 1. Global distribution of malaria. Most of the countries in Sub-Saharan Africa and India (dark blue) are at the risk of malaria. Malaria is controlled in South America and China (lighter blue) where the global contributions to malaria deaths are low. Few countries (yellow) are free of malaria as of now, but there is a risk of reintroduction of malaria if proper control measures are not implemented. This figure is obtained from Alonso *et al.* [4].

1.2 Life cycle of *Plasmodium*

Transmission of *Plasmodium* requires two hosts, an intermediate invertebrate host (vector) and a definitive vertebrate host (mammals or birds). The life cycle of the *Plasmodium*

parasite is very complex (Fig 2). Transmission of malaria to the vertebrate host is initiated by the injection of sporozoites during the bite of an infected female *Anopheles* mosquito while probing for a blood meal. The sporozoites selectively infect hepatocytes and develop into exo-erythrocytic forms (EEFs). Fully grown exo-erythrocytic schizont contains nearly 10,000 to 30,000 merozoites which are released into blood circulation and infect erythrocytes. With in erythrocytes, the parasites transforms through ring, trophozoite and schizont stages. The erythrocyte containing schizont rupture releasing merozoites into blood stream which in turn invade new erythrocytes. Concomitantly, a small portion of merozoites develop into male and female gametocytes that constitute the sexual stages of the life cycle. Upon being taken up by the mosquito, male and female gametocytes differentiate into male and female gametes respectively. Fertilization of male and female gametes results in the formation of non-motile zygote which transforms into motile ookinete within 18-24 h of fertilization. The actively moving ookinete traverses through mosquito midgut wall and forms oocyst on the basal lamina of the midgut. Growth and division of each oocyst produces thousands of sporozoites. After 8-15 days, sporozoites egress by rupture of oocyst into the haemocoel, from where they migrate and invade salivary glands of the mosquito. The cycle of infection re-initiates when the infected mosquito takes a blood meal injecting sporozoites into the blood stream of vertebrates.

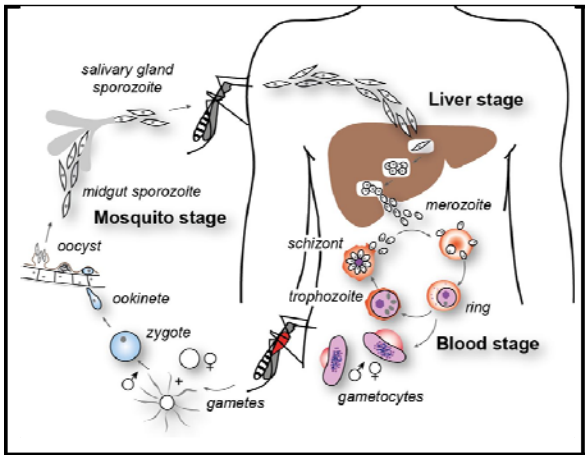

Fig 2. Life cycle of *Plasmodium*. Infection to human (vertebrate) host occurs when female *Anopheles* mosquito injects sporozoites into the dermis. The sporozoites glide through dermal cells and after breaching several cellular barriers, reach blood vessels. Once inside blood circulation, the sporozoites selectively get arrested in hepatocytes of liver. Here the sporozoites transform into liver stages or Exo-Erythrocytic Forms. The EEFs undergo one round of asexual replication and release first generation merozoites. These merozoites initiate the asexual blood stage infection and transforms in to a series of stages called rings, trophozoites, schizonts and gametocytes. Gametocytes are sexually dimorphic forms (male and female) of the parasite that enter the lumen of mosquito midgut after an infective blood meal. Inside the midgut, sexual reproduction occurs resulting in the formation of male and female gametes from respective gametocytes. The gametes fuse to form zygote that transforms into a motile ookinete. The ookinete breaches the midgut epithelium and gets attached on the haemocoel side of the midgut and transforms into oocyst. Sporulation occurs in the oocyst and upon its rupture, sporozoites are released into the haemocoel and migrate to the salivary glands. The sporozoites that lodge in the salivary glands are injected into a vertebrate host, when the infected mosquito attempts to take a blood meal. This figure is obtained from Cowman A.F *et al.* [5].

There is a tight stage specific expression of proteins, that perform unique functions central to that stage. The biology of each of the life cycle stages are described below.

1.2.1 Exo-erythrocytic stages

After release of salivary gland sporozoites into the skin of the vertebrate host during a natural mosquito bite, sporozoites actively migrate through skin cells by gliding motility with the help of actin-myosin motor complex present beneath the sporozoite plasma membrane [6-8]. Sporozoites traverse through different host cell types by disrupting plasma membrane, gliding through the cytosol and exiting the host cells [9]. Sporozoite protein essential for cell traversal (SPECT)-1, SPECT-2 and phospholipase are three important proteins known till to date that are shown to be involved in mediating the cell traversal of sporozoites [10-12]. Mutants of spect-1 and spect-2 are immobilized in the skin as a consequence of impaired cell traversal ability [13]. Sporozoites then enter the blood circulation and are selectively arrested in the liver by interaction of circumsporozite protein (CSP)-one of the major surface proteins of sporozoite with heparin sulfate proteoglycans (HSPGs) present on the surface of hepatocytes. The degree of sulfation is highest in hepatocytes as compared to other cell types and this acts as signal for the sporozoite to switch from cell traversal activity to productive invasion [14, 15] characterized by the formation of a membrane bound compartment, the parasitophorous vacuole (PV) [9] inside which the sporozoites transform into EEFs. Mature *Plasmodium* EEFs, produce first generation merozoites as a result of asexual replication, which are contained within the parasitophorous vacuolar membrane (PVM) [16, 17 and 18]. These are called pre-erythrocytic or liver stages since the development takes place in the liver, and occur prior to blood stages infection. The release of hepatic merozoites into the blood stream takes place through specialized host cell derived membranous structures called merosomes that facilitate a successful evasion from the immune surveillance by highly phagocytic kupffer cells located in the liver lining of sinusoids. Budding of merosomes into hepatic bloodstream facilitates the release of merozoites by membrane disruption thus allowing merozoites to infect red blood cells (RBC) and initiate erythrocytic cycle [19]. Proteases play a crucial role in the egress of merozoites [20]. A conserved *Plasmodium* serine protease, subtilisin like protease (SUB1) was shown to be essential for the egress of merozoites both at blood stages and liver stages [21, 22]. SUB1 secretion is triggered by fluctuations in intracellular calcium concentration facilitated by a cGMP dependent protein kinase (PKG) [21, 23]. While the role of PKG was revealed initially in the release of blood stage merozoites [23], later studies showed that PKG is also essential for merozoite release from hepatic schizonts as *PKG*

conditional knockout sporozoites failed to initiate blood stage infection [24]. Serine repeat antigen (SERA) family proteins act as substrates for SUB1. Cleavage of SERA3 protease by SUB1 initiates a cascade of protease events that are required for the egress process [25, 26]. Transcriptome and proteome of liver stages identified 2000 genes that are active throughout the parasite development in the hepatocytes. Genes selectively upregulated in infected salivary glands (referred to as UIS genes) like *UIS-3, UIS-4* and *P36p* are important for completion of liver stage development. Depletion of *UIS3, UIS4* and *P36p* resulted in the arrest of the EEF development within the hepatocytes, resulting in an inability to initiate a blood stage infection. Mice immunized with *UIS-3, UIS-4* and *P36p* KO parasites were able to generate long lasting pre-erythrocytic immunity that conferred sterile protection against challenge with wild type sporozoites [27-29]. The idea of using these genetically attenuated parasites (GAP) as whole organism vaccines is already gaining significance, as a means to prevent malaria infections [30].

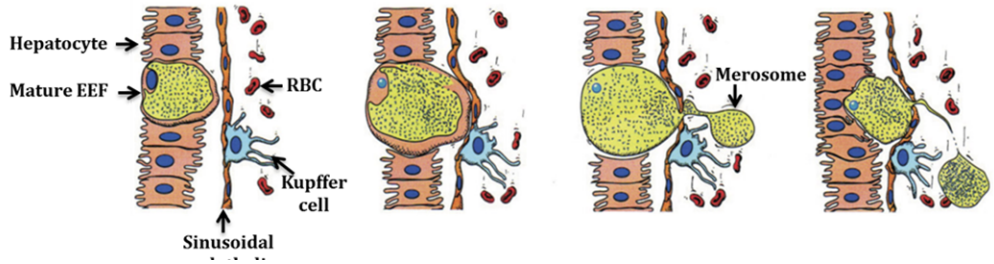

Fig 3. Merozoite release through formation of merosomes. To evade immune clearance, *Plasmodium* liver stages form membrane bound structures called merosomes. Budding of merosomes from fully mature EEFs, results in their release into blood stream that prevents their encounter by kupffer cells residing in liver sinusoids. Rupture of merosome membrane facilitates merozoite release. This figure is obtained from Sturm *et al*. and modified [19].

1.2.2 Erythrocytic stages

Erythrocyte invasion by first generation hepatic merozoites requires multiple receptor-ligand interactions [31]. Invasion of merozoite involves a series of events, attachment of merozoite to RBC followed by reorientation of merozoite apical end to RBC surface and penetration. The invasion process requires two types of proteins; adhesins and invasins. Adhesins are located in the apical organelles of the parasite that binds to receptors on the surface of the erythrocyte [32]. Erythrocyte binding like (EBL) proteins and reticulocyte binding like proteins are two important types of adhesins identified to be localized to micronemes and neck of the rhoptries [33-36]. Invasins play an important role in invasion process that does not involve the direct binding of receptors on the host cell always. Apical membrane antigen -1 (AMA-1) is one of the invasins that is considered to be potential vaccine

candidate that has progressed to clinical trials [37]. The interaction of adhesins with actin myosin motor is crucial for the invasion process. Actin–myosin motor resides in the inner membrane complex (IMC) of the parasite and mediates the motility [38, 39]. Thrombospondin related anonymous protein in merozoite stages is referred to as mTRAP binds to actin filaments through aldolase which further interacts with myosin A (Myo A) tail domain [39-41]. Myosin tail domain interacting protein (MTIP) binds to two IMC proteins referred to as glideosome associated proteins (GAP) - GAP45 and GAP50 in addition to with MyoA. All the components (TRAP-aldolase-actin-MyoA-MTIP-GA45-GAP50) interact together and are collectively referred as motor complex [40]. Drugs that target actin-myosin motor block the process of parasite invasion [38]. Inside the erythrocyte, the parasite develops inside the parasitophorous vacuole. Following invasion, parasites transform into ring stages, where the cytoplasm appears like a crescent like structure surrounding a vacuole with a distinct nuclei at one end of vacuole. The parasite next progresses to trophozoite stage, during which time the parasite metabolic and biosynthetic activity is maximal. During this period, parasite grows in size and occupies one third the volume of the host cell [42]. At this stage, late trophozoite enters into schizont stage in which it multiplies asexually and forms daughter merozoites and release into the blood by rupturing of the host cell membrane. The new generation merozoites are capable of infecting other erythrocytes and continuing the life cycle. A few merozoites differentiate into male and female gametocytes which constitute sexual forms of the life cycle. *Plasmodium* in the erythrocyte uses hemoglobin as energy source and converts free heme which is a non-protein part of the hemoglobin into hemozoin. Hemozoin is the nontoxic pigment and the conversion of free heme to hemozoin is important for the survival of parasites because free heme is toxic to cells [43]. The current antimalarial drugs are designed against the parasites major metabolic pathways. Few anti-malarial drugs like chloroquine and mefloquine are targeted to inhibit hemozoin crystallization. Vaccine approaches are difficult to target erythrocytic stages because of the phenomenon of antigenic variation, a process that involves constant change in the expression of a family of *var* genes that are expressed on the surface of the infected erythrocyte membrane [44-47]. The most extensively studied *var* gene is *PfEMP1* which encodes for *P. falciparum* Erythrocyte Membrane Protein-1. *P. falciparum* infected erythrocytes binds to microvascular endothelial cells of human brain and this adhesion is facilitated by *Pf*EMP-1 domain [48]. In fact, severe malaria and wide spread endothelial activation is associated with the *Pf*EMP-1 expression [49]. Both pregnant women and children living in malaria endemic areas have shown to generate B cell [50] and CD4+ T cell responses [51] respectively against *Pf*EMP-1 implicating it as a natural immune

target in human subjects. The transport of *Pf*EMP-1 to erythrocyte membrane is mediated by an export motif which is conserved among *Plasmodium* species. The export motif includes five amino acid sequence RxLxE/Q/D and termed as *Plasmodium* export element (PEXEL) or vacuolar translocation signal (VTS) [52-54]. More than 300 *Plasmodium* proteins contain PEXEL/VTS motif and participate in protein trafficking from parasite to host [55], which likely play an important role in virulence and survival of the asexual blood stages.

1.2.3 Sexual stages

Schizonts are committed to produce merozoites that either facilitate the propagation of asexual cycle or commit to gametogenesis. The schizonts that are committed to gametocyte formation are pre determined with regard to their gender and differentiate either into male or female gametocytes [56, 57]. Gametocytes are taken up by mosquito while obtaining a blood meal. Gametogenesis occurs in the midgut of the mosquito and is influenced by factors like rise in pH, decrease in temperature, calcium concentration, and presence of xanthurinic acid (XA), a mosquito derived metabolic intermediate [58-60]. Several morphological and functional changes occur during gametogenesis. Male gametocyte undergoes exflagellation and form 8 flagellated male or micro gametes upon activation and are released from the residual body of the erythrocyte. Female gametocyte undergoes nuclear changes and differentiates into female or macro gamete. During fertilization, fusion occurs between micro and macro gamete plasma membrane with the involvement of HAP-2 specific gene product resulting in formation of zygote [61, 62]. In the *Plasmodium* life cycle, zygote is the only stage that is diploid in nature and contains two haploid genome complements. The zygote transforms into motile ookinete within 16-25 h post gamete fusion in the lumen of the mosquito midgut. Ookinete moves from the mosquito midgut by process of gliding. Ookinete resembles a banana shape structure and contains all apical organelles like rhoptries, micronemes and dense granules. The major bottle neck in the *Plasmodium* life cycle is the transition from gamete to zygote and to ookinete and involves several signaling events involving mainly kinases. Serine arginine rich protein kinase (SRPK) [63], a calcium dependent protein kinase (CDPK4) [60] and a mitogen activated kinase (MAP2) [64] that aid in the exflagellation and maturation of flagellated microgametes. NIMA related (never in mitosis *Aspergillus* 1) proteins, NEK-2 and NEK-4 have an essential role in zygote development [65, 66]. Calcium/calmodulin dependent protein kinases are required for the transformation of spherical zygote to elongated ookinete [67]. Ookinete traverses through mosquito midgut epithelium and the parasite secreted chintinase facilitates the degradation of pleotropic matrix of midgut [68, 69]. Within the

mosquito gut lumen, two GPI anchored EGF domain containing proteins p25 and p28 protects the ookinete from proteolytic activity of midgut [70]. Majority of the genes central to zygote and ookinete development are transcribed in gametocytes and stored as P bodies (processing bodies) or stress granules which are not subjected to translation. The process is referred as translational repression which is regulated by a RNA helicase that belongs to DDX family referred to as DOZI (development of zygote inhibited) and is common feature in the development of sexual stages of *Plasmodium*. DOZI binds to pre made transcripts and prevents translation [71, 72]. Translation resumes when gametocytes are ingested by the mosquito. After breaching mosquito midgut epithelium, ookinete transforms into a structure called oocyst under the basal lamina. Oocyst development over 10-14 days depending on *Plasmodium* species and it is the longest developmental stage throughout the *Plasmodium* life cycle [73]. During this process, oocyst grows in size, undergoes several nuclear divisions and produce haploid nuclei [74]. Mature oocysts undergo sporogony and sporozoites are liberated into the haemocoel upon rupture.

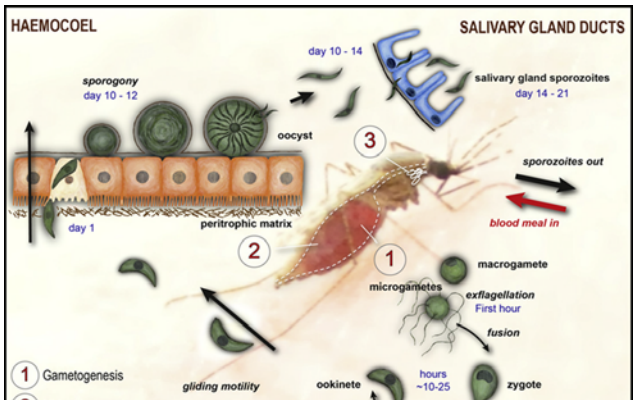

Fig 4. Sexual cycle of *Plasmodium*. Sexual development of *Plasmodium* has a tight temporal regulation. 1) Gametogenesis involves exflagellation of male gametocyte and formation 8 male gametes and female gamete formation. Exflagellation is an important event in sexual development of *Plasmodium* and occurs within 15 min of ingestion of gametocytes. 2) Fertilization, zyote formation and ookinte differentiation take place during 15-25 h post infection. 3) Ookinete is motile and it penetrates midgut epithelium, an event mediated by several ookinete specific proteins. Oocyst formation takes place at basal lamina of midgut. 3) Sporogony takes place within the oocyst and sporozoites invade salivary glands and become ready for next round of infection. This figure is obtained from Angrisano *et al.* [75].

1.2.4 Sporozoites

The development and maturation of sporozoites in oocysts is dependent on circumsporozoite protein (CSP). A mutant line of CSP gene resulted in oocysts without mature sporozoites [76]. The inner surface of oocyst capsule is covered with CS protein, and it is also secreted from sporozoites [77]. It is a major surface protein of sporozoite that contains

signal peptide, a central repeat region that serves as a signature motif for different *Plasmodium* species, two conserved domains referred to as region I and region II plus that flank the repeat region and a TSR (thrombospondin related) domain. Mutation in region II plus inhibits the egress of sporozoites from oocysts [78]. After release, oocyst derived sporozoites reach salivary glands with the movement of haemolymph and invades salivary glands. Sporozoites are unique stages of *Plasmodium* life cycle as is they invades two different types of cells during the life cycle. Midgut sporozoites released from the oocysts invade salivary glands and infectious salivary gland sporozoites invade hepatocytes in mammals. In addition to CSP which is the predominant protein on sporozoite surface, another surface protein referred to as TRAP (thrombospondin related anonymous protein), play an important role in sporozoite gliding motility. TRAP contains two modules: A domain of Willebrand factor and a thrombospondin type I repeat (TSR). These two domains ensure the interaction of the sporozoites with different cell types i.e., the salivary gland cells of mosquitoes and hepatocytes of liver in mammals [79]. In salivary glands, sporozoites mature and wait for several days for successful transmission is facilitated when the mosquitoes are obtaining a blood meal. While residing in salivary glands, the sporozoites achieve enhanced infectivity. The infectivity of salivary gland sporozoites is higher as compared to the oocyst sporozoites. Suppression subtractive hybridization of oocyst versus salivary gland sporozoites identified 30 genes which are upregulated in salivary gland sporozoites and were designated UIS genes (upregulated in infectious sporozoites) [80]. Genome wide expression analysis identified 47 genes that were specifically upregulated in oocyst sporozoites before they invaded salivary glands. These genes were referred as UOS (upregulated in oocyst sporozoites) genes [81]. It has been reported that sporozoite asparagine rich protein (SAP-1) regulates the differential gene expression associated with infectivity changes in the mosquito as the deletion of SAP1 altered the expression of UIS genes [82, 83]. Few transcripts required for hepatocyte invasion and infectivity are translationally repressed in salivary gland sporozoites and are activated upon entering into mammals during blood meal. Translational repression of transcripts required for hepatocyte infectivity is regulated by a puf (pumilio and fem3 transcription binding factor) family protein puf2 [84-86]. Study of differential gene expression of sporozoites is important for understanding proteins involved in the journey of sporozoites from oocysts to salivary glands and finally to hepatocytes. Very few proteins specific to sporozoites are characterized till to date. The gene products corresponding to most highly upregulated UIS transcripts in sporozoite stages have been shown to play a role in liver stage development. Immunization of mice with *uis-3* and *uis-4* KO sporozoites elicited $CD8^+$ T cell responses in mice [87]. Thus

identifying and functional characterization of proteins involved in sporozoite invasion and hepatocytes infectivity can lead to generation of genetically attenuated sporozoites (GAS) that have potential for inducing sterile immunity.

1.3 Control measures of malaria

Control measures to prevent the transmission of malaria include using prophylactic drugs, mosquito eradication and preventing mosquito bites. Residual spraying of insecticides, using mosquito repellants and mosquito nets decreases the transmission of the disease to certain extent. Insecticide treated nets (ITNs) are more effective than untreated nets as they are effective in both killing the mosquitoes as well as reducing the mosquito population and transmission of malaria. Environmental sanitation is an important measure to control the mosquito population. Awareness programs to educate about risk of malaria, vector management and symptom recognition can be effective to bring down the socio economic loss. Usage of prophylactic drugs like mefloquine, atovaquone and proguanil in endemic areas can prevent the parasite multiplication in blood. In malaria endemic regions, control measures are important to reduce the mortality and morbidity.

1.4 Prophylaxis and treatment

To prevent the onset of the disease, prophylactic vaccines are more effective than drugs as parasites tend to acquire resistance against drugs. Different stages in the life cycle are targeted to generate a successful vaccine. Pre-erythrocytic stages are attractive targets for vaccine development because parasites that are not able to complete liver stage development have a potential to elicit protective immunity. Live attenuated parasites obtained by the method of irradiation or through genetic engineering experience a block in liver stage development and are shown to elicit cellular immunity. DNA based subunits vaccines, have also shown to trigger immune response albeit with less protective efficacy [88-92]. Genetically attenuated parasites (GAP) range in their degree of attenuation from early liver stage to late liver stages. For example *uis-3* and *uis-4* knockout parasites are arrested at early stages and immunization with *uis-3* and *uis-4* knockout parasites elicits $CD8^+$ T cell immunity [87, 93]. Depletion of enzymes involved in fatty acid biosynthesis causes mid to late liver stage developmental arrest prior to the formation of merozoite [94]. Targeting genes exppressed in late liver stage development could be effective strategy to develop whole organism vaccines that may be capable of confering cross stage protection. PKG [24], SUB1 [22], PALM (*Plasmodium*-specific Apicoplast protein for Liver Merozoite formation) [95], LISP (Liver

Specific Protein)-1 [96] are examples of few genes essential for liver merozoite formation and release. To treat malaria, anti-malarial drugs like azithromycin and clindamycin are used which inhibit for formation of apicoplast and thus give rise to a generation of non-infectious merozoites which are blocked mid-way during intra erythrocytic development, a phenomenon referred as delayed death phenotype [97]. The other mainstay of chemotherapy are chloroquine and mefloquine that inhibit hemozoin formation in infected RBC and prevent the growth of asexual erythrocytic parasites, however these do not affect liver stage development [98]. Artimisinin is another anti-malarial drug that in combination with other drugs is used to treat malaria [99]. In addition to pre-erythocytic vaccines and drugs that target intra erythrocytic parasites, transmission blocking vaccines are gaining prominence to prevent transmission of malaria to mosquitoes. Genes that play a crucial role in gamete, zygote and ookinete formation are targeted to generate transmission blocking vaccines by inhibiting sexual stage development in the mosquito [100].

1.5 Challenges and Current research on malaria

Increasing resistance to available anti-malarial drugs by *Plasmodium* poses a challenging problem to chemoprophylaxis and treatment leading to mortality and morbidity especially in malaria endemic regions. Chloroquine was widely used anti-malarial which diffuses into the infected RBC and inhibits heme crystallization, resulting in the death of the intra-erythrocytic parasite [101]. As a result of mutations in the chloroquine resistance transporter gene, the parasites have developed resistance to chloroquine resulting in effective efflux of drug [102, 103]. Like wise, mutations in the dihydrofolate reductase (DHFR) gene have resulted in parasite resistance to pyrimethamine and sulfadoxine [104, 105]. Resistance to artemisinin was reported for the first time in 2008 [106]. As a result of resistance to conventional anti-malarial drugs, artimisinin in combination with other drugs (artimisinin combination therapy) became first line defense to curtail malaria. Besides drug resistant parasites, *Anopheles* mosquitoes developed resistance to insecticides. According to world malaria report 2012, *Anopheles* mosquitoes that are insecticide resistant were observed in 64 countries. World health organization is working with governments agencies in several countries where malaria is endemic, thus looping research agencies and industry partners to develop a strategy for insecticide resistance management in malaria vectors. While research is ongoing to understand more about drug resistance, efforts are also underway to identify new gene products against which vaccines can be obtained. Considering the complex digenetic life cycle of *Plasmodium*, the feasibility to develop vaccines exists at three distinct stages: the pre-erythrocytic stages

(sporozoites and liver stages), the erythrocytic stages and the transmission stages. Of all these three stages, vaccines against the pre-erythrocytic stages seem to be more feasible as there is a dual possibility to eliminate the extracellular sporozoites through induction of neutralizing antibodies and the intracellular hepatic forms through generation of parasite specific $CD8^+$ T cells. Thus the pre-erythrocytic vaccines have the potential to clear the parasites before the clinical manifestations of the disease that is associated with the blood stage infections. While radiation attenuated sporozoites remain as gold standard for pre-erythrocytic vaccines, a limited success has also been obtained through use of recombinant vaccines designed at eliciting pre-erythrocytic immunity. For example, RTS, S is one of the recombinant vaccines developed from a central tandem repeats of *P. falciparum* circumsporozoite protein, a major surface protein of sporozoites. According to Phase III clinical trial studies, it was noted that RTS, S/AS01 vaccine provides moderate protection against both clinical and severe malaria in infants [107]. It has been shown that the vaccine induces protection through CD4+ and CD8+ immune response [108]. Owing to the genetic restriction of HLA haplotypes, it is unlikely that any recombinant vaccines elicit a response that is uniform across different individuals. Thus, much of the recent efforts have been towards creating a radiation attenuated *P. falciparum* sporozoite, with an expectation that, when delivered to humans, a customized immune response based on their genetic make-up would offer immunity that can protect against subsequent infections. An equally appealing strategy is the use of genetically attenuated *P. falciparum* parasites obtained through deletion of one or more genes [109-111] critical for completion of the liver stage development. Successful attenuation of the *P. falciparum* liver stage parasites has been shown in human liver tissues grafted in nude mice [112]. These studies provide ample proof for the pre-erythrocytic vaccine to be reality in near future. Vaccine development against blood stages poses extreme challenges because of the phenomenon of antigenic variation associated with the mature asexual blood stages. A family of 150 genes grouped in the *Pf* EMP family, are expressed one at a time, in a mutually exclusive way, so as to preclude the induction of neutralizing antibodies against all the variants at the same time [113]. By constantly switching the expression of the variants, the parasites ensures several waves of asexual cycles, each with a distinct antigenic makeup, thus making highly impossible, the development of an effective vaccines against these stages. Genes important for completion of sexual stage development could also be targeted for generating transmission blocking vaccines. For example, Pfs25 transmission blocking vaccine was generated by targeting a 25kDa ookinete surface protein, Pfs25. This vaccine showed poor immunogenicity and failed to completely block the transmission. To improve its

immunogenicity, a modified vaccine named Pfs25-EPA was developed by conjugating Pfs25 with nontoxic exoprotein A (EPA) from *Pseudomonas aeruginosa.* The Phase 1 clinical trials are currently underway using this vaccine [114]. Several hundred genes are not completely characterized in *Plasmodium* and understanding the function of these genes can lead to the development of more potent anti-malarial vaccine that can target multiple stages of the parasite life cycle.

1.6 *Plasmodium berghei (P. berghei)* – model organism

P. berghei is one of the murine parasites that cause malaria in rodent species. It is used in many research laboratories as a model organism for studies involving basic biology of the parasite and for validation of new drug and vaccines targets. *P. berghei* the first rodent malarial parasite identified and isolated in 1948 and easily maintained in the laboratory [115]. Many aspects of *P. berghei*, like the morphology, physiology and life cycle are similar with human species of malaria with only slight variations making the investigation of human malaria effective. The complete genome of *P. berghei* is sequenced and shows great degree of similarity with *P. falciparum* both in structure and gene content. *P. berghei* can be genetically manipulated by conventional genetic recombination technologies. *P. berghei* offers as a best model organism to investigate the pre-erythrocytic stages and mosquito stages, as the risk of transmission by mosquitoes to humans is none, when compared to *Plasmodium* species that are infective to humans. Because the *P. berghei* species is easily amenable to genetic manipulation, the functional characterization of several stage specifically expressed genes can be performed by disruption of the target gene either through double cross over homologous recombination [116, 117], single cross over recombination [118, 119] or by conditional mutagenesis [120]. Further, several transgenic *P. berghei* lines are already available that constitutively express GFP [121], mCherry/red Star [122, 123] and luciferase genes [124]. These reporter lines have been used as effective tools to study and track the parasites as they go through mosquito and vertebrate host.

CHAPTER 2

Functional characterization of *P. berghei SSPELD* by reverse genetics reveals its role in liver stage development

2.1 Introduction

High throughput methods of gene expression analysis has offered an insight in understanding the malaria parasite biology and allowed the appreciation of stage specifically regulated genes in modulating the infectivity or virulence of parasites [125, 126]. Such insights provide resource and leads towards identification of novel therapeutic and vaccine candidates. The diversity of the parasite life cycle is more appreciable from the point of gene regulation, as distinct stages have different regulatory mechanisms to achieve desired gene expression leading to manifestation of stage specific function. Provided here is a brief overview of the features of the *Plasmodium* transcriptome in stages that occur both in the vertebrate host and the female *Anopheles* mosquito using methods like conventional cDNA library, micro array, suppressive substraction hybridization [SSH], RNA Seq and Serial analysis of gene expression [SAGE].

An obligatory step in the infection of *Plasmodium* to the vertebrate host is invasion of extracellular sporozoites into hepatocytes, where it transforms into liver stages or EEFs [exo-erythrocytic forms]. While it is known that the antigens expressed in the EEF stage are crucial towards achieving protective sterilizing immunity, efforts to identify the genes that are uniquely expressed in this stage were hampered due to the lack of techniques to isolate the EEFs in a pure form from the bulk of uninfected hepatocytes. An axenic liver stage cDNA library obtained from 24h EEFs yielded 1453 expressed sequence tags [ESTs] of which 652 transcripts were unique [127] to this stage. The transcripts recovered in this library were central to processes needed for initiation of sporozoite transformation to EEFs like those involved in protein degradation, cell cycle progression and nutrient transport. Approaches to study the transcriptome of *in vivo* developing EEFs were possible by the use of *P. yoelli* sporozoites that constitutively express GFP all through the life cycle [128]. Transcriptomic analysis of the sorted GFP expressing infected hepatocytes and profiling the genome-wide liver stage gene expression and comparison with other life cycle stages revealed approximately 2000 genes that were active in liver stages. A subset of these genes appeared to be specific to liver stages that encoded for exported parasite proteins and metabolic pathways including FASII pathway enzymes.

Analysis of the asexual blood stage transcriptome of the HB3 strain of *P. falciparum* revealed that nearly 60% of the genome is transcriptionally active where transcriptional regulation occurs in a strictly sequential manner with onset of gene expression associated with

processes like protein synthesis and ending with more specialized functions such as invasion of erythrocytes. Interestingly, there was no co-regulation of genes that were contiguous within a chromosome, though a high co-regulation in the transcription of plastid associated genes were noted. These studies revealed the existence of mechanism that ensured timely expression of genes, that are induced once per cycle and only when required. [129]. Deep sequencing the transcriptome of the developmental stages of the *Plasmodium* infected red blood cells by illumina based RNA Seq has yielded information with better resolution over microarrays [130]. In addition to improving the existing annotation of the *P. falciparum* genome and over 10% of the gene models being modified, it allowed the discovery of 107 novel transcripts and expression of 38 pseudogenes with many showing differential expression across the developmental time series.

Transcriptomic analysis of sexual stages of *Plasmodium* that develop only in the *Anopheles* mosquito midguts were studied by substractionhybridization techniques [SSH] [131], a process that enriches selectively one population of transcripts (target/tester polulation) from the other (driver) population. This approach is based on technique called suppression PCR that combines normalization and subtraction in a single procedure. The abundance of cDNA in the target population is equalized in the normalization step and the common sequences between the target and driver population is excluded in the substraction step. The technique increases the probability of detecting the differentially expressed cDNAs of low abundance. Using this technique, the genes that are specifically expressed in the early stages of *Plasmodium* differentiation in the mosquito were identified by generating two cDNA libraries one enriched for sequences expressed in differentiating *P. berghei* ookinetes and other enriched for sequences expressed in *Anopheles stephensi* guts containing invading ookinetes and early oocysts [132]. Following sequencing of 1485 random clones, 1137 unique expressed sequence tags were identified, of which 608 had data base hits. Of these 608 ESTs, the ones that matched significantly the non-redundant protein data base were 320 [53%], whereas 288 [47%] had matches only to genomic data bases and represented novel *Plasmodium* and *Anopheles* genes. These studies also reported the transcription of six novel parasite genes, together with an unexpected expression of two well characterized asexual candidates, MAEBL and AMA1 induced during oocyst differentiation.

While the importance of stage specific regulation of gene expression across any life cycle stages of *Plasmodium* cannot be undermined, there has been a rejuvenated interest in studying the gene expression of parasites stages that are infective to the vertebrate host.

Gaining insight into these regulatory mechanisms may offer a unique advantage of understanding the parasite biology and devising therapeutic or vaccine oriented strategies to prevent onset of blood stage infections and hence the clinical manifestation of malaria. Referred to as the sporozoite stages, major transcriptional changes occur in these forms of the parasite while residing in the salivary gland of the mosquitoes-a niche that renders them to achieve enhanced infectivity [133]. The first comprehensive transcriptomic analysis of sporozoites [134] opened the possibility of understanding the regulation of *Plasmodium* gene expression in mosquito stages that was previously considered to be technically challenging owing to the limitation of obtaining pure/sizeable preparation of sporozoites, free from mosquito contaminants. By performing a PCR based amplification of the sporozoite transcriptome, sufficient amount of cDNA was generated to construct a library for acquiring EST sequences. An insight into this transcriptome revealed several interesting features. Primarily, an enhanced expression of both CS and TRAP was observed, that was expected owing to the central role of these sporozoite antigens in commitment to hepatocytes infection and in gliding motility. Unexpectedly, there was enhanced expression of chorismate synthase an enzyme of the shikimate pathway that was earlier reported to be functional in the blood stages, making these stages a vulnerable target of herbicide glyphosate [135]. Other two candidates having an unexpected expression in sporozoite stage was MAEBL, which in blood stage stages have been shown to bind to and faciliate the invasion of merozoites into RBC [136] and other was SPATR, that contained a TSR domain whose functional role in CS and TRAP, have been implicated in sporozoite motility, host cell attachment, and invasion [137-139]. Thus transcriptomic analyses redefine our approches to devise more meaningful therapeutic strategies precisely based on the targets that are expressed in the pre erythrocytic stages.

The success with studying the sporozoite transcriptome [134] further led to investigating the differential gene expression across other *Plasmodium* life stages using techniques like suppressive subtraction hybridisation(SSH) to identify the transcripts uniquely upregulated in sporozoite stages. The criterion for such consideration was that distinct compartments of the host/vector offer unique tissue specific environments that influence the regulation of parasite gene expression [131] For example SSH of midgut versus salivary gland sporozoites led to discovery of genes up regulated in infected salivary gland sporozoites (*UIS* genes) [80] and SSH of merozoites versus sporozoites led to the discovery of Sporozoite genes (S genes) [131]. Clearly, the gene products of these upregulated transcripts were

important for functions central to motilitylike S6 [140] and SSP3 [141], in tissue migration like *Pb* LCAT [12] and liver stage development like UIS-3 and UIS-4 [28, 27].

In addition to conventional cDNA library, micro arrays and RNA Seq methods for investigating expression across different life cycle stages, Serial Analysis of Gene Expression (SAGE) [142] has been yet another flat form for studying the stage specific transcriptome and was successfully employed in the blood stages for simultaneous quantifications of multiple mRNA transcripts [143]. SAGE offers quantification of 14-15 nucleotide sequence tags, each sequence being associated with the transcripts of one gene. While this technique is used as popularly as microarrays, it offers several unique advantages. Primarily, it facilitates detection of novel transcripts that cannot be identified based on sequence information alone, thus enhancing the possibilities of discovering novel transcripts. When this technique was applied to analyse the transcriptome of sporozoite infected salivary glands, 530 sequence tags were recovered. By aligning these sequence tags to *P. berghei* genomic sequences, 123 genes were identified, out of which 66 were reported for the first time [144]. Interestingly, these studies revealed that sporozoites not only alter their RNA abundance between the midgut and the salivary gland stages, but also while residing in the salivary glands from day 14-18. The 66 novel transcripts were designated as SIS genes (new Sporozoite expressed gene Identified by SAGE).

Considering that the 66 newly discovered SIS genes were not detected in sporozoite transcriptome [134] nor in the SSH of salivary gland sporozoites versus midgut sporozoites [80], proved uneqivocally the better resolution of gene expression through SAGE method. The 66 newly discovered transcripts were grouped into three categories based on the abundance of the SAGE tags recovered. Group 1 included highly expressed genes with frequency greater than 20, whereas group 2 and 3 included candidates having tag frequency of 10-20 and less than 10 respectively.

The top number one gene with highest expression in the SAGE library of infected salivary gland transcriptome was PBANKA_091090 [144]. To the best of our knowledge no functional investigation of this candidate has been performed till to date. Interestingly, PBANKA_091090 was grouped in a category that clustered frequency wise with previously well characterized transcripts: UIS-4, UIS-7 [80] S23 [131] and TRAP [134] discovered through independently generated substraction or cDNA libraries. Using a rodent model of *P. berghei*, we provide a genetic evidence for the role for PBANKA_091090 in the liver stage development. We designated this protein as *Plasmodium bergheiS*porozoite Surface Protein

Essential for Liver stage Development [*Pb* SSPELD]. One of the unique features of Pb SSPELD has been its association with membrane of sporozoite and developing EEFs, though it lacked canonical membrane targeting motifs like SP, TM and GPI. We implicate the role of *Pb* SSPELD in the liver stage development as *Pb SSPELD* mutants did not complete liver stage development *in vitro* and failed to initiate blood stage infection when malaria was transmitted through natural mosquito bite. We further provide evidence for the ability of *Pb SSPELD* mutants in generating both humoral and cell mediated immunity whose efficacy was nearly 50%.

2.2 Materials and Methods

2.2.1 Retrieval of target genes sequences

Two public domain databases namely Plasmo DB (http://www.plasmodb.org/ plasmo)and Sanger gene data base (http://www.genedb.org/Homepage/Pberghei)were used to retrieve the 5' untranslated region, the ORF and the 3' untranslated regions of any target gene.

2.2.2 Construction of the transfection /knockout vector

Construction of the transfection vector involved cloning of approximately 500bp of 5' and 3' DNA fragments that flanked the *Pb SSPELD* (PBANKA_091090) gene. To clone the 5'fragment, a Polymerase Chain Reaction (PCR) was set up using the following components: 0.5µM of forward primer (FP1- 5'AGTCTCGAGATTATTAAACGTGAGGAATT3') containing Xho1 recognition site (underlined), 0.5µM of reverse primer (RP1-5' ACTATCGATAAAATGTGCTTAAACAATGA3') containing Cla1 recognition site (underlined), 1mM deoxyribonucleoside triphosphates (dNTPs, Invitrogen, Cat#R72501), 0.5U of thermostable DNA polymerase (Invitrogen, Cat#11615010), 40ng of genomic DNA and PCR buffer containing 2.5mM (final concentration) of $MgCl_2$ (Life Technologies, Cat#R0971). The reaction mixture was made up to a final volume of 50µl and the PCR amplification was performed for 35 cycles at following conditions, 94°C for 2 minutes, 94°C for 30sec, 56°C for 30sec and 72°C for 1 minute and final extension at 74°C for 10 minutes using an EppendorfMastercycler personal. A small volume of PCR amplified reaction mixture (5µl) was analyzed in 1% agarose gel containing DNA intercalating dye-ethidium bromide (0.5µg/ml, SRL, Cat# 05481) and was visualized under UV light. The remaining PCR reaction mixture was purified using PureLink PCR purification Kit (Life Technologies,

Cat#K220001) to efficiently remove primers, dNTPs, enzymes and salts from the PCR product. The PCR product was eluted from column and quantified using a nanodrop spectrophotometer at 260 nm wavelength. The 3' fragment was similarly amplified using 0.5µM of forward primer (FP2-5'ATAGCGGCCGCAAGCAAACAATAAACACTTA3') containing Not1 recognition site (underlined) and 0.5µM reverse primer (RP2-5'GTAGGCGCGCCTGCATTATGAAACTGTCA3') containing Asc1 recognition site (underlined). The PCR amplification was performed for 35 cycles at following conditions, 94°C for 2 minutes, 94°C for 30sec, 56°C for 30sec and 72°C for 1 minute and final extension at 74°C for 10 minutes Both the 5' and 3' purified PCR products were ligated in TA sequencing vector, pTZ57R/T. To facilitate the ligation of PCR product into the TA cloning vector, 0.5µl of vector was added to 10µl of fresh PCR product and further incubated in the presence of 0.2mM dATPs(final concentration) for 10 min at 72°C in the EppendorfMastercycler personal. From this mixture, 0.5-1µl was transformed into XL1-Blue strain and streaked on agar plates containing ampicillin (Sigma, Cat# A9518) and tetracycline (Himedia, Cat# CMS219) antibiotics. The positive colonies were screened by performing colony PCR using 5' fragment specific or 3' fragment specific primers and 2µl of bacterial culture as template. Following this preliminary confirmation, plasmid was isolated from the corresponding bacterial culture and further confirmed by releasing the cloned 5' fragment by restriction digestion. In brief, the 5' fragment was released by setting up a restriction enzyme digestion reaction containing 5U of Xho1 (Thermo Scientific and Cat# ER0691) and 5U of Cla1 (Thermo Scientific and Cat#ERO141) in the presence of buffer BamHI(Thermo Scientific and Cat #B57) with 0.1mg/ml BSA (Sisco research laboratories private limited and Cat#0141105) in a final volume of 30µl and the reaction mixture was incubated at 37°C for 1 hr. Similarly, the presence of the 3' fragment into the TA vector was confirmed by setting up a restriction enzyme digestion reaction containing 5U of Not1 (Thermo Scientific and Cat #ERO592) and 5U of Asc1 (Theromo Scientific and Cat #ER1892) in the presence of buffer BamHIwith 0.1mg/ml BSA in a final volume of 30µl and the reaction mixture was incubated at 37°C for 1 hr. A mini plasmid preparation was made from colony that contained either the 5' or 3' part cloned into the TA vector. Following nanodrop quantification of plasmid DNA at 260nm, 150ng/µl of this plasmid was sequenced using same set of primers (as described above) as used for amplifying the 5' and 3' fragment. Following sequence confirmation, both 5' and 3' inserts were released from the TA sequencing vector and further subcloned into the

multiple cloning sites of the targeting vector pBC-GFP-hDHFR. The targeting vector was a generous gift from Dr. Robert Menard, Pasteur Institute.

2.2.3 Sub cloning into targeting vector pBC-GFP-hDHFR

The targeting vector pBC-GFP-hDHFR contained multiple cloning sites (MCS-1 and MCS-2) flanking the GFP cassette (containing 5' HSP70 promotor sequence and 3' UTR of HSP70) and hDHFR cassette (containing 5' EF1α promoter sequence and 3' UTR of PBDHFR/TS) respectively. The 5' fragment of PBANKA_091090 was ligated into the MCS-1 utilizing Xho1 and Cla1 sites in the presence of T4 DNA ligase (Thermo Scientific, Cat#EL0011) at 22°C for 16 h. The resulting intermediate vector 5'+pBC-GFP-hDHFR was transformed into XL-1Blue competent cells and dispersed on to chloramphenicol (Sigma, Cat# C0378) and tetracycline (Himedia, Cat#CMS219) plate and incubated at 37°C for overnight. Positive colonies were screened by colony PCR using 5' specific primers and 2µl of bacterial culture as template. A single positive colony was selected and inoculated into 5ml LB broth and incubated at 37°C for overnight. The intermediate vector 5'+pBC-GFP-hDHFR was isolated by byGeneJET Plasmid Miniprep Kit (Thermo Scientific, Cat#K0503). This vector was further used to clone the 3' fragment utilising the Not1 and Asc1 sites present in the MCS-2 to generate the final vector 5'+pBC-GFP-hDHFR+3'. This vector was reconfirmed by releasing the targeting construct and the vector back bone using restriction enzymes Xho1 and Asc1 that gave DNA fragment of 5654bp and 3276bp respectively. Following this confirmation, the final vector was expanded by bacterial culturing and plasmid was purified using mini plasmid isolation kit.

2.2.4 Preparation of the transfection plasmid by maxi preparation method

Approximately 20-30ng of final transfection vector [5'+pBC-GFP-hDHFR+3'] containing the cloned 5' and 3' fragments of SAGE-1 was transformed into XL-1 Blue competent cells and plated on chloramphenicol tetracycline plate. One colony was selected and inoculated into 5ml of primary culture was grown over night at 37°C. The primary culture was further used to inoculate 500ml of LB-broth containing chloramphenicol and tetracycline antibiotics. Inoculated medium was incubated at 37°C for overnight. Following day, culture was harvested at 10,000 rpm for 10 min at 4°C. A maxi preparation of the final transfections vector was made using EndoFree Plasmid Maxi Kit (QIAGEN, Cat#12362). The bacterial pellet was resuspended in 10ml of P1 resuspension buffer. Next, 10 ml of P2lysis buffer was

added and mixed by inverting the tube for 4-6 times followed by the addition of 10ml of chilled P3 buffer. The contents were mixed thoroughly by vigorously inverting the tube for 4-6 times. The lysates were poured into the barrel of QIA filter cartridge and incubated at room temperature for 10 min. Equilbration of QIAGEN column was done by adding 10ml QBT buffer and the column was allowed to empty by gravity flow. The cell lysates was filtered into equilibrated QIAGEN column. The QIAGEN column was washed with 60ml of QC buffer. The DNA was eluted with 15ml QF buffer and precipitated by adding 10.5 ml isopropanol and centrifuged at 15,000 rpm for 30 min at 4°C. The DNA pellet was washed with 5 ml of 70% ethanol at 15,000 rpm for 10 min and air dried briefly (2-3 min). The DNA pellet was resuspended in 150µl of 1X TE buffer and the concentration was estimated by nanodrop using 1X TE as blank.

2.2.5 Release of targeting cassette by double restriction digestion

Plasmids were digested with Xho1 and Asc1 to release the cassette from plasmid back bone. For efficient digestion, five independent reactions were set up, each reaction containing 45µg of plasmid, 5µl of 10X BamH1 buffer and 5U each of both the enzymes. The restriction digestion reaction mixture was incubated at 37°C for 20h and products were analyzed on 1% agarose gel. To achieve clear separation of the cassette from plasmid back bone, electrophoresis was performed at 30V for 16 h. The targeting cassette was excised from the gel and purified using Purelink Gel extraction kit (Life Technologies Cat#K220001). In brief, the procedure involved the excision of gel slice containing the construct, followed by estimating its weight and addition of three volumes of the gel solubilisation buffer (to the weight of gel). The contents were incubated at 50^0C until the gel slice was completely dissolved. One volume of isopropanol was added and loaded on to the PureLink Gel extraction column and centrifuged at 11,000g for one minute. The column was washed by 500µl buffer PW4 and the flow through was discarded. The column was centrifuged for 2 min at maximum speed to remove any residual wash buffer. DNA was eluted in 50µl of nuclease free water and quantified using a nanodrop spectrophotometer at 260nm.

2.2.6 Transfection of the rodent malaria parasite *Plasmodium berghei (P. berghei)*

Plasmodium transfections were done essentially as described earlier [145]. Four to six weeks old BALB/c mice was intraperitonealy injected with wild type *P. berghei* infected blood from frozen stock. Blood smears were made from day 3 post injection. When parasitaemia reached around 0.5%, blood was collected from donor mice and passaged to five BALB/c

mice such that each mouse received nearly 2-3X10^7 infected erythrocytes. When the donor mice developed around 4-5% parasitaemia, blood was collected by cardiac puncture and an *in vitro* overnight culture was set up [Fig 5]

2.2.7 *In vitro* culture of schizonts

Following is the brief procedure for setting up an *in vitro* parasite culture. On day 4 post infection, blood was collected from mice by cardiac puncture using heparinised syringe. The collected blood was pooled into 50ml tube containing 0.25ml of 200U/ml heparin (Sigma, Cat#H3393). Approximately 5ml of blood was collected from 5 mice. Culture media used for maintaining asexual blood stages contained RPMI supplemented with 20% FBS and gentamycin (Sigma, Cat #G1397) at a concentration of 350μg/ml of medium. Ten milliliter of culture medium was added to 5 ml of blood and centrifuged at 200g (Eppendorf 5810R) without brake for 8 min at room temperature using a swinging bucket rotor. Supernatant was discarded and RBC pellet (approximately 3 ml) was resuspended gently in 20ml of culture media and was split into 4X5 ml cultures and transferred into four T75 flasks each containing 20ml of culture medium. The cultures were gently gassed with mixture containing (5% CO_2, 5%O_2, 90%N_2) swirled for 3 min under the hood and further incubated at 36.5°C with 77 rpm for 16-23 hours. Following day, 0.5 ml of schizont culture was taken into 1.5 ml tube and spun for 5 sec at maximum speed at room temperature. The pellet was resuspended in minimal amount of schizont medium and was smeared. The smears were fixed in methanol and Giemsa stained. The slides were observed for the presence of mature schizonts and their numbers were determined under light microscope (Lawrence and Mayo XSZ-N107T).

2.2.8 Schizont purifications

Schizonts were purified by pouring 35ml of overnight culture into 50 ml (Falcon) tube and by gently adding 10ml of 60% Nycodenz(Sigma, Cat#D2158) made in 1X phosphate buffered saline (PBS) diluted from 10X PBS stock, pH 7.4 (Gibco, Cat#70011). This resulted in the appearance of sharp phase between the two suspensions. The tubes were centrifuged at 200g (Eppendorf 5810R) without break for 25 min at room temperature in swinging bucket rotor. The brown layer (schizont) at the interphase between the two suspensions was carefully collected and pooled into one fresh 50 ml tube. Approximately 30-40 ml schizont suspension was collected from four tubes. Schizonts were pelleted down to 200g (Eppendorf 5810R) without brakes for 8 min at room temperature and pellet was washed with 20 ml schizont

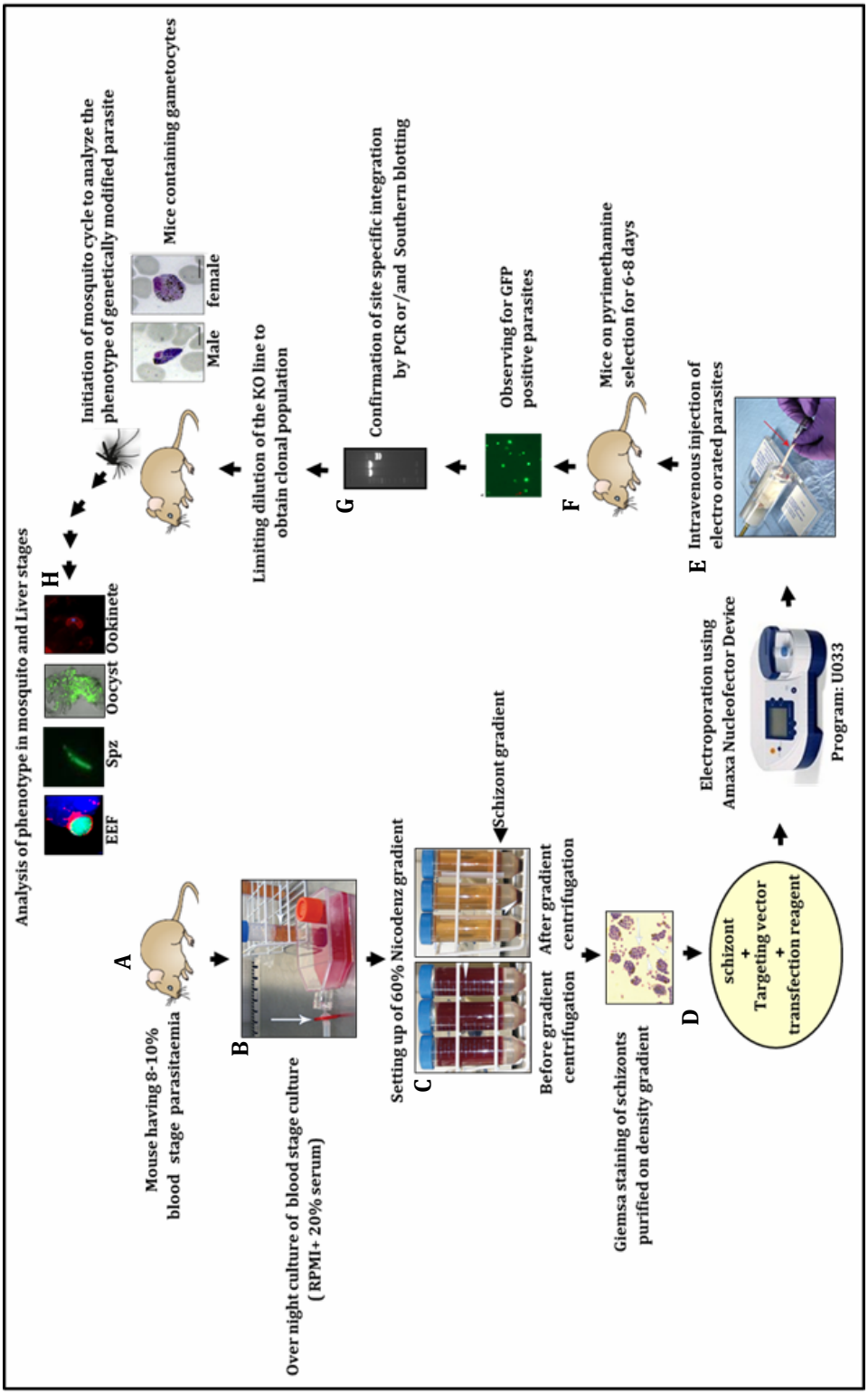

Fig 5. Schematic representation *Plasmodium berghei* transfection, drug selection, confirmation of the site specific integration and phenotypic characterization of the genetically modified transgenic/ knockout/reporter line. Blood is collected from mouse having 8-10% parasitemia (A) and an overnight culture is set up (B). Next day, the schizonts are enriched on a 60% density gradient (C). The purified schizonts are collected and electroporated with the targeting construct (D) and immediately injected intravenously into mouse (E). The mice are kept on a Pyrimethamine, an antimalarial drug that facilitates selection of the transfectants (F). The success of stable site specific integration is confirmed either by PCR or Southern (G). The transfectants are cloned out and passed through mosquito stages to analyze the phenotype in other life cycle stages like oocyst stages, sporozoite stages and liver stage (H). This figure is obtained from Janse, C.J, Ramesar, J and Water, A.P [203] and modified and reproduced from the thesis of Togiri J (2015)

medium at 200g for 8 min at room temperature. Schizonts were resuspended in 1 ml of culture medium and transferred into 1.5ml tube and centrifuged for 5 sec at room temperature.

2.2.9 Electroporation of schizonts

In fresh 1.5 ml tube, 10µg of DNA [targeting cassette] was mixed with 100µl of nucleofector transfection reagent (Lonza, Cat#VBZ-1001) was transferred into tube containing nearly 50-60 million schizonts. The mixture (schizonts, DNA and nucleofector reagent) was gently transferred into transfection cuvette without air bubbles. The cuvette was placed into an Amaxanucleofector device (Nucleofector II AAD 10015) and electroporated using program U033. Immediately after electroporation, 100µl schizont medium was added in the cuvette and the transfected parasites were transferred into 1.5ml tube. Transfected parasites were immediately injected into tail vein of mice using an insulin syringe.

2.2.10 Drug selection

On second day of transfection, parasitemis was monitored by Giemsa staining of the blood smears. Under optimal transfections conditions, the parasitemia will be around 0.5-1%. To facilitate the selection of the transfected population, injected mice were treated with pyrimethamine (Sigma, Cat# 46706), an antimalarial drug that eliminated the wild type (nontransfected) population. Pyrimethamine was provided in drinking water and was prepared by dissolving 7 mg in 100 ml water and pH was adjusted to 3.5 ml with HCL. The parasitemia was monitored daily that showed a gradual decrease until no infected RBC was seen in the smear on day 7 post infection. On day 8-9, parasitemia (resistant parasites) started gradually increasing and reached around 3-5% on day 12 post infection. A minimum of two independent transfections were performed with the targeting construct. Samples obtained from independent transfections were labeled as T1 (transfection 1) and T2 (transfection 2). Both T1 and T2 blood samples were collected in an anticoagulant as described below and stored at -80°C. A small volume of T1 and T2 were taken for gDNA isolation.

2.2.11 Microscopic enumeration of *P. berghei* infections by Giemsa staining

Blood smears were prepared on a microscopic glass slide by drawing blood from the tail tip of an infected mouse. The smear was fixed in 100% methanol for 10 seconds and dried using a hair drier. Giemsa staining solution (Sigma Cat#GS1L) was diluted in a 1:5 ratio in deionised water and was over layered on the fixed smear and was stained for 15 minutes. The

slides were washed in tap water and air dried. Smears were examined under light microscope at 100X magnification with oil immersion. Parasitaemia was typically determined in an area where the smear appeared as monolayer. The slide was viewed in 50 random fields and the number of infected erythrocytes was counted and averaged. The following formula was used to determine the percentage of parasitaemia:

(Average number of infected erythrocytes)/ (average number of all erythrocytes X 50) X 100= % of parasitemia.

2.2.12 Cryopreservation of *P. berghei* infected blood

P. berghei infected blood was collected by ocular puncture using a disposable Pasteur pipet (Corning, Cat# 7095B-5X) that was pre rinsed in heparin (200U/ml)]. One part of the blood was mixed with two parts of freezing medium. The freezing medium was prepared by adding 9 parts of Alsevier Solution (Sigma Cat#A3551) with one part of glycerol (Invitrogen, Cat# 15514-011). The contents were gently mixed and 250µl of samples was distributed in each cryo vial. The cryo vials were gradually frozen by first maintaining at -20°C for 4 h followed by shifting them into -80°C for overnight. The frozen samples were finally preserved in liquid nitrogen container.

2.2.13 Observation of GFP parasites under fluorescent microscope

Approximatey 20µl of *P. berghei* infected blood (both T1 and T2) were collected by caudal vein puncture and placed into 1.5ml tube containing 1-2µl of 200U/ml heparin solution. Blood was washed twice with 1X PBS and RBC pellet was re suspended in 200µl of same buffer containing 2µl of 100X DAPI (4', 6' diamidino-2 phenyl indole, Sigma, Cat# 9542) prepared by adding 1 mg of DAPI in 1ml of double distilled water. The suspension was incubated at 37°C for 10 min. The cells were centrifuged at 5000 rpm for 1 min and supernatant was discarded. Pellet was washed with 1X PBS and resuspended in 20µl of 1X PBS. Two microlitres of suspension was spread on the slide and covered with coverslip and observed under fluorescent microscope.

2.2.14 Genomic DNA isolation from transfected *P. berghei* population

Genomic DNA was isolated from transfected (T1 and T2) *P. berghei* blood stages using a genomic DNA isolated kit (Genetix and Cat #NP-61305), following manufacturer's instructions. In brief, 700µl of blood was collected from infected mice into 1.5ml tube

containing 60µl of heparin (200U/ml). RBC were centrifuged at 13,000 rpm for 10 min. The supernatant was discarded and pellet was washed with 1ml of 0.5% saponin (Sigma Cat# 47036) at maximum speed for 10 min. The pellet was washed twice with 1X PBS at 13,500 rpm in Eppendorf centrifuge (Model 5415R) for 10 min and the supernatant was discarded. The pellet was resuspended sequentially in 200µl of LBT buffer, 200µl of BT3 and 25µl of proteinase K having concentration of 20mg/ml. Mixture was incubated at 70°C for 10-15 min followed by precipitation of DNA with 210µl of 100% ethanol. The lysates were applied onto column and centrifuged for 1 min at 11,000g. The flow through was discarded and the column was placed again into the collection tube and washed with 600µl of WBT buffer followed by WBT5 buffer at 11,000g centrifuged [Model 5415R] for 1 minute. The flow through was discarded and column was air dried for 2 min by spinning at 11,000g. The column was placed in fresh centrifuge tube and 35µl of BET elution buffer [pre heated to 70°C for 10 min] was added into the center of column and incubated at room temperature for 1 min. The gDNA was eluted at 11,000 rpm followed by a 1 min centrifugation and was quantified at 260/280nm using a nanodrop spectrophotometer.

2.2.15 Confirmation of targeted gene knockout by site specific integration PCR

To confirm the site specific integration of the targeting cassette, PCR was performed using gDNA as a template. Diagnostic primers were designed, such that the forward primer (FP3-5'TGTCTATTTCTAATGTTCTTA3') flanked upstream of the 5' recombined fragment and the reverse primer (RP3-TTCCGCAATTTGTTGTACATA3') was with in the GFP cassette. A single amplified product of 863bp in PCR confirmed the stable 5' integration at the gene locus. Similarly, a second set of diagnostic primers were designed where the forward primer (FP4-5'GTTGTCTCTTCAATGATTCATAAATAG3') had sequence within the hDHFR cassette and reverse primer (RP4-5'ACCCAAACGAGACATATATA3') was a sequence beyond of the site of 3' fragment integration. Again a single amplified product of 825bp in PCR confirmed the stable 3' integration at the gene locus.

2.2.16 Limiting dilution of transfected/ knockout parasites

Two hundred micro liters of infected blood was collected by ocular puncture using a Pasteur pipet that was pre rinsed with heparin (200U/ml) and placed in a 1.5ml tube. This was considered as a stock solution on infected blood. A thin smear was made from the stock blood that was Giemsa stained and the percentage of parasitaemia was calculated using the

formula as describe earlier. The stock blood was diluted at 1:10,000 dilution and 10µl of this dilution was observed in a haemocytometer to estimate the total RBC present in 1µl of stock blood. Based on the percentage of infection and total number of RBC count, further dilutions of the stock blood was made in incomplete RPMI such that one infected RBC was intravenously injected into each of 20 BALB/c mice to achieve clonal dilution of the KO. Blood smears were made from all 20 mice on day 8 post infection. Out of twenty, 2 mice were found to be positive for infection. When the parasiteaemia reached around 3-5%, the blood was collected both mice. A portion of the blood was taken for genomic DNA isolation while remaining was frozen for future use. Diagnostic PCR was performed using forward primer-FP5-5'ACTATTTATTACCCTGCG3' and reverse primer- RP5-5'TTAAGGATAAAATATAGCAGT3' from within the target gene ORF. A PCR was set up using genomic DNA as template from WT parasites and the cloned line. The PCR gave a product of 395bp from WT genomic DNA while complete absence of the product confirmed that the KO line was successfully cloned.

2.2.17 Maintenance of *Anopheles stephensi* colony

To generate the mosquito stages of *P. berghei*, a colony of *Anopheles stephensi* was continuously maintained. Following is the brief description of the activity associated with breeding and maintenance of the colony. Adult male and female mosquitoes were allowed to mate in capitivity within 24-36 hours following their emergence from pupae. Following mating the mosquitoes received a blood meal from an anesthesised rabbit. The rabbit was anethesised using a combination of ketamine and xylazine [0.8 ml ketamine [50mg/ml] + 0.3 ml of xylazine (20mg/ml) + 3.9 ml of 1X PBS) and 0.5ml was introduced intramuscularly into the rabbit. The sedated rabbit was placed on the top of the mosquito cages to facilitate the uptake of blood meal by the female mosquitoes. The blood meal was given two times within the interval of 24 h. After 36 h of second blood meal, a blow of water was placed inside the mosquito cage to allow egg laying by female mosquitoes. The eggs were collected over a period of 4 days. The eggs were transferred into water trays and shifted into a chamber that was maintained at 27°C and 80% RH [relative humidity]. The eggs hatched under these conditions and transformed through a series of instars resulting in the pupae. The pupae were manually collected and placed in a new cage to facilitate the emergence of adult mosquitoes.

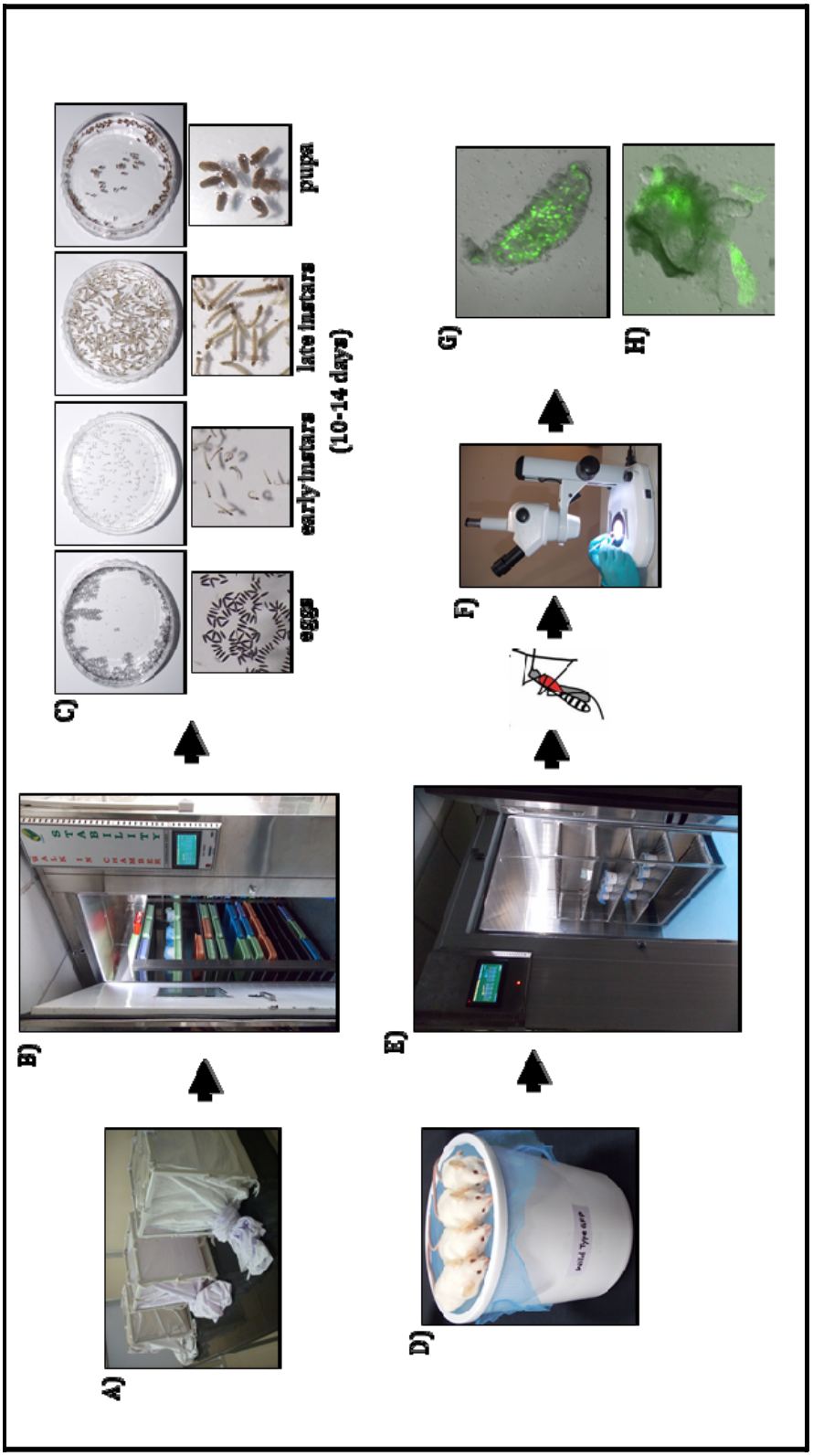

Fig 6. Maintenance of *Anopheles stephensi* colony. Maintenance of *Anopleles stephensi* colony includes activities like preparation of breeding cages, where pupa are placed in water bowls that emerge and mate within 24-36 hours (A). Two successive blood meals from anesthetized rabbit are given to the mated female mosquitoes at an interval of 24 hours. Thirty six hours after second blood meal, a bowl of water is placed inside the breeding cage and eggs are collected for four consecutive days. The eggs are then transferred into environmental chamber maintained at 27°C and RH 80% (B). Under these conditions the eggs hatch and transforms into a series of instars and finally into pupae (C). The pupae and collected and placed inside the breeding cage for emergence of adult mosquitoes. For preparation of infection cages, female mosquitoes are separated using a vacuum pump. The cage containing female *Anopheles* mosquitoes were allowed to obtain an infected blood meal from mice carrying *Plasmodium berghei* gametocytes (D). The infected cage was placed in an environmental chamber maintained at 22°C and RH 80% to facilitate the completion of sexual reproduction of *Plasmodium berghei* (E). Mosquitoes were dissected under dissection microscope (F) on D14 (G) and D18 (H) post infection to observe respectively the oocyst and sporozoite in the salivary glands under a fluorescent microscope. Schematic reproduced from thesis of Togiri J (2015).

2.2.18 Transmission of malaria into *Anopheles* mosquitoes

To allow malaria transmission into mosquitoes, a separate cage containing only female *Anopheles* mosquito was prepared. The separation of the female mosquitoes was achieved by placing the hand palm on the outer side of the adult mosquito cage that attracted the female mosquitoes by sensing the body temperature (37°C). All the female mosquitoes (on inside of the cage) gathered in the region of the palm were collected into a tube attached to a vacuum pump. The female mosquitoes were immediately transferred into a new plastic cage and were maintained in another chamber maintained at 20°C and 80% RH. The mosquitoes received a 10% sugar solution soaked in cotton as food. Immediately before obtaining an infective blood meal, the mosquitoes were starved for 2 hours by removing the sugar soaked cotton pads. Four to five BALB/c mice that were positive for *P. berghei* gametocytes were sedated by injecting 200µl of anesthesia into each mouse. The mice were placed on top of the female mosquito cage to transmit malaria. The mice were allowed to take a blood meal for a total time of 18 minutes, with three changes in the position of the mice during this time so that all mosquitoes received blood meal from all the mice. The feeding was done for two times within a 24 h interval. After second feeding the mosquito cage was placed back in same chamber maintained at 20°C and 80% RH for 18-22 days to facilitate the completion of sexual development and for the formation of salivary gland sporozoites. During this entire period, the mosquitoes were fed with sugar soaked cotton pads that were replaced on a daily basis.

2.2.19 Observing the midgut oocyst

Successful transmission of malaria in the mosquitoes was monitored by observing the oocysts on mosquito midguts. Since both the WT and KO parasites were constitutively expressing GFP, all the mosquito stage were readily monitored under a fluorescent microscope. On day 14 post infection, 20-25 mosquitoes were dissected to isolate the midguts that provided an idea about the parasite burden in the mosquito.

2.2.20 Dissection and purification of salivary gland sporozoites

To isolate the salivary glands, day 18 post infection mosquitoes were collected and were washed in 50% ethanol for three times. Followed by this, the mosquitoes were additionally washed in DMEM containing 1X antibiotic and antimycotic (Life Technologies, Cat# 152400-062, 100X) for three times. The salivary glands were dissected and collected into a 1.5ml of eppendorf tube in small volume of 80-100µl. The glands were crushed using a

plastic pestle and disrupted to release the sporozoites. The crushed samples were spun at 800rpm for 3 min at 4°C in Eppendorf centrifuge (Model 5415R). The supernatants were collected in a 1.5ml eppendorf tube. A small volume [2-3µl] was diluted in a 1:10 ratio and 10µl of this dilution was placed on a haemocytometer and the number of sporozoites was counted. Sporozoite count from all the four quandrants was averaged and the actual sporozoite numbers were calculated using the following formula:

No. of sporozoites = Average number of sporozoites from 4 quadrants X 10 (dilution fold) $X10^4$(Hemocytomter correction factor)/ml

2.2.21 HepG2 cell culturing

Hepatoma cell line [HepG2] were preserved as frozen stock in a solution of 80% Fetal Calf Serum and 20% dimethyl sulfoxide [DMSO] in liquid nitrogen. For initiating the culture, the cells were thawed quickly by placing them in a water bath maintained at 37°C. The thawed cell suspension was transferred into a 15ml tube containing 5 ml of pre warmed complete Dulbeco's Modified Eagle Medium [DMEM] containing 2mM L-glutamine and 4.5 g/liter glucose supplemented with 10% FCS (Hyclone laboratories). The cells were washed once by centrifuging at 1500 rpm for 3 minutes. The supernatant was discarded and the pellet was resuspended in 5ml of complete DMEM medium and transferred into T-25 culture flasks. The cells were maintained in a CO_2 incubator (having 5% CO_2 concentration) at 37°C until a confluent monolayer was grown. Cells were sub cultured periodically before they reached 100% confluency by adding 0.25% Trypsin EDTA (Gibco, Cat#25200056) and by incubating at 37°C for 3-4 minutes. Following trypsinisation the cells were washed in 5ml of complete medium by centrifuging at 1500 rpm for 5 min. The cells were resuspended in 250-300µl of complete DMEM medium. This was considered as a stock solution of cells. From the stock, a 1: 10 dilution was made that contained 50% (v/v) trypan blue solution (Himedia, Cat# TCL005, 0.5% solution). Ten microliters of this cell suspension was placed in a haemocytometer and the number of viable cells was counted. The following formula was used to obtain the cell density:

Average number of cells in 8 quadrants X 10 (dilution factor) X 10^4 (haemocytometer correction factor) = number of cells/ml

2.2.22 Infection of HepG2 cells for obtaining exo erythrocytic forms

For obtaining the liver stages or exo erythrocytic forms (EEFs), the HepG2 cells were either cultured in 8 well glass LAB-TEK chamber slides (NalgeNunc International, Cat# 177402) or in 24 well culture plates (Corning Cat# 3526) that were coated with collagen (Type 1, Rat tail) (BD Bioscience, Cat# 354236) and placed in culture wells. When HepG2 cells reached nearly 70-80% confluency, $2X10^4$ sporozoites were added to each well. To facilitate instant attachment of sporozoites to the host cells, the labtek slides or 24 well plates were spun at 1500 rpm for 4 min. Following the spin, the cultures were placed in a CO_2 incubator. Two hours post addition of sporozoites to cultures; the supernatants were gently removed and replenished with fresh complete DMEM medium. To prevent contamination of the cultures, the medium was changed for every 8 hours until 62h time point. Cultures were fixed at different stages of sporozoite transformation like 12h, 36h and 62 hours. Cells were also trypsinised at these time points for isolation of RNA that was required for gene expression analysis by quantitative real time PCR and for microarrays.

2.2.23 Immunofluorescence assay

To visualize the progressive transformation of the sporozoites occurring inside the HepG2 cells, the cultures were fixed at different time points (12h, 36h and 62h) in formalin solution (Sigma, Cat# HT50-1-2, 10% neutral buffered) for 20 min at room temperature. The cultures were then washed once with 1X PBS (pH 7.4), followed by permeabilisation with chilled methanol and acetone (1:1 ratio) for 20 min at 4°C. The cultures were washed once in 1X PBS and further incubated in 2% BSA solution (SRL, Cat# 0140105) for one hour at 37°C to allow nonspecific blocking. Following this step, the cultures were incubated for 1h at 37°C with an anti-rabbit primary antibody (1:1000 dilution) generated against UIS-4, a parasitophorous vacuolar membrane (PVM). The cultures were washed three times, with 15 minutes duration at 37°C with 1X PBS, followed by PBST (0.1% of Tween 20, Himedia, Cat# MB067) followed by a final wash with 1X PBS. To reveal the immunoreactivity, the cultures were further treated with anti-rabbit secondary antibody (1:300 dilution) conjugated to Alexa Fluor 594 (Life Technologies, Cat# A11062) and DAPI (Sigma, Cat#9564) were diluted in 1% PBS BSA solution and incubated for 1h at 37°C. The cultures were washed for three times with PBS, PBST and PBS identically as described above. After final wash the cultures were air dried and 4-5µl of antifade mounting reagent (Life Technologies, Cat#P36930) was added to the each sample and a coverslip was placed over it. The cover slips were further

sealed with nail polish and preserved in dark. The samples were visualised using a Nikon (Ni-E AR) upright fluorescent microscope.

2.2.24 RNA isolation from *P. berghei* infected HepG2 cultures

The HepG2 cultures were trypsinised as described above in the cell culturing method. The cells were washed once in sterile 1X PBS (pH 7.4), at 4°C by centrifuging at 4000 rpm for 5 min. The pellet was taken for RNA extraction by using a micro to midi RNA isolation kit (Life Technologies, Cat# 12183018A) following manufacturer's instructions. In brief, the pellet was resuspended in 150µl of RNA lysis buffer containing guanidiumthiocyanate and β-mercaptoethanol (SRL, Cat# 1324196) used at a concentration of 10µl/ml. The cells were lysed in this solution by passing them through an insulin syringe 10-15 times. To this lysate, an equal volume (150µl) of 70% ethanol (Hayman, Cat#F203408) was added and vortex briefly. The contents were transferred to a RNA spin column and centrifuged at 8000 rpm for 1 minute at room temperature. The RNA spin column was washed once with 500µl of wash buffer I at 8000 rpm followed by two washes (600µl each) with wash buffer II at 8000 rpm. The RNA spin column was air dried by spinning at 8000 rpm for 2 minutes. The total RNA was recovered by placing 25µl of RNAse free water at the center of the spin column and centrifuging at 12,000 rpm. The concentration of the eluted RNA was quantified on a nanodrop spectrophotometer.

2.2.25 RNA isolation from all *P. berghei* life cycle stages to study expression of *Pb SSPELD*

To study expression of *Pb SSPELD*, RNA was obtained from all life cycle stages. In brief, mice were infected with WT *P. berghei* asexual blood stages and after obtaining 10-12% parasitemia, the blood was harvested by cardiac puncture. The blood was lysed using 0.5% saponin and the pelleted at 15,000 rpm at 4°C. Following 3-4 washes with sterile RNAse free PBS, the pellet was used for RNA extraction. The midguts and salivary glands were obtained on D14 and on D18 respectively following dissection of infected *Anopheles stephensi* mosquitoes. Different stages of developing liver stages or EEFs were harvested from HepG2 culture, following trypsinisation. The cells were washed 3-4 times with sterile RNAse free PBS and pellet was used for RNA extraction. The samples obtained from different stages were subjected to RNA extraction using a micro to midi RNA isolation kit as described above.

2.2.26 cDNA synthesis

For cDNA synthesis, 2µg of RNA was reverse transcribed in a reaction mixture containing 1X PCR buffer, 2.5mM dNTPs, 5mM $MgCl_2$, 1.5 units RNAse inhibitor, 2.5 mM random hexamers and 1.5 units reverse transcriptase. All reagents required for synthesis of cDNA were procured from Applied Biosystems. The thermal cycling conditions were 25°C for 10 min, 42°C for 20 min and 98°C for 5 min.

2.2.27 Expression analysis of *Pb SSPELD* by quantitative real time PCR

Pb SSPELD gene expression was quantified by absolute method of real time PCR. Towards this end, a 120 bp fragment of *Pb SSPELD* was generated using forward primer (RT FP-5'TATTTATTACCCTGCGGATA3' and reverse primer (RT RP-5'ATACTCAACGTGATATTTCCA3') and cloned into a pTZ57R/T vector. The cloned was expanded by transformation and following purification of the plasmid by mini-prep method, a log dilution of the plasmid was generated to be used as gene specific standard with a dynamic range that covered from 10^2 copies/µl to 10^8 copies/µl. Similarly, a standard was generated for *Pb 18S rRNA* that was used as internal control. For performing real time PCR, cDNA obtained from various stages of *P. berghei* was used as template that was added to SYBR green master mix (Biorad) along with 0.25µM concentration of forward and reverse primer corresponding to either *Pb SSPELD* or *Pb 18S rRNA*. The samples were run alongside with both *Pb SSPELD* or*Pb 18S rRNA* standards. The data normalisation was done by obtaining ratio of *Pb SSPELD*/*Pb 18S rRNA* for each sample.

2.2.28 Microarray of *P. berghei*

For microarray analysis**,** an Agilent Custom *Plasmodium berghei* gene expression microarray slide having 4X44k format designed by Genotypic Technology Private Limited was used that comprised of a total number of 43803 features including 5155 numbers of probes, and 1417 Agilent control features. The array covered 5106 number of transcripts sourced from Plasmodb database.

2.2.29 RNA Extraction and RNA Quality Control

RNA concentration and purity was determined at an optical density ratio of 260/280 using the Nanodrop® ND-1000 spectrophotometer (Nanodrop Technologies, Wilmington,

DE) and the integrity of total RNA was verified on an Agilent 2100 Bioanalyzer using the RNA 6000 Nano Lab Chip (Agilent Technologies).

2.2.30 Labeling and microarray hybridization

The samples for Gene expression were labeled using Agilent Quick-Amp labeling Kit (p/n5190-0442). 500ng each of total RNA were reverse transcribed at 40°C using oligodT primer tagged to a T7 polymerase promoter and converted to double stranded cDNA. Synthesized double stranded cDNA were used as template for cRNA generation. cRNA was generated by in vitro transcription and the dye Cy3 CTP(Agilent) was incorporated during this step. The cDNA synthesis and in vitro transcription steps were carried out at 40°C. Labeled cRNA was cleaned up using QiagenRNeasy columns (Qiagen, Cat No: 74106) and quality assessed for yields and specific activity using the Nanodrop ND-1000.

2.2.31 Hybridization and Scanning

1650ng of labeled cRNA sample were fragmented at 60°C and hybridized on to an Agilent Custom *Plasmodium berghei* Gene Expression Microarray 4x44k designed by Genotypic Technology Private Limited. (AMADID No: 067226). Fragmentation of labeled cRNA and hybridization were done using the gene expression hybridization kit of (Agilent Technologies, In situ Hybridization kit, Part Number 5190-0404). Hybridization was carried out in Agilent's surehyb chambers at 65º C for 16 hours. The hybridized slides were washed using Agilent gene expression wash buffers (Agilent Technologies, Part Number 5188-5327) and scanned using the Agilent Microarray Scanner (Agilent Technologies, Part Number G2600D) at 5 micron resolution.

2.2.32 Feature Extraction: Image Analysis

Data extraction from Images was done using Agilent Feature Extraction software.

2.2.33 Microarray Data Analysis

Feature extracted raw data was analyzed using Agilent GeneSpring GX software. Normalization of the data was done in GeneSpring GX using the 75th percentile shift method. Percentile shift normalization is a global normalization, where the locations of all the spot intensities in an array are adjusted. This normalization takes each column in an experiment independently, and computes the n^{th} percentile of the expression values for this array, across all spots (where n has a range from 0-100 and n=75 is the median). It subtracts

this value from the expression value of each entity and fold change values were obtained by comparing test samples with respect to specific control samples. Significant genes up regulated fold> 0.8 (logbase2) and down regulated <-0.8 (logbase2) in the test samples with respect to control sample were identified. Statistical student T-test p-value among the replicates was calculated based on volcano Plot Algorithm. Differentially regulated genes were clustered using hierarchical clustering based on Pearson coefficient correlation algorithm to identify significant gene expression patterns**.**Genes were classified based on functional category and pathways using Biological Analysis tool DAVID (http://david.abcc.ncifcrf.gov/)

2.2.34 Analysis of co-relates of protection following immunization with *Pb SSPELD* KO parasites

Immunisation of mice

Six to eight weeks old C57BL/6 mice were immunized twice with $2X10^4$ *Pb* SSPELD KO sporozoites. The duration between priming and boosting was 14 days. Ten days after boosting, a group of 6 mice were challenged with $2X10^4$ *P. berghei* WT sporozoites and monitored for the prepatent period, by performing Giemsa staining of blood smears from D3 post infection.

For analysis of correlates of T cell mediated protection, whole spleens were removed from immunized and naive mice and a splenocyte suspension was made using frosted glass slides. The cell suspension was filtered through 70µm nylon filter into 50ml tube. One hundred micro liters of purified splenocyte suspension was placed in 1.5 ml eppendorf tube and lysed by adding 1ml of RBC lysis buffer and the cells were centrifuged at 6000 rpm at 4 °C for 5 min. Supernatant was discarded and pellet was washed with 1x PBS two times at 6000 rpm at 4 °C for 5 min. Splenocytes were resuspended in 100µl of 1x PBS. One micro litre of each anti-CD4 (BD, Cat #553650), anti-CD8 (BD, Cat#553032) and anti-CD3e (BD, Cat#561108) antibodies were added to the splenocytes and incubated on ice for 30 min in dark. The CD3e antibody was added to differentiate between T cells and other cell types in splenocyte suspension. From the gated CD3 positive T cells, we estimated the percentage of $CD4^+$ and $CD8^+$T cells. Following staining, the splenocytes were washed at 4000 rpm at 4 °C for 6 min. The supernatant was discarded and splenocytes were resuspended in 300µl of 1X PBS and subjected to FACS analysis using BD FACS Aria.

To determine sporozoite antibody titers, a small volume of immune sera was collected from a group of 6 mice before challenge. The sera were pooled and sporozoite IFA was

performed. The dilutions of the pooled immune sera were made in the range of 1:50 to 1: 100,000. The dilutions of the immune sera were made in 96 well plates. Sporozoites obtained from dissected salivary glands were spotted on IFA slides. Each well was spotted with approximately $1X10^4$ sporozoites.

2.2.35 Generation of *Pb SSPELD mCherry* transgenic parasites for studying the localization of SSPLED

In order to reveal the promoter activity of *Pb SSPELD* and investigate its localization across different parasite stages, we generated a *mCherry* transgenic of *Pb SSPELD*. In brief, following strategy was employed for generating the mCherry targeting construct. *mCherry* open reading frame was PCR amplified using forward primer, FP-ATACTCGAGATGGTGAGCAAGGGCGAG (Xho1) and reverse primer, RP-ACCACTAGTTTACTTGTACAGCTCGTCC (Spe1) using vector PL0017 as a template (a kind gift from the laboratory of Prof. Volker Heussler's Lab, Germany). The PCR product was sequenced and confirmed. The mCherry ORF with restriction sites Xho1 and Spe1 was cloned in pTZ57R/T vector. A 3' regulatory sequence of HSP70 was PCR amplified using forward primer, FP- TATACTAGTTTATTGTTCTGTACTTCTTTT (Spe1) and reverse primer, RP-ACTCCCGGGAAAATACCAATAATACCGTTT (Xma1) from pBC-GFP-hDHFR vector (kind gift from Dr. Robert Menard, Pasteur Institute, France) and following sequence confirmation, this fragment was cloned into the TA vector in tandem to mCherry ORF using restriction sites Spe1 and Sma1/Xma1. The mCherry ORF along with HSP70 3' UTR was released from TA vector and cloned into pBC-GFP-hDHFR vector using Xho1 and Xma1 replacing GFP cassette. The vector was named pBC-mCherry-hDHFR vector and used for localization of *Pb* SSPELD. A 614bp of *Pb* SSPELD ORF was amplified using forward primer (FP1-5'ATAGGGCCCATGACCAATCAAGTGTTAGA3'), Apa1 restriction site underlined and reverse primer RP1-5'AGTCTCGAGAGGATAAAATATAGCAGTAGG3', Xho1 site underlined. The sequence was confirmed and cloned into pBC-mCherry-hDHFR vector using Apa1 and Xho1 and the sequence was confirmed. To facilitate double crossover, 3'UTR of *Pb* SSPELD was PCR amplified using forward primer (FP2-5' ATAGCGGCCGCAAGCAAACAATAAACACTTA3') and reverse primer (RP2-5'GTAGGCGCGCCTGCATTATGAAACTGTCA3') and cloned into pBC-mCherry-hDHFR vector using Not1 and Asc1 restriction enzymes. Following sequence confirmation, *Pb SSPELD* localization plasmid was prepared in large scale and digested with Apa1 and Asc1 restriction enzymes. The digested construct was gel extracted and used for parasite

transfection. After obtaining successful transfectants, the site specific integration was confirmed using a set of diagnostic primers- forward primer, FP3- 5'TAACGTTATTTTATTTTTCTTGT3' and reverse primer (RP3- 5'AAAGACATGAAGATTAATAAG3') that gave differential product sizes of 820bp in *mCherry* transgenics and 3960bp in WT parasites, that also formed the basis for confirming the clonal lines.

2.2.36 Immuno Fluorescence Assay to confirm the sporozoite membrane localization of *Pb* SSPELD

To show the localization of *Pb* SSPELD on sporozoite plasma membrane, the dissected salivary gland sporozoites were spotted on IFA slides and air dried briefly. The parasites were fixed in 4% Paraformaldehyde for 15 min at 4°C, followed by nonspecific blocking in 3% BSA made in PBS, for one hour at 37°C. Monoclonal antibody 3D11 [146] specific for the *Plasmodium berghei* CS repeats was used to stain the sporozoite plasma membrane for one hour at 37°C. Following three washes with PBS, PBST (0.5% Tween), and PBS, the parasites were stained with antimouse secondary antibody conjugated to Alexafluor 488 (Cat#A11001) for one hour at 37°C. After washing with PBS, PBST (0.5% Tween), and PBS briefly, 20 minutes each, the sample were mounted and visualized using Nikon (Ni-E AR) upright fluorescent microscope.

2.3 Results

2.3.1 *Pb SSPELD* is conserved amongst other *Plasmodium* species

Alignment of amino acid sequence of *Pb* SSPELD from various rodent and human species revealed nearly 33% identity in the sequence (Fig 7).

```
pvivSal1          ------MAPLVVDTLDCVYLRPQPTST--YYYPLGMTWKYVVSSKSTGCFGTTKKYTLTP 52
pknoH             ------MSPLVVDTYDCVYLRPQPART--YYYPLGMTWKYVVSSKSTGCFGTTKKYTLTP 52
pberANKA          ------MTNQVLETYECSILKPHPVNT--IYYPADITWKYVLSSKPSGCFGSTKKYVAVP 52
pyoeyoelii17X     ------MSNQVLETYECSLLKPQLVNT--LYYPADITWKYVLSSKPSGCFGSTKKYVAVP 52
pchachabaudi      ------MTNQMLETYECSLLRPQPFST--LYYPANITWKYVLNSKPSGCFGSTQKYVAVP 52
pfal3D7           MCSTYSVEPLVYDSYEYVYLKPKKAGTSAVYYPLNISWKYVAKKRSVGCFGSRKKYTLTP 60
                        :   : :: :   *:*:   *   *** .::**** ..:. ****: :**. .*

pvivSal1          ET--YYYPYYYYYVYYTPAESPIVCLSSKKVIKDKKKKKDEDKQELKDESSKEGSEKEEG 110
pknoH             ET--YYYPYYYYYVYYTPVESSTVCSSNKKVIKDKKKKKDEDKKELKDESSKEGSEKEEE 110
pberANKA          ES--YSYPYYYYYVYYRPYTLGNITLSIKNADKSKKKVNESNDQEKKEESNDE-----NG 105
pyoeyoelii17X     ETYTYSYPYYYYYVYYRPYVLGNVTLSIKNADQSKKKVNELNNQEKKEEPSDE-----NG 107
pchachabaudi      ET--YSYPYYYHYVYYRPYPLANITLSIKHEDKNKKKVNELNNQEKKEELNDE-----DE 105
pfal3D7           EA--YYYPYYYYYVYYYPSAARLVRTTRK-----EKVLKENNNKESEDENKQD------N 107
                  *:  * *****:**** *     :  : *     :*  :: :.:* ::* ..:

pvivSal1          SKKSSGKKKYEYVEREKVVRTYLPVVEPFYY-TSSYYVPR-AILFP 154
pknoH             LKKSSGKKKNEYAEGERVVRTYLPVVEPFYY-TSSYYVPR-AILFP 154
pberANKA          TKTS--KKNDECNDRENNTKKYVSVLTPPYY-IGSLFYPT-AIFYP 147
pyoeyoelii17X     SKTS--KKNDECNDRENNTKKYVSILTPPYY-IGSLFYPT-AIVFP 149
pchachabaudi      SKTS--KKNNECNDKENNTKKYVSVVSPPYY-IGSLYYPT-AIFYP 147
pfal3D7           VGTE--KKECDCSEKEKYIPTYVPLTESYYFPPSALYVPHYSVLVP 151
                    ..  **: :  : *.   .*:.:  . *:  .: : *  ::. *
```

Fig 7. Amino acid sequence alignment of orthologues of *Pb SSPELD* amongst *Plasmodium* species. PvivSal1: *P. vivax*, pknoH: *P. knowlesii*, pber: *P. berghei*, pyoeyoelli: *P. yoelli*, pchaubchaudi: *P. chaubadi*, pfal3D7: *P. falciparum*

2.3.2 Gene expression analysis by quantitative real time PCR revealed maximal expression of *Pb SSPELD* in salivary gland sporozoite stages

In order to quantify the gene expression of *Pb SSPELD*, gene specific standards were generated for *Pb SSPELD* and *Pb 18S rRNA*. The cDNA samples generated from various life cycle stages were run alongside with standards. At the end of PCR, the gene expression was expressed as absolute copy numbers of either *Pb SSPELD* or *Pb18S rRNA*. Data normalization was done by obtaining a ratio of *Pb SSPELD* copy numbers versus *Pb 18S rRNA* copy number. The normalized data revealed highest expression of *Pb SSPELD* in salivary gland sporozoite stages (Fig 8)

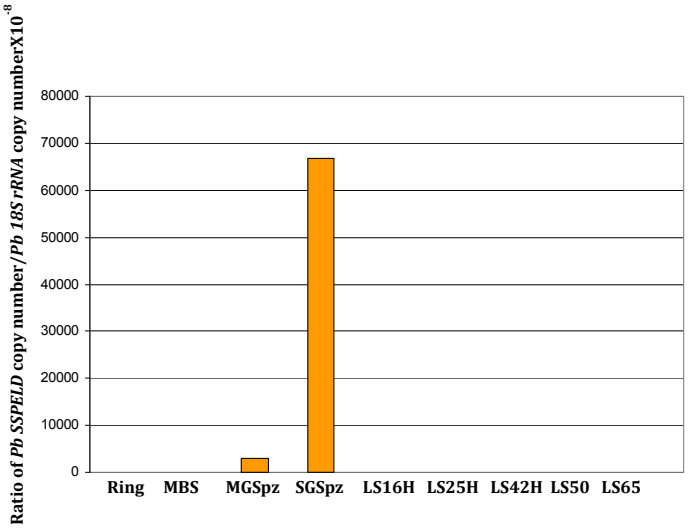

Fig 8. Normalized gene expression for *Pb SSPELD* across *Plasmodium berghie* life cycle stages. Analysis of gene expression by quantitative real time PCR revealed highest gene expression in the salivary gland sporozoites (SG Spz) followed by day14 midgut sporozoites (MG Spz). The normalized data was expressed as a ratio of absolute copy numbers of *Pb SSPELD* versus *Pb 18S rRNA* (internal control) for each stage of the *Plasmodium* life cycle. Ring: Ring stages, MBS: mixed blood stages, MG Spz: Midgut sporozoites, SGSpz: salivary gland sporozoites, LS16H: Liver stage 16h, LS25H: Liver stage 25h, LS42H: Liver stage 42h, LS50H: Liver stage 50h, LS65H: Liver stage 65h.

2.3.3 Successful replacement of *Pb SSPELD* locus by GFP-hDHFR cassette by double homologous recombination method

The organisation of the *Pb SSPELD* locus is shown Fig 9A. To achieve a successful double homologous recombination for replacement of the *Pb SSPELD* locus with *GFP-hDHFR* cassette, the 5' fragment and 3' fragments were cloned on either ends of the *GFP-hDHFR* cassette (Fig 9B). The organization of the genomic locus of *Pb SSPELD* following its replacement is shown in Fig 9C. The 5' and 3' fragments of *Pb SSPELD* amplified by PCR and resolved on 1% agarose gel are shown in Fig 9D and 9E. Following cloning of these fragments into the targeting vector, these fragments were further reconfirmed by release of the 5' fragment by using restriction enzymes Xho1 and Cla1, the 3' fragment by using restriction enzymes Not1 and Asc1, and targeting vector was release from the plasmid back bone using restriction enzymes Xho1 and Asc 1 (Fig 9F). The linearized *Pb SSPELD* KO targeting construct was electroporated into *P. berghei ANKA* schizonts using U-033 program in Amaxa nucleofector device and injected intravenously into mice. The mice were kept under pyrimetamine drug pressure and parasitemia was monitored daily by Giemsa stained blood smears. Genomic DNA was isolated from drug resistant parasites and site specific 5' and 3' integration was confirmed by primers designed at beyond sites of recombination, that indicated correct integration (Fig 9G). Limiting dilution was performed to obtain clonal

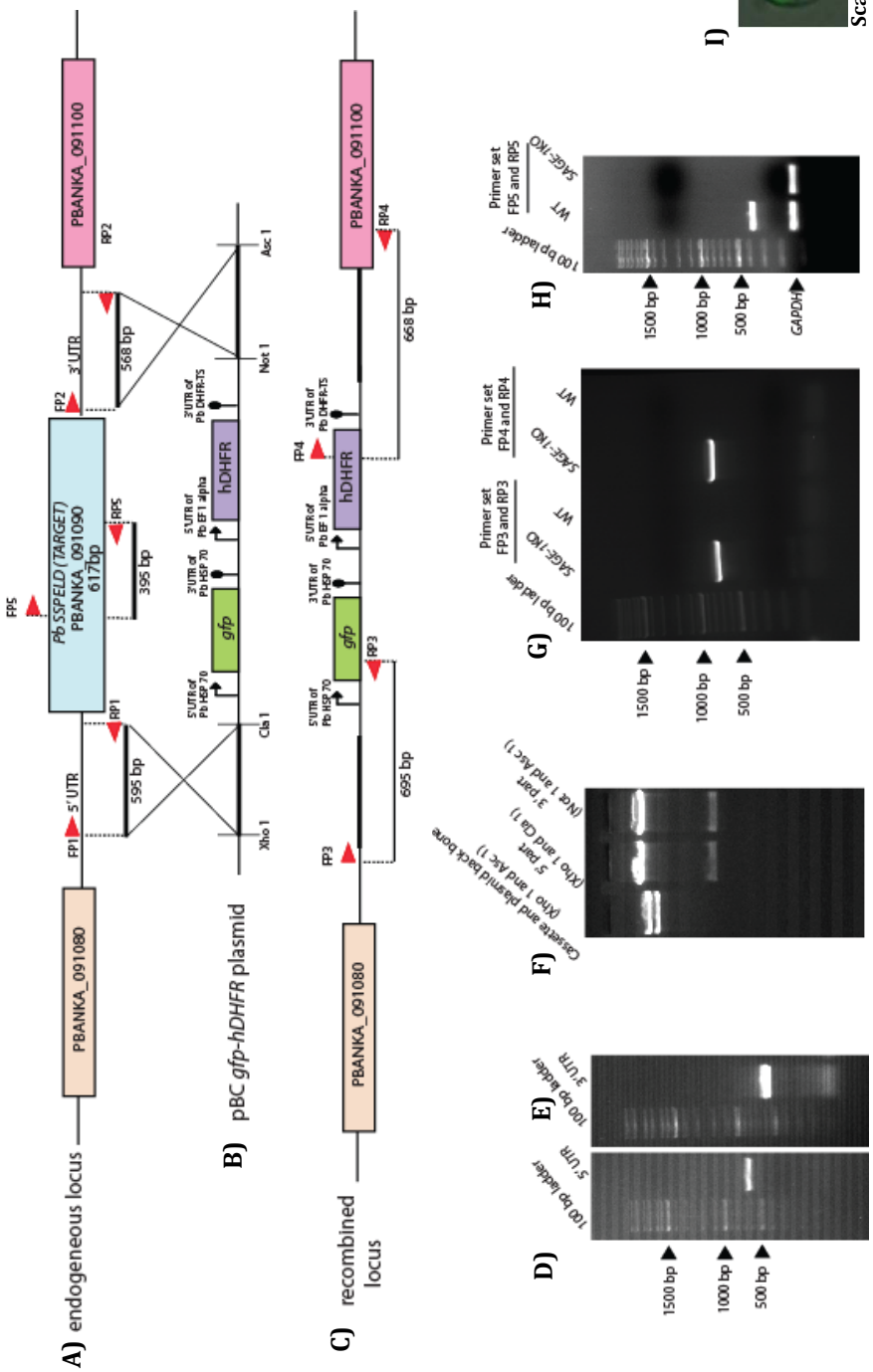

Fig 9. Generation of *Pb SSPELD* KO parasite line. A) Genomic locus of *Pb SSPELD* (PBANKA_091090) showing 5' and 3' UTRs. B) Elements of the targeting vector showing pBC-GFP-hDHFR. A 595 bp 5' fragment of *Pb SSEPLD* was cloned in XhoI/ClaI site of the targeting vector. A 568 bp of 3' fragment was cloned into NotI/AscI site of the targeting vector. C) Recombined locus following successful double cross over recombination resulting in replacement of target gene, *Pb SSPELD* by GFP-DHFR cassette. A 1% agarose gel showing the PCR product of : D) 5' and E) 3' UTRs. The 5' UTR fragment was amplified with primers FP1 and RP1. The 3' UTR fragment was amplified with primers FP2 and RP2. F) Release of targeting cassette (5' UTR fragment+GFP-DHFR cassette+3' UTR fragment) and vector backbone using restriction enzymes XhoI/AscI. Release of 5' UTR fragment from transfection vector using restriction enzymes XhoI/ClaI and release of 3'UTR fragment from transfection vector using restriction enzymes NotI/AscI. G) Diagnostic PCR using primers within the targeting cassette and beyond sites of recombination revealing the correct site specific integration. A PCR product with primers FP3 and RP3 indicated a correct 5' integration and a PCR product with primers FP4 and RP4 indicated a correct 3' integration. H) Genomic DNA isolated from cloned *Pb SSPELD* KO parasites does not amplify a PCR product from the ORF whereas WT parasites amplify a product of 527bp with primer set FP5 and RP5 H) A merged DIC image showing a GFP expressing *Pb SSPELD* KO parasite inside RBC.

population of *Pb SSPELD* KO parasites. *Pb SSPELD* ORF specific primers were used to confirm the deletion of *Pb SSPELD* locus, that gave a PCR product only with WT *P. berghei* genomic DNA and not with *Pb SSPELD* KO genomic DNA (Fig 9H). The cloned line of *Pb SSPELD* KO expressed GFP constitutively (Fig 9I).

2.3.4 *Pb SSPELD* is not essential for asexual blood stages

To monitor, if *Pb SSPELD* depletion affected asexual blood stage propagation, two groups of BALB/c mice (3 mice per group) were intravenously injected with $1X10^3$ iRBC (infected RBC) of either WT or *Pb SSPELD* KO and the asexual blood stage replication was monitored for 7 days by making Giemsa stained blood smears. The identical propagation of *Pb SSPELD* KO as that of WT parasites and presence of all stages of asexual forms in *Pb SSPELD* KO revealed its non-essential role in asexual blood stages (Fig 10).

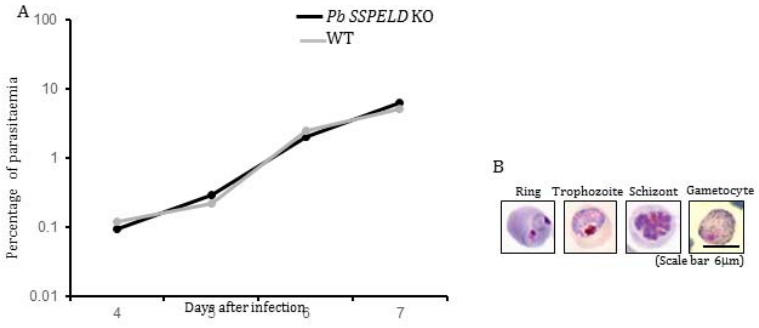

Fig 10. *Pb SSPELD* KO asexual parasites propagate identically as WT parasites. A) $1X10^3$ infected RBC of either WT or *Pb SSPELD* KO were intravenously injected in two groups of mouse (3 mouse/group) and monitored for propagation of the parasites daily for 7 days by making Giemsa stained smears. B) Representative pictures showing asexual blood stages obtained from Rathore et al (147].

2.3.5 *Pb SSPELD* is not essential for mosquito stages

Transmission of *Pb SSPELD* KO parasites to mosquitoes resulted in formation of oocysts, whose numbers were comparable to the oocysts derived from the WT parasites (Fig. 11 A and B). The sporulation pattern inside oocyst (Fig 11 C and D) and the ability of the egressed sporozoites to reach salivary gland (Fig 11 E and F) also were comparable to that of WT parasites suggesting that *Pb SSPELD* KO manifested no defect in the mosquito stages of *P. berghei.*

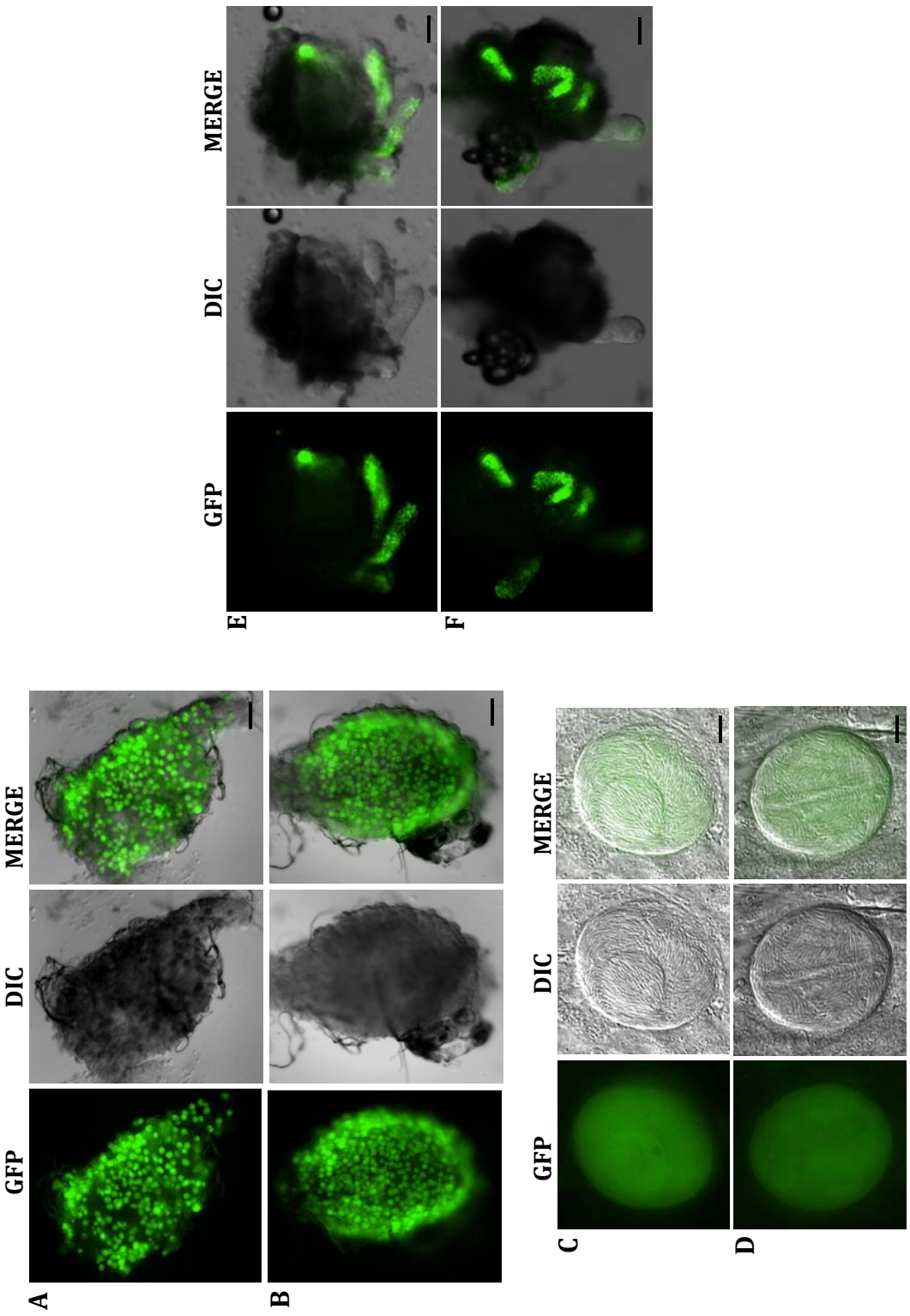

Fig 11. Mosquito stages of *Pb SSPELD* KO do not show any defect in oocyst development, sporulation and its ability to reach salivary gland. Malaria was transmitted to female *Anopheles* mosquitoes from mouse harboring gametocyte stages of either WT or *Pb SSPELD* KO. Midguts showing oocyst derived from WT parasites (A) and *Pb SSPELD* KO parasites (B), scale bar 200µm. A single magnified oocyst from WT (C) and *Pb SSPELD* KO (D), scale bar 10µm. Dissected salivary glands showing similar loads of WT sporozoites (E) and *Pb SSPELD* KO sporozoites (F), scale bar 10µm.

2.3.6 *Pb SSPELD* sporozoites fail to initiate blood stage infection when malaria is transmitted though natural mosquito bite

Inoculation of *Pb SSPELD* KO sporozoites through natural mosquito bite did not initiate blood stage infection in three independent experiments (Fig 12, Table A). All blood meal positive mosquitoes that were used for transmission were dissected and majority of them had high loads of sporozoites in the salivary glands. Thus lack of break through infection was not due to absence of salivary gland sporozoites in the batch of mosquitoes used for transmission experiments. However high doses ($2X10^4$) of sporozoites delivered through intravenously route led to occasional break through infection with delayed pre patent period of D8/9 (Fig 13 and Table B Table)

Fig 12. Transmission of *Pb SSPELD* KO sporozoites to mouse by natural mosquito bite does not induce blood stage infection. A) 12-15 mosquitoes infected with WT or *Pb SSPEDL* KO were placed in a small container and covered with mosquito net. Anesthesized C57BL/6 mice were placed on the top of cage and the mosquitoes were allowed to obtain a blood meal for 15 minutes. During the process of uptake of blood meal, salivary gland sporozoites are injected into the dermis of the mouse leading to successful malaria transmission to mouse. All blood meal positive mosquitoes following bite experiment were dissected to collect salivary glands to confirm the presence of GFP expressing sporozoites (WT or ***Pb SSPELD* KO**) under fluorescent microscope.

Table A

Parasite Strain	Experiment No.	Number of animals used for bite	Number of animals positive for blood stage infection	*Pre-patent period
WT	I	3	3/3	D4
	II	3	3/3	D4
***Pb SSPELD* KO**	I	3	0/3	ND
	II	3	0/3	ND
	III	2	0/2	ND
	IV	2	0/2	ND

Table A. Showing the kinetics of the mosquito bite experiment, the details of number of experiments performed, number of animals used in each experiment, the number of animals that became positive for blood stage infection and the pre patent period (* defined as the time required for the appearance of blood stage infection following infection with sporozoites). ND: not detected.

Fig 13. High dose (2X10^4) of *Pb SSPELD* KO sporozoites delivered through intravenous (i.v.,) route induces occasional break through infection in mice.

Table B

Parasite Strain	Experiment No.	Number of animals used for intravenous injection	Number of animals positive for blood stage infection	*Pre-patent period
WT	I	3	3/3	D4
	II	3	3/3	D4
***Pb SSPELD* KO**	I	4	1♣/4	D9
	II	4	0/4	ND
	III	3	0/3	ND
	IV	2	0/2	ND

Table B. Showing the kinetics of i,v., experiment, the details of number of experiments performed, number of animals used in each experiment, the number of animals that became positive for blood stage infection and the pre patent period (*defined as the time required for the appearance of blood stage infection following infection with sporozoites). ND: not detected. ♣The occasional break through infection in mouse following *Pb SSPELD* sporozoite injection gave a delayed pre patent period

2.3.7 *Pb SSPELD* exhibit growth arrest at 36 hour time point

Pb SSPELD knockout sporozoites were indistinguishable in growth at 12 h (Fig 14 D) as compared to WT EEFs (Fig 14 A). However, a dramatic arrest in the growth was observed at 36h (Fig 14 E) and 62h (Fig 14 F) time points in *Pb SSPELD* KO as compared to the same time points in WT EEFs (Fig 14 B and C). Measurement of parasite area (WT and *Pb SSPELD* KO) from 15 random EEFs at 62h time point revealed difference that was statistically significant (Fig 15 and Table C).

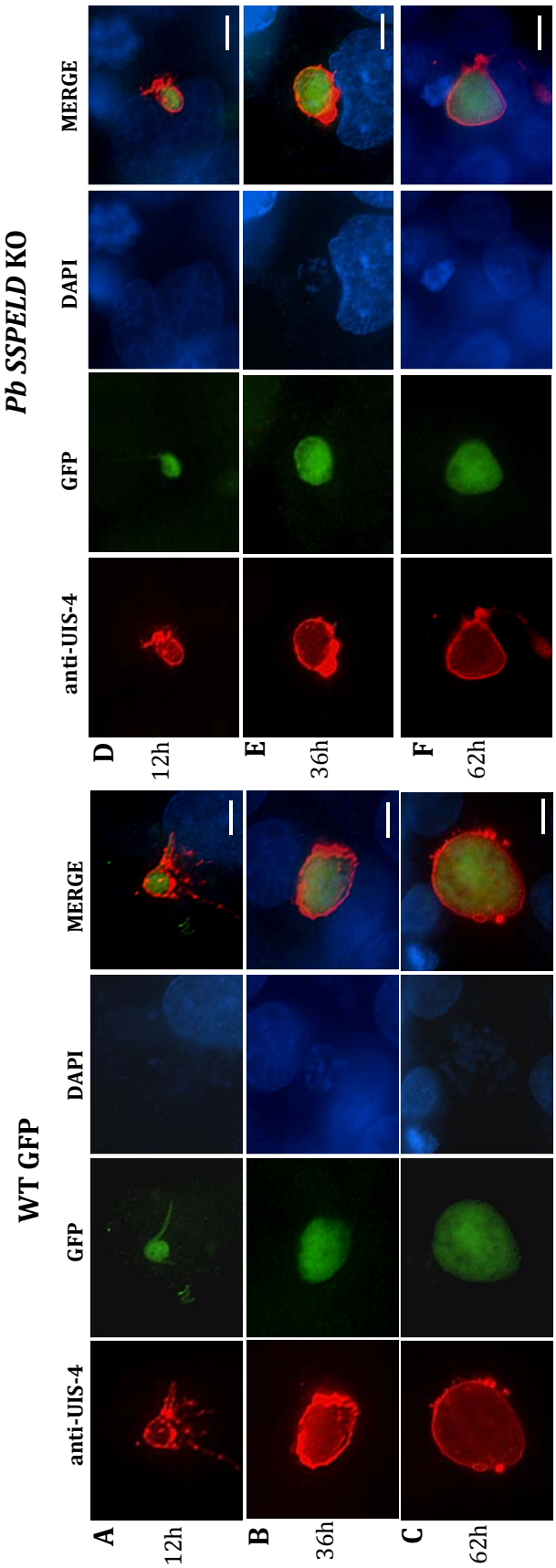

Fig 14. The Exo Erythrocytic Forms (EEF's) of *Pb SSPELD* show arrested growth at 36h and 62h when compared to WT liver stages. Salivary gland sporozoites were isolated by dissection and $2X10^4$ sporozoites of either WT or *Pb SSPELD* KO were added to HepG2 cultures, that supported the complete development of the *P. berghei* EEF's. The cultures were fixed at different time points: 12h, 36h and 62h. The cultures were stained with anti-UIS-4 antibody that reacts with the parasitophorous vacuolar membrane (PVM) of EEF and DAPI (4', 6' diamidino-2 phenyl indole) for visualization of HepG2 and parasite nuclei. EEF's derived from *Pb SSPELD* KO sporozoites at 12h (D) were comparable to that of the WT EEF's (A), where as the 36h (E) and 62h (F) EEF's derived from *Pb SSPELD* KO showed growth defect as compared to the corresponding WT EEF's at 36h (B) and 62h (C).Scale bar 10μm.

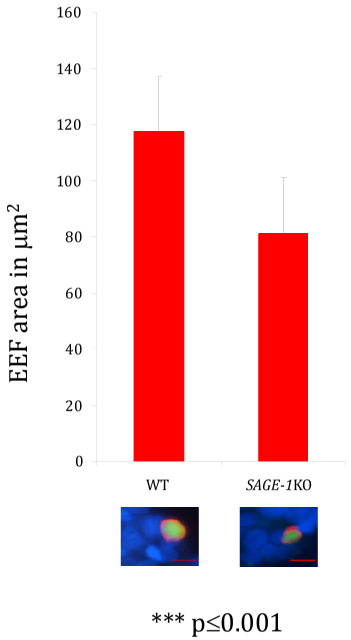

Table C

S.No.	WT	*Pb SSPELD* KO
1	63.53	132.78
2	115.73	94.12
3	104.7	168.61
4	102.71	134.27
5	85.09	131.7
6	49.38	102.57
7	88.63	89.34
8	104.83	137.3
9	72.34	124.5
10	62.96	84.17
11	55.64	80.76
12	63.37	143.3
13	72.82	76.87
14	75.07	78.56
15	98.12	144.47
Average area in microns	114.888	81.03733

Fig 15. Measurement of EEF area at 62h reveals arrested growth in *Pb SSPELD* KO. A) Average area of the 62H EEF is indicated in the bar graph. P value < 0.005. B) and C) are representative pictures of EEF's derived from WT and *Pb SSPELD* KO respectively.
Table C. Values corresponding to the area measurement of 15 individual EEF's derived from WT and *Pb SSPELD* KO.

2.3.8 Successful replacement of *Pb SSPELD* 3' UTR with mCherry -hDHFR cassette by double homologous recombination method

The organisation of the *Pb SSPELD* locus is shown Fig 16 A. To achieve a successful double homologous recombination resulting in placing mCherry cassette in frame with the *Pb SSPELD* locus, the complete ORF of *Pb* SSPELD and the 3' UTR were cloned respectively on either ends of the mCherry-hDHFR vector (Fig 16B). The organization of the genomic locus of *Pb SSPELD* following successful double cross over recombination is shown in Fig 16C. The *Pb* SSPELD ORF and and 3' fragments were amplified by PCR and resolved on 1% agarose gel are shown in Fig 16D and E. Following cloning of these fragments into the targeting vector, these fragments were further reconfirmed by release of the 5' fragment by using restriction enzymes Apa1 and Xho1, and the 3' fragment by using restriction enzymes Not1 and Asc1 (Fig 16 F). The targeting vector was released from the plasmid back bone using restriction enzymes Apa1 and Asc 1 (Fig 16G). The linearized *Pb SSPELD* KO targeting construct was electroporated into *P. berghei ANKA* schizonts using U-033 program in Amaxanucleofector device and injected intravenously into mice. The mice were kept under pyrimetamine drug pressure and parasitemia was monitored daily by Giemsa stained blood smears. Genomic DNA was isolated from drug resistant parasites and after obtaining a clonal line, site specific integration was confirmed by using a set of diagnostic primers that amplified different products in WT and *Pb SSPELD mCherry* transgenics (Fig 16 H).

2.3.9 *Pb SSPELD mCherry* transgenics express reporter in oocyst, salivary gland sporozoite and EEF stage

To study the mCherry expression and localization of *Pb SSPELD,* the cloned *Pb SSPELD mCherry* trangenics were infected to mouse and analysed for the reporter expression. We observed no mCherry expression in the asexual stages. However, the mosquito stages ie., the D14 sporulating oocyst (Fig 17 A and B) and D18-21 salivary glands sporozoites (Fig 18 and 19) showed expression of the reporter. Deconvulted images of intact salivary glands harbouring sporozoites revealed the localization of mCherry to the sporozoite plasma membrane (Fig 20). This was further confirmed by the co-localisation of mCherry with CSP, a major sporozoite surface protein (Fig 21 A, B, C and D). To monitor if mCherry continued to express in the liver stages, sporozoites were added to HepG2 cultures that facilitated their transformation into EEFs. Observation of 36h fixed culture revealed the localization of the mCherry to the PVM membrane of the EEF (Fig 21 E, F and G).

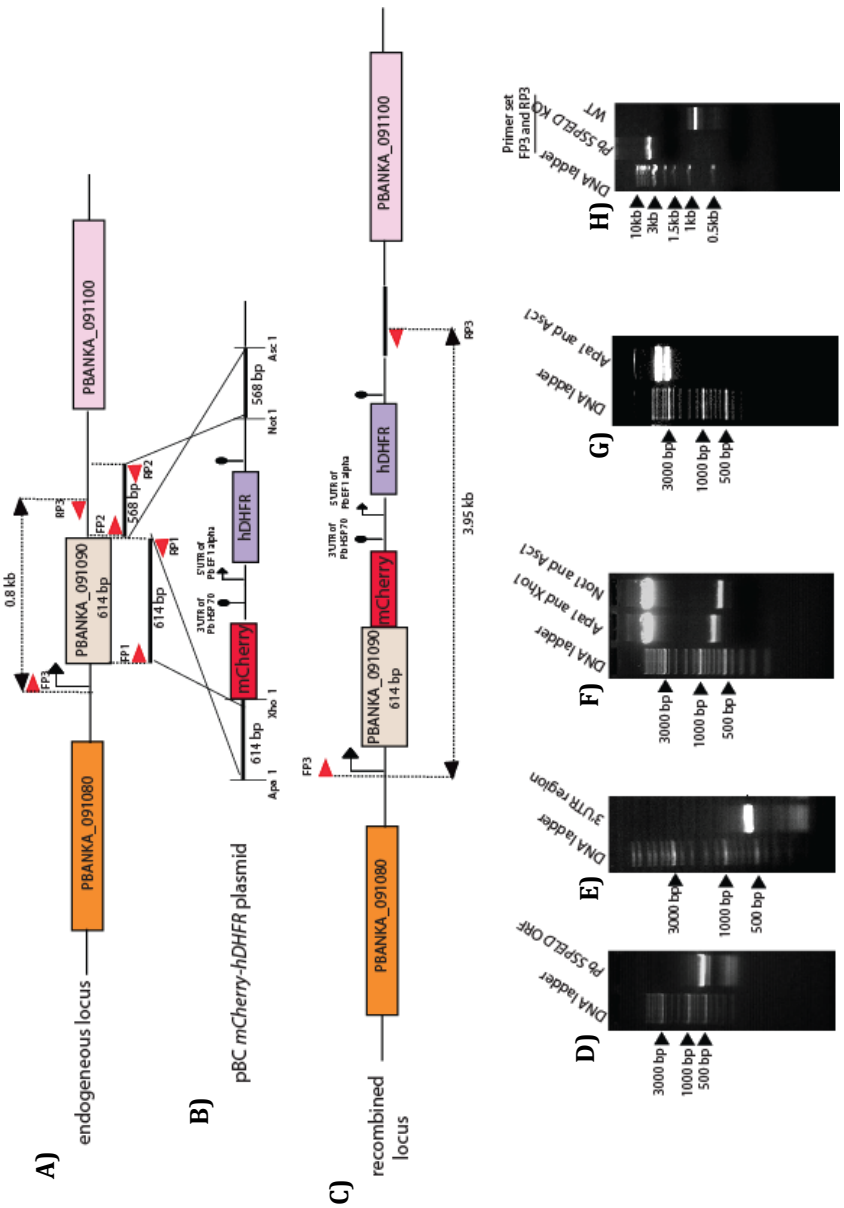

Fig 16. Generation of Pb SSPELD mCherry transgenic. A) Genomic locus of *Pb SSPELD* (PBANKA_091090) showing 5' and 3' UTRs. B) Elements of the targeting vector showing pBC-mCherry-hDHFR. The complete ORF (without stop codon) of *Pb SSEPLD* was cloned in Apa 1/Xho1 site of the targeting vector. A 568 bp of 3' fragment was cloned into NotI/AscI site of the targeting vector. C) Recombined locus following successful double cross over recombination resulting in placing mCherry ORF in tandem to the *Pb SSPELD*. A 1% agarose gel showing the PCR product of : D) *Pb SSPELD* ORF and E) 3' UTRs. The *Pb SSPELD* ORF was amplified with primers FP1 and RP1. The 3' UTR fragment was amplified with primers FP2 and RP2. F) Release of 5' UTR fragment from transfection vector using restriction enzymes Apa1/Xho1 and release of 3'UTR fragment from transfection vector using restriction enzymes NotI/AscI. G) Release of targeting cassette (Pb SSPELD +mCherry-hDHFR cassette+3' UTR fragment) and vector backbone using restriction enzymes ApaI/AscI. H) Diagnostic primers FP3 and RP3 beyond the *Pb SSPELD* ORF amplifies differential PCR product from WT and Pb SSPELD mCherry transgenic indicating a correct site specific integration,

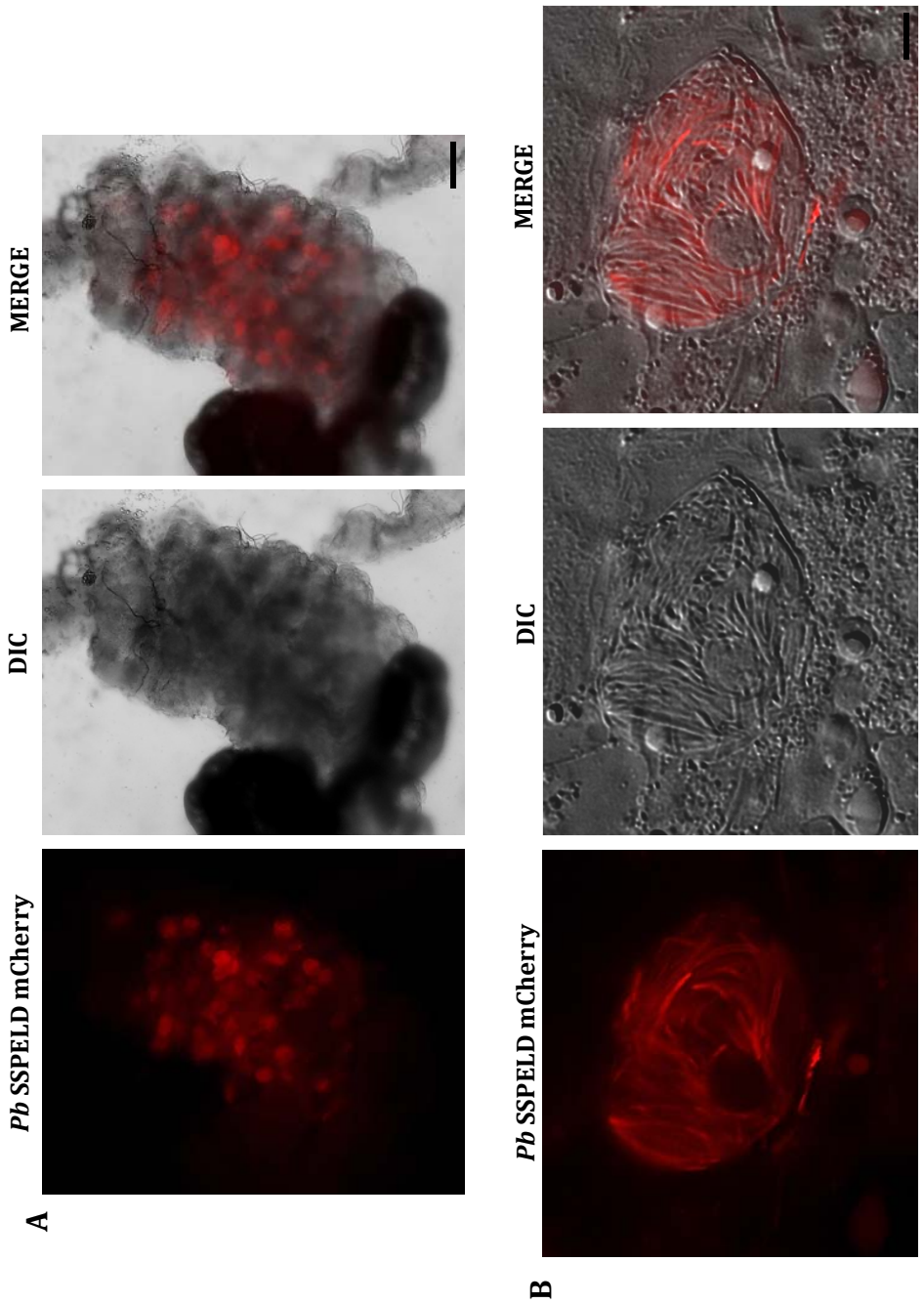

Fig 17. mCherry transgenic of *Pb SSPELD* express the reporter in oocyst stages. (A) Dissected mosquito midgut showing oocyst expressing *Pb* SSPELD mCherry. Scale bar 200μm (B) Higher magnification (100x) of oocyst showing mcherry expression in sporozoites within oocyst. Scale bar 10μm

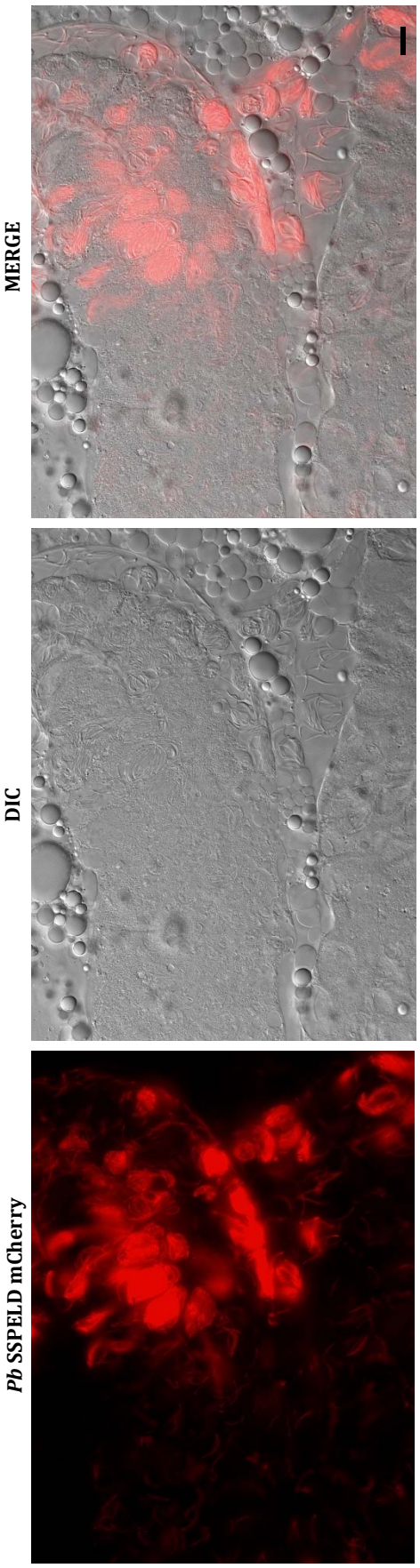

Fig 18. mCherry transgenic of *Pb SSPELD* express the reporter in salivary gland sporozoite stages. Dissected mosquito salivary gland lobe showing sporozoites expressing *Pb* SSPELD mCherry. Scale bar 10μm

Fig 19. Higher magnification (100X) of infected salivary gland lobe showing sporozoites expressing *Pb* SSPELD mCherry. Scale bar 5μm

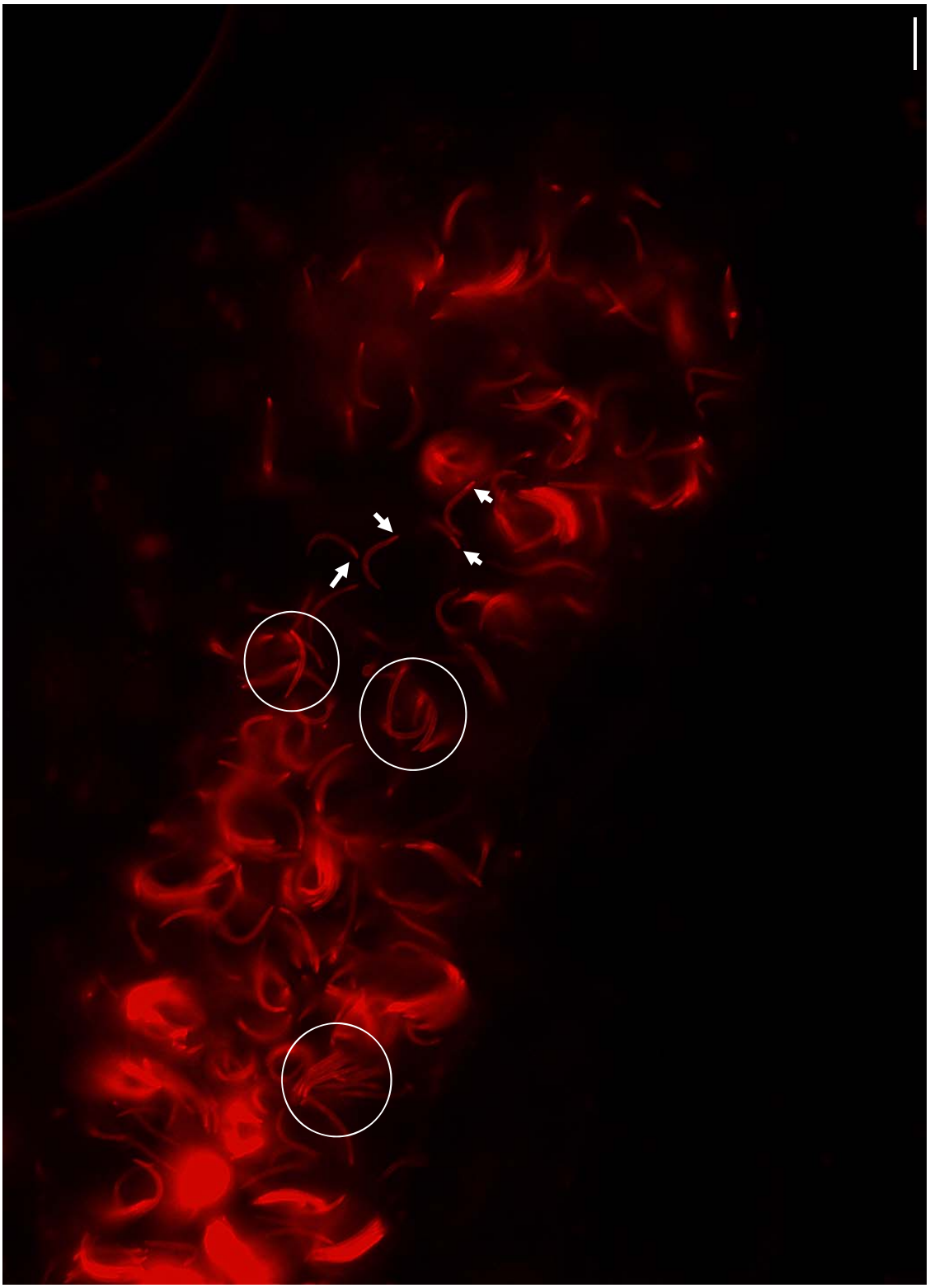

Fig 20. mCherry localizes to salivary gland sporozoite plasma membrane in *Pb* SSPELD mCherry transgenics and shows a likely accumulation at apical end of the sporozoite. Circles with while out line indicate sporozoites showing *Pb* SSPELD mCherry localization to the plasma membrane. Indicated in white arrows is the *Pb* SSPELD mCherry concentrated at the apical end of the sporozoite. Scale bar 5µm

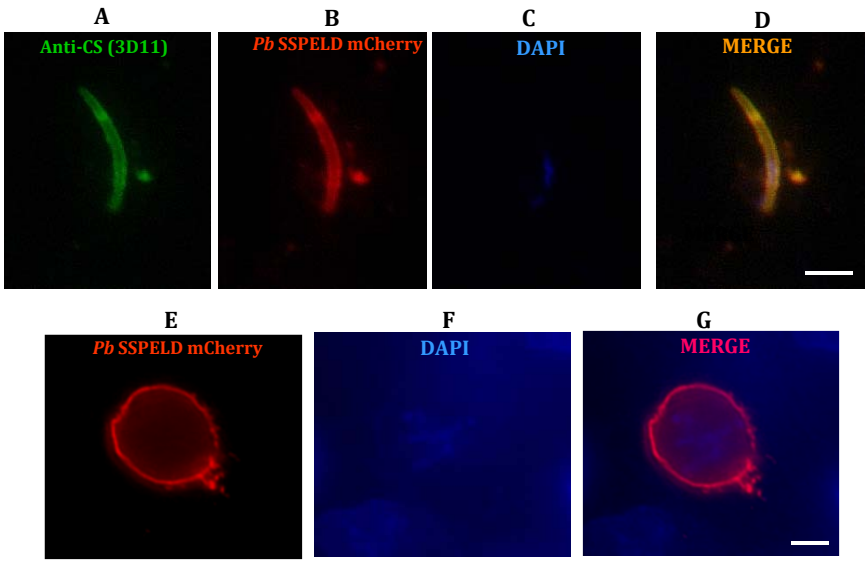

Fig 21. *Pb* SSPELD mCherry co- localizes with circumsporozoite protein on sporozoite plasma membrane and to PVM membrane on 36 hr EEF. A) Immunoreactivity of circumsporozoite protein on sporozoite surface following staining with 3D11 monoclonal antibody specific for *P. berghei* CS and revealed with anti-mouse secondary antibody conjugated to Alexa fluor 488. B) Sporozoite Surface localization of *Pb* SSPELD mCherry. C) DAPI staining of sporozoite nuclei. D) Merge of CSP immunoreactivity, mCherry and DAPI. Scale bar 5µm. E) Localization of mCherry on PVM of 36h EEF. F) DAPI staining of the EEF nuclei. G) Merge of mCherry and DAPI. Scale bar 10µm

2.3.10 Immunisation with *Pb SSPELD* KO generates pre erythrocytic immunity

To test the ability of *Pb SSPELD* KO to generate protective immunity and analyse the co relates of protection, C57BL/6 mice were primed and boosted at an interval of 2 weeks. Ten days after boosting, all immunized mice, along with naïve (nonimmunised) mice were challenged with $2X10^4$ WT sporozoites. Analysis of prepatent period in three independent experiments revealed respectively 3/6, 2/5 and 3/7 mice that gave pre patent period between D8/9, whereas all naïve mice became positive for blood stages on D4 (Table D in Fig 22). We conclude that a two times immunization with*Pb SSPELD* KO induces immunity whose efficacy is nearly 50%. Using pooled immune sera, sporozoite IFA titers were determined that ranged from 1:1600-1:3200 (Fig 22 A,B and C). Splenocytes collected from immunised mice were stained for CD4+ and CD8+ T cells and quantified by FACS. While we observed a significant increase in the CD4 T cells that from 49% to 56%, we noted only a marginal increase in CD8+ T cells from 26.6% to 30.1%.

2.3.11 Microarray of *Pb SSPELD* KO reveals dramatic changes in the global gene expression

Microarray revealed global changes in the gene expression of *Pb SSEPLD* KO where 1197 genes were upregulated and 552 genes were down regulated (Fig 23 A). The important functional clusters that were upregulated belonged to mRNA splicing pathway, purine metabolism pathway, DNA replication pathway, ubiquitin mediated proteolysis pathway, fatty acid synthesis pathway and nucleotide excision repair pathway (Fig 23 B and Fig 24). The important clusters that were down regulated belonged to spliceosome pathway, glycolysis/gluconeogenesis pathway, general transcription by RNA pol 1 pathway, cell cycle pathway, Cadherin signaling pathway, oxidative phosphorylation pathway, proteosome pathway (Fig 23 C, Fig 25 and Fig 26). Consistent with the attenuation of the *Pb SSPELD* KO at 36 hours, several late liver stage specific transcripts like UIS-4, LISP2, EXP-1, FABL, were significantly down regulated (Fig 27). SERA-4, a member of serine repeat antigen family was also down regulated. While no role of SERA-4 in liver sage development exists, the other member of this family in *P. berghei* like SERA V (ECP-1) and SERA III were shown to be essential respectively in egress of oocyst sporozoites and mature liver schizonts. Amongst other down regulated genes were the putative orthologues of *P. yoelli* that were shown to be inducedin the transcriptomic studies of the *in vivo*late liver stages (Kappe, Combined

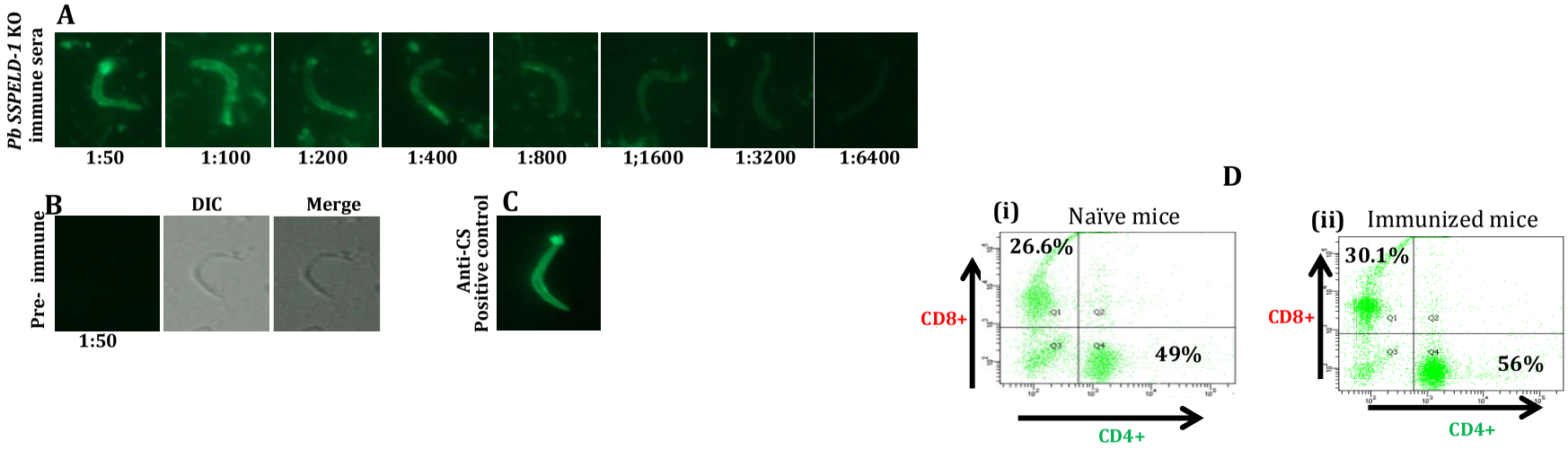

Table D

S. No	Immune status of C57BL/6 mice	No. of mice used for challenge with WT sporozoites	Challenge dose/mouse	No of mice positive for blood stage infection	Pre patent period
1.	Naive	3	$2X10^4$	3/3	D4
2.	*Pb SAGE-1* KO immunized mice (2X)	6	$2X10^4$	3*/6	D8/9
		5		2*/5	
		2		3*/7	

*** The mice that became positive for blood stage infection gave a delayed pre patent period**

Fig 22. Analysis of co-relates of protection in C57BL6 mice immunized with *Pb SSPLED* KO. A) Immune sera collected from 4-5 mice were pooled and serial 2 fold dilutions were made in PBS. The sera at different dilution as indicated in Fig A was incubated with fixed and immobilized sporozoites and the immunoreactivity was revealed using an anti-mouse secondary antibody conjugated to Alexa fluor 488. Pre immune sera (B) was used as a negative control and 3D11 monoclonal antibody specific for *P. berghei* CSP was used as positive control (C). D) FACS analysis of splenocytes obtained from C57BL/6 mice were stained with mouse anti-CD4 antibody conjugated to FITC and mouse anti CD8a antibody conjugated to PE (i) Splenocyes obtained from naïve mice show 26.6% CD8+ T cells and 49% CD4+ T cells. (ii) Splenocyes obtained from mice that were twice immunized *Pb SSPELD* KO show 30.1% CD8+ T cells and 56% CD4+ T cells.

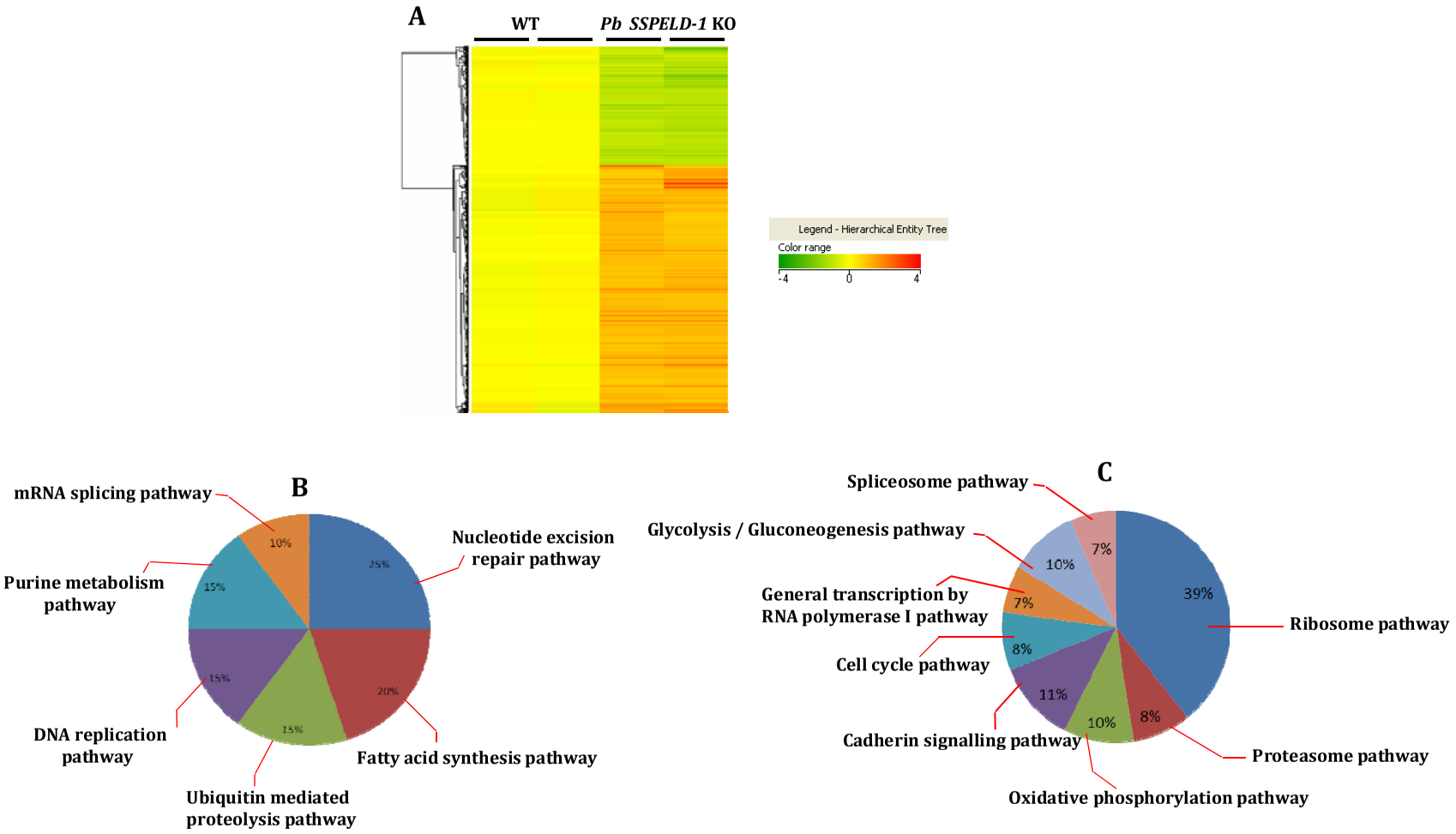

Fig 23. Micro array of 36H liver stages of WT and *Pb SSPELD* KO: A) Heat map showing global gene expression changes in *P. berghei* liver stages at 36h from WT and *Pb SSPELD* KO. B) Pie diagram indicating the major functional clusters up regulated in *Pb SSPELD* KO. C) Pie diagram indicating the major functional clusters down regulated in *Pb SSPELD* KO.

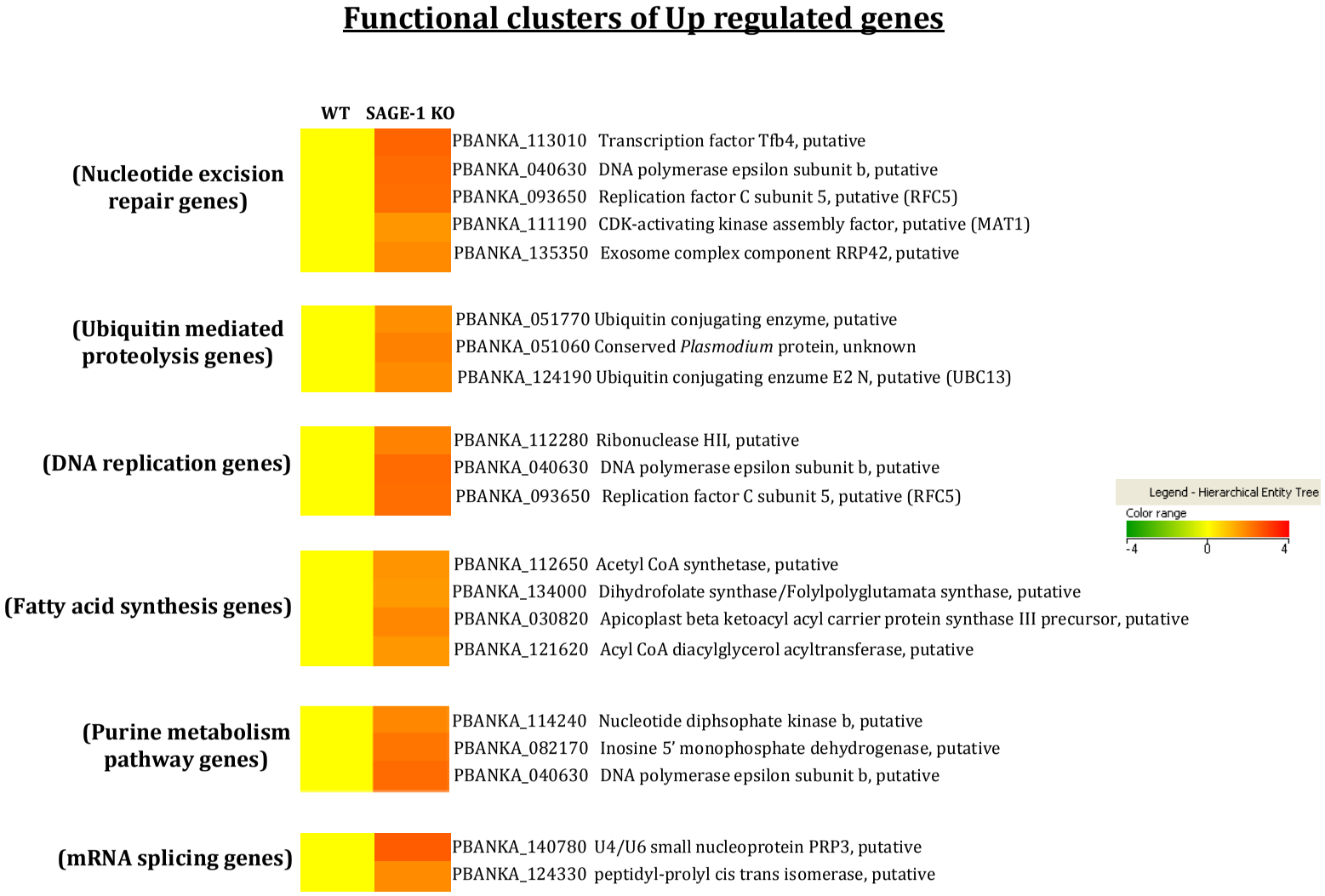

Fig 24. Genes included in functional clusters belonging to nucleotide excision repair, ubiquitin mediated proteolysis, DNA replication , fatty acid synthesis, purine metabolism and mRNA splicing are up regulated in *Pb SSPELD* KO. The plasmo DB ID of each of these genes with their likely function are indicated.

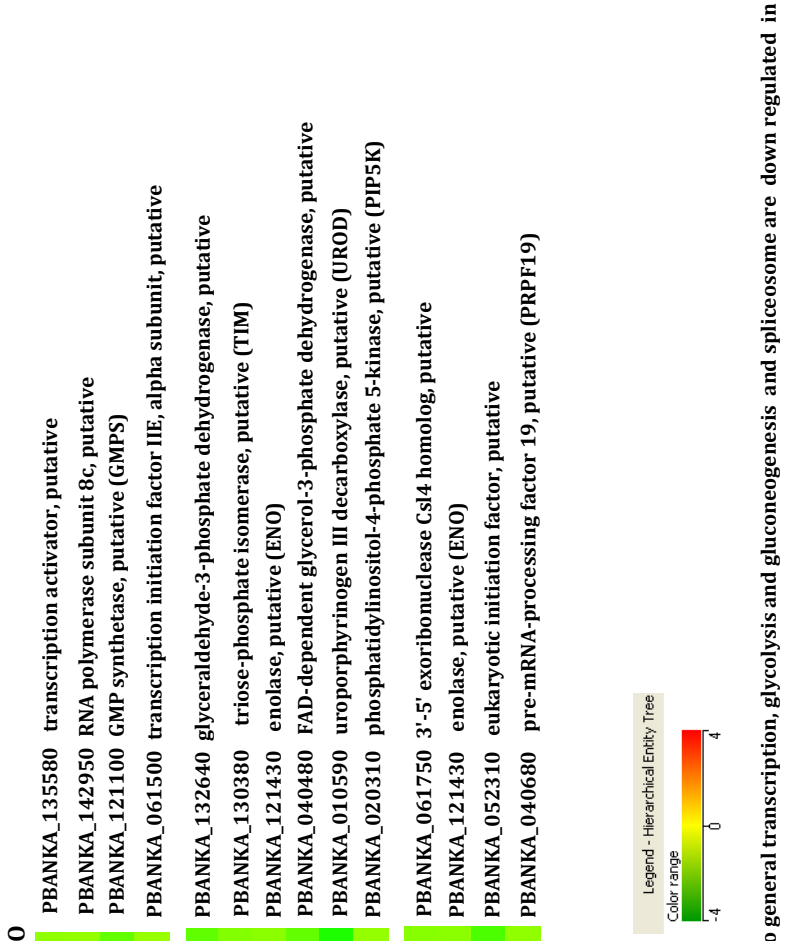

Fig 25 . Genes included in functional clusters belonging to general transcription, glycolysis and gluconeogenesis and spliceosome are down regulated in *Pb SSPELD* KO. The plasmo DB ID of each of these genes with their likely function are indicated.

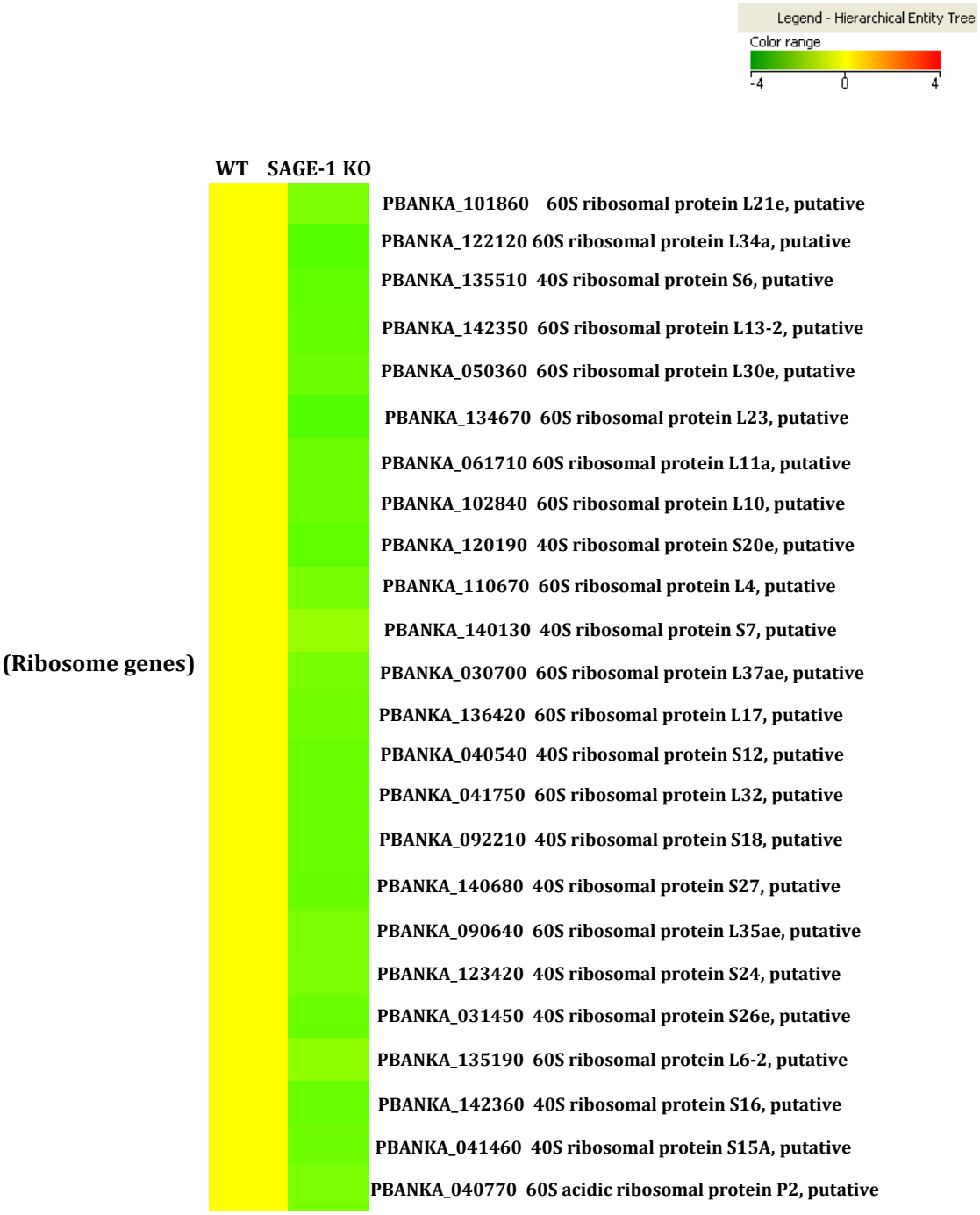

Fig 26. Ribosomal genes down regulated in *Pb SSPELD* KO. The plasmo DB ID of each of these genes with their likely function are indicated.

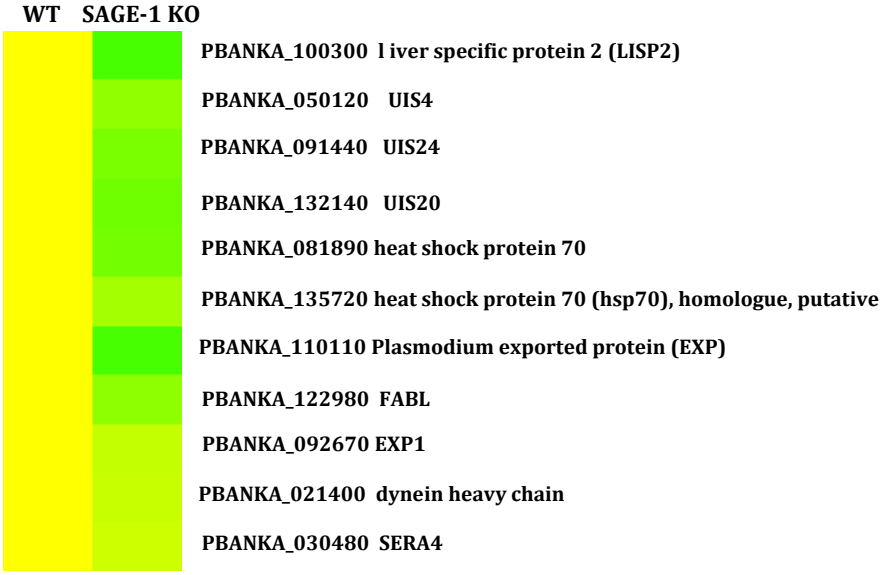

Fig 27. Some of the well characterized liver stage specific genes and late liver state specific genes down regulated in *Pb SSPELD* KO. The plasmo DB ID of each of these genes with their likely function are indicated.

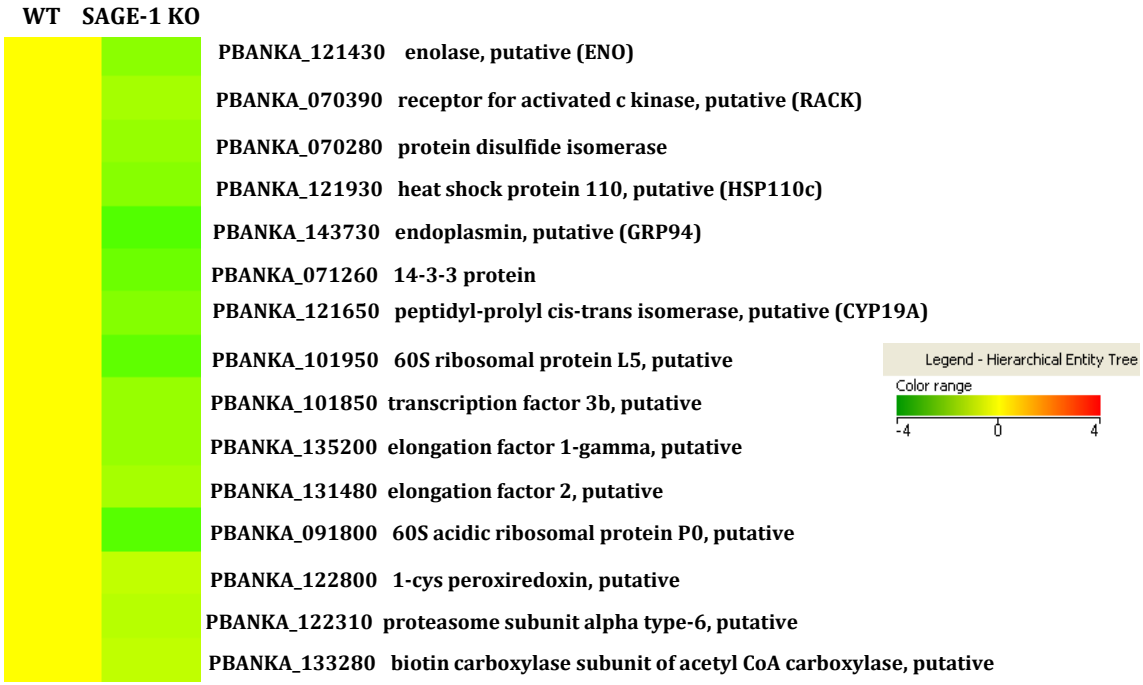

Fig 28. List of few putative genes that have been reported to be expressed in the late liver stages (Tarun AS et al., PNAS (2008) 105; 1 (305-310)) **are down regulated in Pb SSPELD KO. The plasmo DB ID of each of these genes with their likely function are indicated.**

transcriptome and Proteomic analysis) and included enolase, receptor activated c kinase (RACK), protein disulfide isomerase, heat shock protein 110, endoplasmin (GRP94), peptidyl-prolylcis-trans isomerase, 1-cys peroxiredoxin, proteosome subunit alpha type 6, biotin carboxylase subunit of acetyl CoA carboxylase (Fig 28). The list of up regulated and down regulated genes are indicated respectively in tables 1 and 2.

Table 1 showing the list of up regulated genes in *Pb SSPELD* knock out

S.No	GeneID	Function
3-4fold		
1	PBANKA_132550	CCAAT-box DNA binding protein subunit B
2	PBANKA_050730	Dynein heavy chain, putative.
3	PBANKA_000020	Pb-fam-1 protein, pseudogene
4	PBANKA_010420	calcium-binding protein, putative
5	PBANKA_130040	BIR protein
6	PBANKA_141450	protein kinase, putative
7	PBANKA_050265	conserved Plasmodium protein, unknown function
8	PBANKA_010440	nucleoside diphosphate kinase, putative
9	PBANKA_110800	transcription factor IIb, putative
10	PBANKA_060650	50S ribosomal protein L29, putative
11	PBANKA_050190	conserved Plasmodium protein, unknown function
2-3 fold		
12	PBANKA_103450	conserved Plasmodium protein, unknown function
13	PBANKA_060925	unspecified product
14	PBANKA_021590	BIR protein, pseudogene
15	PBANKA_123770	zinc finger protein, putative, fragment
16	PBANKA_120030	BIR protein
17	PBANKA_132360	biotin protein ligase, putative
18	PBANKA_000570	BIR protein
19	PBANKA_093570	conserved Plasmodium protein, unknown function
20	PBANKA_123780	multidrug resistance protein, putative (MDR1)
21	PBANKA_041720	conserved Plasmodium protein, unknown function
22	PBANKA_080010	BIR protein
23	PBANKA_136170	conserved Plasmodium protein, unknown function
24	PBANKA_144830	homocysteine S-methyltransferase, putative
25	PBANKA_124610	Pb-fam-1 protein
26	PBANKA_122030	lysophospholipase, putative
27	PBANKA_101420	conserved Plasmodium protein, unknown functio
28	PBANKA_103880	conserved Plasmodium protein, unknown function
29	PBANKA_070850	conserved Plasmodium protein, unknown function
30	PBANKA_141700	conserved Plasmodium protein, unknown function
31	PBANKA_122020	lysophospholipase, putative
32	PBANKA_120330	methionine-tRNA ligase, putative
33	PBANKA_092650	petidase, M16 family, putative
34	PBANKA_132150	conserved Plasmodium protein, unknown function
35	berg11:tRNA:rfamscan	unspecified product
36	PBANKA_103570	conserved Plasmodium protein, unknown function
37	PBANKA_070410	ubiquitination-mediated degradation component, putative
38	PBANKA_114670	BIR protein
39	PBANKA_111990	DnaJprotein, putative
40	PBANKA_081950	DNA helicase, putative
41	PBANKA_111030	conserved Plasmodium protein, unknown function

42	PBANKA_114610	conserved rodent malaria protein, unknown function
43	PBANKA_141980	3',5'-cyclic nucleotide phosphodiesterase, putative
44	PBANKA_131390	conserved Plasmodium protein, unknown function
45	PBANKA_020110	BIR protein, pseudogene
46	berg03:tRNA:rfamscan	unspecified product
47	PBANKA_050060	Plasmodium exported protein, unknown function
48	PBANKA_083610	phosphatidylinositol N- acetylglucosaminyltransferase subunit P, putative
49	PBANKA_141200	conserved Plasmodium protein, unknown function
50	PBANKA_010240	conserved Plasmodium protein, unknown function
51	PBANKA_093900	ion channel protein, putative
52	PBANKA_072270	BIR protein, pseudogene
53	PBANKA_103460	conserved Plasmodium protein, unknown function
54	PBANKA_140010	BIR protein
55	PBANKA_031665	BIR protein, pseudogene, fragment
56	PBANKA_144790	conserved Plasmodium protein, unknown function
57	PBANKA_132900	conserved Plasmodium protein, unknown function
58	PBANKA_020960	conserved Plasmodium protein, unknown function
59	PBANKA_060390	conserved Plasmodium protein, unknown function
1-2 fold		
60	PBANKA_142820	conserved Plasmodium protein, unknown function
61	PBANKA_102120	conserved Plasmodium protein, unknown function
62	PBANKA_111960	merozoite surface protein 10, putative (MSP10)
63	PBANKA_130180	conserved Plasmodium protein, unknown function
64	PBANKA_101920	conserved Plasmodium protein, unknown function
65	PBANKA_031050	conserved Plasmodium protein, unknown function
66	PBANKA_091110	conserved Plasmodium protein, unknown function
67	PBANKA_090240	conserved Plasmodium protein, unknown function, fragment
68	PBANKA_090040	BIR protein
69	PBANKA_041360	zinc finger protein, putative
70	PBANKA_131680	conserved Plasmodium protein, unknown function
71	PBANKA_API0017	RNA polymerase D (rpoD)
72	PBANKA_051790	conserved Plasmodium protein, unknown function
73	PBANKA_051200	DHHC-type zinc finger protein, putative
74	PBANKA_101750	lipase, putative (UIS28)
75	PBANKA_141740	conserved Plasmodium protein, unknown function
76	PBANKA_134250	conserved Plasmodium protein, unknown function
77	PBANKA_081830	conserved Plasmodium protein, unknown function
78	PBANKA_112320	conserved Plasmodium protein, unknown function
79	PBANKA_112320	conserved Plasmodium protein, unknown function
80	PBANKA_080150	conserved Plasmodium protein, unknown function
81	PBANKA_146380	conserved Plasmodium protein, unknown function
82	PBANKA_120100	conserved Plasmodium protein, unknown function
83	PBANKA_051960	conserved Plasmodium protein, unknown function
84	PBANKA_040890	conserved Plasmodium protein, unknown function
85	PBANKA_062150	conserved Plasmodium protein, unknown function
86	PBANKA_092730	zinc finger, DHHC-type, putative
87	PBANKA_082400	OTU-like cysteine protease, putative
88	PBANKA_071980	conserved Plasmodium protein, unknown function
89	PBANKA_050080	BIR protein, pseudogene
90	PBANKA_146020	conserved Plasmodium protein, unknown function
100	PBANKA_136090	GTPase, putative
101	PBANKA_133130	conserved Plasmodium protein, unknown function
102	PBANKA_070020	BIR protein
103	PBANKA_070020	BIR protein
104	PBANKA_133650	conserved Plasmodium protein, unknown function

105	PBANKA_083680	Pb-fam-1 protein
106	PBANKA_050110	early transcripted membrane protein (SEP3)
107	PBANKA_091100	conserved Plasmodium protein, unknown function
108	PBANKA_131900	conserved Plasmodium protein, unknown function
109	PBANKA_146390	conserved Plasmodium protein, unknown function
110	PBANKA_080680	conserved Plasmodium protein, unknown function
111	PBANKA_141810	conserved Plasmodium protein, unknown function
112	PBANKA_131270	gamete egress and sporozoite traversal protein (GEST)
113	PBANKA_API_tRNA7	unspecified product
114	PBANKA_103020	conserved Plasmodium protein, unknown function
115	PBANKA_132390	conserved Plasmodium protein, unknown function
116	PBANKA_000380	BIR protein
117	PBANKA_000360	BIR protein
118	PBANKA_101100	protein kinase, putative, fragment
119	PBANKA_041760	LCCL domain-containing protein (CCp4)
120	PBANKA_021300	RNA-binding protein, putative
121	PBANKA_082890	conserved Plasmodium protein, unknown function
122	PBANKA_112300	conserved Plasmodium protein, unknown function
123	PBANKA_093060	conserved Plasmodium protein, unknown function
124	PBANKA_000670	BIR protein, pseudogene, fragment
125	PBANKA_020460	photosensitized INA-labeled protein 1, putative
126	PBANKA_101820	conserved Plasmodium protein, unknown function
127	PBANKA_083500	conserved Plasmodium protein, unknown function
128	PBANKA_104050	BIR protein, pseudogene
129	PBANKA_000630	BIR protein
130	PBANKA_082430	conserved Plasmodium protein, unknown function
131	berg08:tRNA:rfamscan:20764-20836	unspecified product
132	PBANKA_132080	conserved Plasmodium protein, unknown function
133	PBANKA_060040	Pb-fam-1 protein
134	PBANKA_000990	BIR protein, pseudogene, fragment
135	PBANKA_133090	conserved Plasmodium protein, unknown function
136	PBANKA_061780	conserved Plasmodium protein, unknown function
137	PBANKA_061780	conserved Plasmodium protein, unknown function
138	PBANKA_080780	conserved Plasmodium protein, unknown function
139	PBANKA_110850	conserved Plasmodium protein, unknown function
140	PBANKA_092120	conserved Plasmodium protein, unknown function
141	PBANKA_110075	Pb-fam-1 protein
142	PBANKA_121410	tubulin binding cofactor c, putative
143	PBANKA_093310	conserved Plasmodium protein, unknown function
144	PBANKA_010020	Plasmodium exported protein, unknown function
145	PBANKA_020890	conserved Plasmodium protein, unknown function
146	PBANKA_121910	heat shock protein 90, putative
147	PBANKA_114010	conserved Plasmodium protein, unknown function
148	PBANKA_062260	conserved Plasmodium protein, unknown function
149	PBANKA_070080	conserved Plasmodium protein, unknown function
150	PBANKA_050340	conserved Plasmodium protein, unknown function
151	PBANKA_062380	BIR protein, fragment
152	PBANKA_092190	conserved Plasmodium protein, unknown function
153	PBANKA_146230	conserved Plasmodium protein, unknown function
154	PBANKA_021390	dynein light chain, putative
155	PBANKA_000340	BIR protein
156	PBANKA_094390	BIR protein
157	PBANKA_060010	BIR protein
158	PBANKA_031370	conserved Plasmodium protein, unknown function
159	PBANKA_102240	dynein-associated protein, putative
160	PBANKA_144280	leucine-rich repeat protein (LRR13)

161	PBANKA_020120	Pb-fam-1 protein, pseudogene
162	PBANKA_101890	conserved Plasmodium protein, unknown function
163	PBANKA_030240	conserved Plasmodium protein, unknown function
164	PBANKA_031390	conserved Plasmodium protein, unknown function
165	PBANKA_121060	conserved Plasmodium protein, unknown function
166	PBANKA_132000	conserved Plasmodium protein, unknown function
167	PBANKA_111200	conserved Plasmodium protein, unknown function
168	PBANKA_031690	BIR protein
169	PBANKA_000790	BIR protein, pseudogene, fragment
170	PBANKA_072290	BIR protein, pseudogene
171	PBANKA_052150	conserved Plasmodium protein, unknown function
172	PBANKA_102760	conserved Plasmodium protein, unknown function
173	PBANKA_070030	BIR protein
174	PBANKA_052370	conserved Plasmodium protein, unknown function
175	PBANKA_124310	F-actin capping protein, alpha subunit, putative
176	PBANKA_135680	conserved Plasmodium protein, unknown function
177	PBANKA_134050	conserved Plasmodium protein, unknown function
178	PBANKA_031620	Plasmodium exported protein, unknown function, fragment
179	PBANKA_114030	conserved Plasmodium protein, unknown function
180	PBANKA_050140	conserved Plasmodium protein, unknown function
181	PBANKA_136080	conserved Plasmodium protein, unknwon function
182	PBANKA_082580	conserved Plasmodium protein, unknown function
183	PBANKA_093880	conserved Plasmodium protein, unknown function
184	PBANKA_081030	conserved Plasmodium protein, unknown function
185	PBANKA_113310	serine/threonine protein kinase, putative (ARK3)
186	PBANKA_120790	protein phosphatase, putative
187	PBANKA_124700	BIR protein
188	PBANKA_062350	Pb-fam-1 protein
189	PBANKA_060540	conserved Plasmodium protein, unknown function
190	PBANKA_091500	apical membrane antigen 1 (AMA1)
191	PBANKA_091340	protein phosphatase 2C, putative
192	PBANKA_041590	conserved Plasmodium protein, unknown function
193	PBANKA_040270	membrane skeletal protein, putative
194	PBANKA_101990	conserved Plasmodium protein, unknown function
195	PBANKA_141930	conserved Plasmodium protein, unknown function
196	PBANKA_132570	thioredoxin-like protein (TLP1)
197	PBANKA_122550	conserved Plasmodium protein, unknown function
198	PBANKA_132520	conserved Plasmodium protein, unknown function
199	PBANKA_050780	conserved Plasmodium protein, unknown function
200	PBANKA_030840	dolichol-linked oligosaccharide biosynthesis enzyme, putative
201	PBANKA_143660	inner membrane complex protein 1h (IMC1h)
202	PBANKA_123200	conserved Plasmodium protein, unknown function
203	PBANKA_114590	conserved rodent malaria protein, unknown function
204	PBANKA_114590	conserved rodent malaria protein, unknown function
205	PBANKA_000890	BIR protein, pseudogene, fragment
206	PBANKA_100210	6-cysteine protein (P36)
207	PBANKA_000780	BIR protein, pseudogene, fragment
208	PBANKA_112450	poly(A) polymerase PAP, putative
209	PBANKA_114600	conserved rodent malaria protein, unknown function
210	PBANKA_082920	conserved Plasmodium protein, unknown function
211	PBANKA_131970	transcription factor with AP2 domain(s), putative (ApiAP2)
212	PBANKA_111980	conserved Plasmodium protein, unknown function
213	PBANKA_094080	apicoplast ribosomal protein S15 precursor, putative
214	PBANKA_131470	conserved Plasmodium protein, unknown function
215	PBANKA_133900	vacuolar protein sorting protein 52, putative
216	PBANKA_080250	conserved Plasmodium protein, unknown function
217	PBANKA_143720	conserved Plasmodium protein, unknown function

218	PBANKA_134150	RNA binding protein, putative
219	PBANKA_082320	conserved Plasmodium protein, unknown function
220	PBANKA_121320	conserved Plasmodium protein, unknown function
221	PBANKA_110940	phosphatidylinositol 4-kinase, putative
222	PBANKA_100420	conserved Plasmodium protein, unknown function
223	PBANKA_143450	conserved Plasmodium protein, unknown function
224	PBANKA_020030	BIR protein
225	PBANKA_030060	Plasmodium exported protein, unknown function
226	PBANKA_060620	blood stage antigen 41-3 precursor, putative
227	PBANKA_123230	conserved Plasmodium protein, unknown function
228	PBANKA_050030	conserved rodent malaria protein, unknown function
229	PBANKA_110990	conserved Plasmodium protein, unknown function
230	PBANKA_000165	Pb-fam-1 protein, pseudogene
231	PBANKA_030470	serine repeat antigen 5 (SERA5)
232	PBANKA_062070	conserved Plasmodium protein, unknown function
233	PBANKA_050390	conserved Plasmodium protein, unknown function
234	PBANKA_050440	conserved Plasmodium protein, unknown function
235	PBANKA_102050	conserved Plasmodium protein, unknown function
236	PBANKA_010080	conserved Plasmodium protein, unknown function
237	PBANKA_094020	dna2/nam7 helicase family member, putative
238	PBANKA_111510	amino acid transporter, putative
239	PBANKA_080050	chitinase (CHT1)
240	PBANKA_000710	BIR protein, pseudogene, fragment
241	PBANKA_000935	BIR protein, pseudogene, fragment
242	PBANKA_040740	serine/threonine protein kinase, putative (ARK2)
243	PBANKA_110930	conserved Plasmodium protein, unknown function
244	PBANKA_142290	conserved Plasmodium protein, unknown function
245	PBANKA_083390	conserved Plasmodium protein, unknown function
246	PBANKA_140870	conserved Plasmodium protein, unknown function
247	PBANKA_100050	conserved rodent malaria protein, unknown function
248	PBANKA_146410	coronin, putative
249	PBANKA_020360	conserved Plasmodium protein, unknown function
250	PBANKA_083620	conserved Plasmodium protein, unknown function
251	PBANKA_072300	BIR protein
252	PBANKA_090400	conserved Plasmodium protein, unknown function
253	PBANKA_091940	conserved Plasmodium protein, unknown function
254	PBANKA_104040	BIR protein
255	PBANKA_092260	conserved Plasmodium protein, unknown function
256	PBANKA_132620	conserved Plasmodium protein, unknown function
257	PBANKA_100630	perforin like protein 1 (SPECT2)
258	PBANKA_100760	conserved Plasmodium protein, unknown function
259	PBANKA_145110	conserved Plasmodium protein, unknown function
260	PBANKA_082830	dynein light chain, putative
261	PBANKA_120910	dolichyl-phosphate-mannose protein mannosyltransferase, putative
262	PBANKA_113010	Transcription factor Tfb4, putative
263	PBANKA_070710	membrane skeletal protein, putative
264	PBANKA_135970	6-cysteine protein (P47)
265	PBANKA_052480	early transcribed membrane protein (SEP1)
266	PBANKA_130270	conserved Plasmodium protein, unknown function
267	PBANKA_050040	BIR protein, fragment
268	PBANKA_041290	circumsporozoite- and TRAP-related protein (CTRP)
269	PBANKA_146560	BIR protein
270	PBANKA_124550	conserved Plasmodium protein, unknown function
271	PBANKA_090250	kinesin-like protein, putative
272	PBANKA_091050	conserved Plasmodium protein, unknown function
273	PBANKA_060970	conserved Plasmodium protein, unknown function

274	PBANKA_000130	BIR protein, fragment
275	PBANKA_124300	cell cycle regulator with zn-finger domain, putative
276	PBANKA_072220	BIR protein, pseudogene
277	PBANKA_141770	conserved Plasmodium protein, unknown function
278	PBANKA_141940	conserved Plasmodium protein, unknown function
279	PBANKA_020900	conserved Plasmodium protein, unknown function
280	PBANKA_123320	cyclin, putative
281	PBANKA_145770	conserved Plasmodium protein, unknown function
282	PBANKA_135490	conserved Plasmodium protein, unknown function
283	PBANKA_140430	conserved Plasmodium protein, unknown function
284	PBANKA_136150	conserved Plasmodium protein, unknown function
285	PBANKA_120950	conserved Plasmodium protein, unknown function
286	PBANKA_140780	U4/U6 small nuclear ribonucleoprotein PRP3, putative
287	PBANKA_020020	Pb-fam-1 protein
288	PBANKA_120950	conserved Plasmodium protein, unknown function
289	PBANKA_140780	U4/U6 small nuclear ribonucleoprotein PRP3, putative
290	PBANKA_020020	Pb-fam-1 protein
291	PBANKA_114580	conserved rodent malaria protein, unknown function
292	PBANKA_091665	conserved Plasmodium protein, unknown function
293	PBANKA_100860	conserved Plasmodium protein, unknown function
294	PBANKA_090940	conserved Plasmodium protein, unknown function
295	PBANKA_120890	conserved Plasmodium protein, unknown function
296	PBANKA_120830	conserved Plasmodium protein, unknown function
297	PBANKA_010010	Pb-fam-1 protein
298	PBANKA_000960	BIR protein, pseudogene, fragment
299	PBANKA_083070	procollagen lysine 5-dioxygenase, putative
300	PBANKA_020700	calcium-transporting ATPase, putative (SERCA)
301	PBANKA_102420	conserved Plasmodium protein, unknown function
302	PBANKA_121770	ATP-dependent RNA Helicase (DOZI)
303	PBANKA_130490	conserved Plasmodium protein, unknown function
304	PBANKA_081220	conserved Plasmodium protein, unknown function
305	PBANKA_090320	conserved Plasmodium protein, unknown function
306	PBANKA_051070	conserved Plasmodium protein, unknown function
307	PBANKA_020480	secreted ookinete protein, putative (PSOP24)
308	PBANKA_103180	conserved Plasmodium protein, unknown function
309	PBANKA_051280	merozoite TRAP-like protein, putative (MTRAP)
310	PBANKA_000490	conserved rodent malaria protein, unknown function
311	PBANKA_122190	conserved Plasmodium protein, unknown function
312	PBANKA_113390	conserved Plasmodium protein, unknown function
313	PBANKA_020090	conserved rodent malaria protein, unknown function
314	PBANKA_010410	serine/threonine protein kinase, putative (ARK1)
315	PBANKA_082800	zinc finger protein, putative
316	PBANKA_082820	conserved Plasmodium protein, unknown function
317	PBANKA_083450	conserved Plasmodium protein, unknown function
318	PBANKA_121800	conserved Plasmodium protein, unknown function,pyrazinamidase/nicotinamidase, putative
319	PBANKA_144770	elongation factor G, putative
320	PBANKA_114230	rhoptry protein, putative
321	PBANKA_061260	conserved Plasmodium protein, unknown function
322	PBANKA_133760	translation initiation factor EIF-2B subunit, putative
323	PBANKA_081070	subpellicular microtubule protein 1, putative (SPM1)
324	PBANKA_142420	conserved Plasmodium protein, unknown function
325	PBANKA_144340	conserved Plasmodium protein, unknown function
326	PBANKA_092580	conserved Plasmodium protein, unknown function
327	PBANKA_121710	protein kinase, putative
328	PBANKA_112610	mitochondrial import inner membrane translocase subunit, putative

329	PBANKA_110080	BIR protein
330	PBANKA_081940	conserved Plasmodium protein, unknown function
331	PBANKA_031200	conserved Plasmodium protein, unknown function
332	PBANKA_072260	Plasmodium exported protein, unknown function
333	PBANKA_124595	BIR protein, pseudogene
334	PBANKA_132820	conserved Plasmodium protein, unknown function
335	PBANKA_120290	conserved Plasmodium protein, unknown function
336	PBANKA_143030	conserved Plasmodium protein, unknown function
337	PBANKA_052380	asparagine rich protein, putative
338	PBANKA_081730	conserved Plasmodium protein, unknown function
339	PBANKA_131800	serine/threonine protein kinase, putative
340	PBANKA_000040	BIR protein, fragment
341	PBANKA_136570	BIR protein
342	PBANKA_102320	splicing factor 3B subunit 4, putative (SF3B4)
343	PBANKA_041370	conserved Plasmodium protein, unknown function
344	PBANKA_001000	BIR protein, pseudogene, fragment
345	PBANKA_112710	conserved Plasmodium protein, unknown function
346	PBANKA_051535	OTU-like cysteine protease, putative
347	PBANKA_000530	BIR protein
348	PBANKA_000530	BIR protein
349	PBANKA_094010	protein kinase, putative
350	PBANKA_123610	ribosomal large subunit pseudouridylate synthase, putative
351	PBANKA_062315	conserved rodent malaria protein, unknown function
352	PBANKA_051930	conserved Plasmodium protein, unknown function
353	PBANKA_020580	serine/threonine protein kinase, putative (IK2)
354	PBANKA_143140	conserved Plasmodium protein, unknown function
355	PBANKA_141230	conserved Plasmodium protein, unknown function
356	PBANKA_090030	BIR protein
357	PBANKA_000840	BIR protein, pseudogene, fragment
358	PBANKA_145040	conserved Plasmodium protein, unknown function
359	PBANKA_031350	conserved Plasmodium protein, unknown function
360	PBANKA_082440	conserved Plasmodium protein, unknown function
361	PBANKA_111810	N-acetylglucosaminetransferase, putative
362	PBANKA_082590	conserved Plasmodium protein, unknown function
363	PBANKA_081700	sugar transporter, putative
364	PBANKA_090010	conserved rodent malaria protein, unknown function
365	PBANKA_130035	Pb-fam-1 protein, pseudogene
366	PBANKA_091740	armadillo repeat protein PF16 (PF16)
367	PBANKA_145840	conserved Plasmodium protein, unknown function
368	PBANKA_062030	conserved Plasmodium protein, unknown function
369	PBANKA_145390	conserved Plasmodium protein, unknown function
370	PBANKA_010070	Plasmodium exported protein, unknown function
371	PBANKA_110410	conserved Plasmodium protein, unknown function
372	PBANKA_092690	conserved Plasmodium protein, unknown function
373	PBANKA_030160	conserved Plasmodium protein, unknown function
374	PBANKA_133810	conserved Plasmodium protein, unknown function
375	PBANKA_143630	conserved Plasmodium protein, unknown function
376	PBANKA_090460	conserved Plasmodium protein, unknown function
377	PBANKA_122530	conserved Plasmodium protein, unknown function
378	PBANKA_102570	conserved Plasmodium protein, unknown function
379	PBANKA_050010	Pb-fam-1 protein, pseudogene
380	PBANKA_090790	conserved Plasmodium protein, unknown function
381	PBANKA_100390	sexual stage-specific protein precursor, putative
382	PBANKA_100640	conserved Plasmodium protein, unknown function
383	PBANKA_130550	acid cluster protein 33 homologue, putative
384	PBANKA_133490	conserved Plasmodium protein, unknown function
385	PBANKA_144960	conserved Plasmodium protein, unknown function

386	PBANKA_000120	Pb-fam-1 protein, pseudogene
387	PBANKA_146550	BIR protein
388	PBANKA_101170	conserved Plasmodium protein, unknown function
389	PBANKA_010060	schizont membrane associated cytoadherence protein (SMAC)
390	PBANKA_100240	protease, putative
391	PBANKA_000610	BIR protein, pseudogene, fragment
392	PBANKA_144730	conserved Plasmodium protein, unknown function
393	PBANKA_121510	Rh5 interacting protein, putative
394	berg11:tRNA:rfamscan:1692721-1692792	unspecified product
395	PBANKA_040200	binding protein, putative
396	PBANKA_040070	Pb-fam-1 protein, pseudogene
397	PBANKA_050200	conserved Plasmodium protein, unknown function
398	PBANKA_030010	BIR protein
399	PBANKA_082740	conserved Plasmodium protein, unknown function
400	PBANKA_030220	dynein light chain, putative
401	PBANKA_120340	conserved protein, unknown function
402	PBANKA_144290	conserved Plasmodium protein, unknown function
403	PBANKA_060370	conserved Plasmodium protein, unknown function
404	PBANKA_144160	conserved Plasmodium protein, unknown function
405	PBANKA_081210	phosphatidylinositol N- acetylglucosaminyltransferase, putative
406	PBANKA_030670	transporter, putative
407	PBANKA_143230	cell traversal protein for ookinetes and sporozoites (CelTOS)
408	PBANKA_060330	conserved Plasmodium protein, unknown function
409	PBANKA_093460	conserved Plasmodium protein, unknown function
410	PBANKA_050290	conserved Plasmodium protein, unknown function
411	PBANKA_000620	BIR protein, pseudogene, fragment
412	PBANKA_040010	BIR protein
413	PBANKA_094100	conserved Plasmodium protein, unknown function
414	PBANKA_092180	steryl ester hydrolase, putative
415	PBANKA_093490	conserved Plasmodium protein, unknown function
416	PBANKA_091240	conserved Plasmodium protein, unknown function
417	PBANKA_120990	conserved Plasmodium protein, unknown function
418	PBANKA_123260	apicortin, putative
419	PBANKA_143700	conserved Plasmodium protein, unknown function
420	PBANKA_133050	conserved Plasmodium protein, unknown function
421	PBANKA_000240	BIR protein
422	PBANKA_122900	Plasmodium exported protein, unknown function
423	PBANKA_011150	conserved Plasmodium protein, unknown function
424	PBANKA_052430	tryptophan/threonine-rich antigen, putative
425	PBANKA_021180	conserved Plasmodium protein, unknown function
426	PBANKA_071140	perforin like protein 4 (PPLP4)
427	PBANKA_100750	actin-like protein, putative
428	PBANKA_020560	DNA repair exonuclease, putative
429	PBANKA_101390	conserved Plasmodium protein, unknown function
430	PBANKA_145870	conserved Plasmodium protein, unknown function
431	PBANKA_001040	BIR protein, pseudogene, fragment
432	PBANKA_071060	phosphatidylglycerophosphate synthase, putative
433	PBANKA_010040	rhoptry protein, putative
434	PBANKA_020550	conserved Plasmodium protein, unknown function
435	PBANKA_102530	cyclic nucleotide-binding protein, putative (cNBP)
436	PBANKA_104030	Plasmodium exported protein, unknown function
437	PBANKA_124690	BIR protein, pseudogene
438	PBANKA_144360	conserved Plasmodium protein, unknown function
439	PBANKA_140040	Plasmodium exported protein, unknown function

440	PBANKA_070630	GTP-binding protein, putative
441	PBANKA_060790	3',5'-cyclic-nucleotide phosphodiesterase, putative
442	PBANKA_090850	myosin heavy chain subunit, putative
443	PBANKA_146430	conserved Plasmodium protein, unknown function, fragment
444	PBANKA_020270	kinesin, putative
445	PBANKA_113540	riboflavin kinase / FAD synthase family protein, putative
446	PBANKA_020105	BIR protein, pseudogene, fragment
447	PBANKA_000560	BIR protein, pseudogene
448	PBANKA_145190	conserved Plasmodium protein, unknown function
449	PBANKA_110040	BIR protein
450	PBANKA_124620	Plasmodium exported protein, unknown function
451	PBANKA_101300	conserved Plasmodium protein, unknown function
452	PBANKA_120350	conserved Plasmodium protein, unknown function
453	PBANKA_082100	chaperone protein, putative
454	PBANKA_040120	ABC transporter, putative
455	PBANKA_071680	conserved Plasmodium protein, unknown function
456	PBANKA_071340	conserved Plasmodium protein, unknown function
457	PBANKA_136565	Pb-fam-1 protein, pseudogene
458	PBANKA_070050	Pb-fam-1 protein
459	PBANKA_122880	protein kinase, putative
460	PBANKA_134920	MSP7-like protein (MSRP1)
461	PBANKA_082670	conserved Plasmodium protein, unknown function
462	PBANKA_114160	conserved Plasmodium protein, unknown function
463	PBANKA_093650	replication factor C subunit 5, putative (RFC5)
464	PBANKA_050960	conserved Plasmodium protein, unknown function
465	PBANKA_100120	conserved Plasmodium protein, unknown function
466	PBANKA_090160	farnesyltransferase beta subunit, putative
467	PBANKA_120680	zinc finger C-x8-C-x5-C-x3-H type, putative
468	PBANKA_094370	conserved Plasmodium protein, unknown function
469	PBANKA_111690	conserved Plasmodium protein, unknown function
470	PBANKA_082570	telomeric repeat binding factor 1, putative
471	PBANKA_135790	conserved Plasmodium protein, unknown function
472	PBANKA_134170	conserved Plasmodium protein, unknown function
473	PBANKA_131510	transcriptional regulatory protein sir2b (Sir2b)
474	PBANKA_141170	peptidyl-prolyl cis-trans isomerase, putative
475	PBANKA_110880	leucine-rich repeat protein (LRR2)
476	PBANKA_082850	serine/threonine protein phosphatase, putative
477	PBANKA_070790	conserved Plasmodium protein, unknown function
478	PBANKA_000100	BIR protein
479	PBANKA_030450	conserved Plasmodium protein, unknown function
480	PBANKA_061360	Phosphopantothenoylcysteinesynthetase, putative
481	PBANKA_132240	conserved Plasmodium protein, unknown function
482	PBANKA_142760	conserved Plasmodium protein, unknown function
483	PBANKA_011220	myosin-like protein, putative
484	PBANKA_000730	BIR protein, pseudogene, fragment
485	PBANKA_110880	leucine-rich repeat protein (LRR2)
486	PBANKA_082850	serine/threonine protein phosphatase, putative
487	PBANKA_070790	conserved Plasmodium protein, unknown function
488	PBANKA_000100	BIR protein
489	PBANKA_030450	conserved Plasmodium protein, unknown function
490	PBANKA_061360	Phosphopantothenoylcysteinesynthetase, putative
491	PBANKA_132240	conserved Plasmodium protein, unknown function
492	PBANKA_142760	conserved Plasmodium protein, unknown function
493	PBANKA_011220	myosin-like protein, putative
494	PBANKA_000730	BIR protein, pseudogene, fragment
495	PBANKA_136340	conserved Plasmodium protein, unknown function
496	PBANKA_146205	conserved Plasmodium protein, unknown function

497	PBANKA_040630	DNA polymerase epsilon subunit b, putative
498	PBANKA_141540	conserved Plasmodium protein, unknown function
499	PBANKA_110290	conserved Plasmodium protein, unknown function
500	PBANKA_091580	pre-mRNA splicing factor, putative
501	PBANKA_102510	conserved Plasmodium protein, unknown function
502	PBANKA_144480	conserved Plasmodium protein, unknown function
503	PBANKA_090920	conserved Plasmodium protein, unknown function
504	PBANKA_000650	BIR protein, pseudogene, fragment
505	PBANKA_114390	conserved Plasmodium protein, unknown function
506	PBANKA_144850	sentrin-specific protease 1, putative
507	PBANKA_101210	conserved Plasmodium protein, unknown function
508	PBANKA_145080	conserved Plasmodium protein, unknown function
509	PBANKA_093890	IWS1-like protein, putative
510	PBANKA_031680	Plasmodium exported protein, unknown function
511	PBANKA_030980	Leu/Phe-tRNA protein transferase, putative
512	PBANKA_070060	Plasmodium exported protein, unknown function
513	PBANKA_113640	conserved Plasmodium protein, unknown function
514	PBANKA_136040	conserved Plasmodium protein, unknown function
515	PBANKA_020850	conserved Plasmodium protein, unknown function
516	PBANKA_010150	conserved Plasmodium protein, unknown function
517	PBANKA_110890	conserved Plasmodium protein, unknown function
518	PBANKA_051340	conserved Plasmodium protein, unknown function
519	PBANKA_110170	conserved Plasmodium protein, unknown function
520	PBANKA_092410	conserved Plasmodium protein, unknown function
521	PBANKA_040730	conserved Plasmodium protein, unknown function
522	PBANKA_100590	zinc-finger, RAN binding protein, putative
523	PBANKA_093680	conserved Plasmodium protein, unknown function
524	PBANKA_090360	dynamin-like protein, putative
525	PBANKA_132380	conserved Plasmodium protein, unknown function
526	PBANKA_060670	cysteine repeat modular protein 3 (CRMP3)
527	PBANKA_121560	40S ribosomal protein S3A, putative
528	PBANKA_132240	conserved Plasmodium protein, unknown function
529	PBANKA_142760	conserved Plasmodium protein, unknown function
530	PBANKA_011220	myosin-like protein, putative
531	PBANKA_000730	BIR protein, pseudogene, fragment
532	PBANKA_136340	conserved Plasmodium protein, unknown function
533	PBANKA_146205	conserved Plasmodium protein, unknown function
534	PBANKA_040630	DNA polymerase epsilon subunit b, putative
535	PBANKA_141540	conserved Plasmodium protein, unknown function
536	PBANKA_110290	conserved Plasmodium protein, unknown function
537	PBANKA_091580	pre-mRNA splicing factor, putative
538	PBANKA_102510	conserved Plasmodium protein, unknown function
539	PBANKA_144480	conserved Plasmodium protein, unknown function
540	PBANKA_090920	conserved Plasmodium protein, unknown function
541	PBANKA_000650	BIR protein, pseudogene, fragment
542	PBANKA_114390	conserved Plasmodium protein, unknown function
543	PBANKA_144850	sentrin-specific protease 1, putative
544	PBANKA_101210	conserved Plasmodium protein, unknown function
545	PBANKA_145080	conserved Plasmodium protein, unknown function
546	PBANKA_093890	IWS1-like protein, putative
547	PBANKA_031680	Plasmodium exported protein, unknown function
548	PBANKA_030980	Leu/Phe-tRNA protein transferase, putative
549	PBANKA_070060	Plasmodium exported protein, unknown function
550	PBANKA_113640	conserved Plasmodium protein, unknown function
551	PBANKA_136040	conserved Plasmodium protein, unknown function
552	PBANKA_020850	conserved Plasmodium protein, unknown function

553	PBANKA_010150	conserved Plasmodium protein, unknown function
554	PBANKA_110890	conserved Plasmodium protein, unknown function
555	PBANKA_051340	conserved Plasmodium protein, unknown function
556	PBANKA_110170	conserved Plasmodium protein, unknown function
557	PBANKA_092410	conserved Plasmodium protein, unknown function
558	PBANKA_040730	conserved Plasmodium protein, unknown function
559	PBANKA_100590	zinc-finger, RAN binding protein, putative
560	PBANKA_093680	conserved Plasmodium protein, unknown function
561	PBANKA_090360	dynamin-like protein, putative
562	PBANKA_132380	conserved Plasmodium protein, unknown function
563	PBANKA_060670	cysteine repeat modular protein 3 (CRMP3)
564	PBANKA_121560	40S ribosomal protein S3A, putative
565	PBANKA_142730	ABC1 family, putative
566	PBANKA_052420	early transcribed membrane protein (SEP2)
567	PBANKA_090600	alpha/beta hydrolase, putative
568	PBANKA_090490	conserved Plasmodium protein, unknown function
569	PBANKA_136000	DNA topoisomerase III, putative
570	PBANKA_112920	conserved Plasmodium protein, unknown function
571	PBANKA_093840	endoplasmic reticulum-resident calcium binding protein, putative
572	PBANKA_091030	guanylyl cyclase, putative (GCalpha)
573	PBANKA_081650	conserved Plasmodium protein, unknown function
574	PBANKA_132060	conserved Plasmodium protein, unknown function
575	PBANKA_062370	BIR protein, fragment
576	PBANKA_131130	conserved Plasmodium protein, unknown function
577	PBANKA_102960	conserved Plasmodium protein, unknown function
578	PBANKA_140990	clathrin-adaptor medium chain, putative
579	PBANKA_110060	BIR protein, pseudogene
580	PBANKA_050690	conserved Plasmodium protein, unknown function
581	PBANKA_133730	conserved Plasmodium protein, unknown function
582	PBANKA_093470	conserved Plasmodium protein, unknown function
583	PBANKA_091860	phosphatidylinositol-4-phosphate 5-kinase, putative
584	PBANKA_090950	AAA family ATPase, putative
585	PBANKA_060030	BIR protein
586	PBANKA_072210	BIR protein, pseudogene;
587	PBANKA_114640	BIR protein
588	PBANKA_020570	conserved Plasmodium protein, unknown function
589	PBANKA_144440	conserved Plasmodium protein, unknown function
590	PBANKA_093480	conserved Plasmodium protein, unknown function
591	PBANKA_091890	conserved Plasmodium protein, unknown function
592	PBANKA_121220	conserved Plasmodium protein, unknown function
593	PBANKA_113180	histone-lysine N-methyltransferase, putative
594	PBANKA_031650	Pb-fam-1 protein, pseudogene
595	PBANKA_134570	GPI transamidase subunit PIG-U, putative
596	PBANKA_103280	conserved Plasmodium protein, unknown function
597	PBANKA_090100	Pb-fam-1 protein
598	PBANKA_140840	conserved Plasmodium protein, unknown function
599	PBANKA_134420	conserved Plasmodium protein, unknown function
600	PBANKA_120180	conserved Plasmodium protein, unknown function
601	PBANKA_070430	SPRY domain, putative
602	PBANKA_123350	mRNA-binding protein PUF1 (PUF1)
603	PBANKA_135890	conserved Plasmodium protein, unknown function
604	PBANKA_113280	conserved Plasmodium protein, unknown function
605	PBANKA_142170	secreted ookinete protein, putative (PSOP20)
606	PBANKA_000770	BIR protein, pseudogene, fragment
607	PBANKA_020065	Pb-fam-1 protein

608	PBANKA_052390	glideosome associated protein with multiple membrane spans 2, putative
609	PBANKA_082170	inosine-5'-monophosphate dehydrogenase, putative
610	PBANKA_112890	conserved Plasmodium protein, unknown function
611	PBANKA_020130	lysophospholipase, putative
612	PBANKA_101040	conserved Plasmodium protein, unknown function
613	PBANKA_110640	conserved Plasmodium protein, unknown function
614	PBANKA_061670	NIMA related kinase 4 (NEK4)
615	PBANKA_010050	BIR protein
616	PBANKA_070040	Plasmodium exported protein, unknown function
617	PBANKA_100060	erythrocyte membrane antigen 1
618	PBANKA_140020	BIR protein
619	PBANKA_090770	conserved Plasmodium protein, unknown function
620	PBANKA_113800	conserved Plasmodium protein, unknown function
621	PBANKA_093280	conserved Plasmodium protein, unknown function
622	PBANKA_110650	rhomboid protease, putative (ROM4)
623	PBANKA_000440	BIR protein
624	PBANKA_070290	SET domain protein, putative
625	PBANKA_031510	DEAD/DEAH helicase, putative
626	PBANKA_122940	conserved Plasmodium protein, unknown function
627	PBANKA_140890	conserved Plasmodium protein, unknown function
628	PBANKA_102640	conserved Plasmodium protein, unknown function
629	PBANKA_021510	Pb-fam-1 protein, pseudogene
630	PBANKA_101630	proliferation-associated protein 2g4, putative
631	PBANKA_112690	protein kinase PK4 (PK4)
632	PBANKA_083560	cAMP-dependent protein kinase catalytic subunit (PKAc)
633	PBANKA_144660	conserved Plasmodium protein, unknown function
634	PBANKA_030120	ERCC1 nucleotide excision repair protein, putative
635	PBANKA_041850	Plasmodium exported protein, unknown function, fragment
636	PBANKA_062345	Pb-fam-1 protein, pseudogene
637	PBANKA_113690	SUMO ligase, putative
638	PBANKA_110090	Pb-fam-1 protein
639	PBANKA_082960	serine/threonine protein kinase, putative
640	PBANKA_111890	conserved Plasmodium protein, unknown function
641	PBANKA_062390	BIR protein
642	PBANKA_081870	XPA binding protein 1, putative
643	PBANKA_112880	CPW-WPC family protein, putative
644	PBANKA_030290	conserved Plasmodium protein, unknown function
645	PBANKA_000580	BIR protein
646	PBANKA_122500	serine/threonine protein kinase, FIKK family
647	PBANKA_092600	conserved Plasmodium protein, unknown function
648	PBANKA_143300	conserved Plasmodium protein, unknown function
649	PBANKA_100040	Pb-fam-1 protein
650	PBANKA_134450	conserved Plasmodium protein, unknown function
651	PBANKA_020125	BIR protein, pseudogene
652	PBANKA_000200	BIR protein
653	PBANKA_081850	conserved Plasmodium protein, unknown function
654	PBANKA_000880	BIR protein, pseudogene, fragment
655	PBANKA_140300	small heat shock protein, putative
656	PBANKA_122110	conserved Plasmodium protein, unknown function
657	PBANKA_120550	conserved Plasmodium protein, unknown function
658	PBANKA_120200	membrane skeletal protein, putative
659	PBANKA_121960	cg1 protein, putative
660	PBANKA_110780	longevity-assurance (LAG1) protein, putative
661	PBANKA_136440	conserved Plasmodium protein, unknown function
662	PBANKA_146300	osmiophilic body protein (G377)
663	PBANKA_051480	calmodulin, putative

664	PBANKA_140570	DnaJ protein, putative
665	PBANKA_070930	small ribosomal subunit processing microtubule-associated protein, putative
666	PBANKA_130480	conserved Plasmodium protein, unknown function
667	PBANKA_090840	conserved Plasmodium protein, unknown function
668	PBANKA_113890	conserved Plasmodium protein, unknown function
669	berg04:tRNA:rfamscan:399257-399330	unspecified product
670	PBANKA_081900	secreted acid phosphatase, putative,glideosome-associated protein 50, putative (GAP50)
671	PBANKA_101090	protein kinase, putative, fragment
672	PBANKA_070140	U6 snRNA-associated Sm-like protein LSm8, putative (LSM8)
673	PBANKA_101020	methionine aminopeptidase, type II, putative
674	PBANKA_100580	conserved Plasmodium protein, unknown function
675	PBANKA_072150	conserved Plasmodium protein, unknown function
676	PBANKA_061570	dynein heavy chain, putative
677	PBANKA_060090	conserved Plasmodium protein, unknown function
678	PBANKA_133220	translation initiation factor IF-1, putative
679	PBANKA_111820	conserved Plasmodium protein, unknown function
680	PBANKA_092110	methyltransferase, putative
681	PBANKA_082410	flavodoxin-like protein
682	PBANKA_110100	Pb-fam-1 protein
683	PBANKA_114080	conserved Plasmodium protein, unknown function
684	PBANKA_030610	6-cysteine protein (P230)
685	PBANKA_135120	conserved Plasmodium protein, unknown function
686	PBANKA_144300	NIMA related kinase 1, putative (NEK1)
687	PBANKA_020930	actin-related protein (ARP1)
688	PBANKA_100830	conserved Plasmodium protein, unknown function
689	PBANKA_070860	quinone oxidoreductase, putative
690	PBANKA_121260	male gamete fusion factor HAP2 (HAP2)
691	PBANKA_082710	protein kinase, putative
692	PBANKA_000350	Pb-fam-1 protein, pseudogene
693	PBANKA_120420	conserved Plasmodium protein, unknown function
694	PBANKA_062250	exonuclease I, putative
695	PBANKA_143440	secreted ookinete protein, putative (PSOP17)
696	PBANKA_101460	phosphotyrosyl phosphatase activator, putative
697	PBANKA_130110	conserved Plasmodium protein, unknown function
698	PBANKA_111450	conserved Plasmodium protein, unknown function
699	PBANKA_141360	serine/threonine protein kinase, putative
700	PBANKA_124250	RNA helicase, putative
701	PBANKA_142150	conserved Plasmodium protein, unknown function
706	PBANKA_114620	Plasmodium exported protein, unknown function
707	PBANKA_113290	regulator of chromosome condensation, putative
708	PBANKA_142660	conserved Plasmodium protein, unknown function
709	PBANKA_132610	conserved Plasmodium protein, unknown function
710	PBANKA_041540	conserved Plasmodium protein, unknown function, pseudogene
711	PBANKA_146590	BIR protein
712	PBANKA_131930	ferlin, putative
713	PBANKA_122370	conserved Plasmodium protein, unknown function
714	PBANKA_146340	adaptor-related protein complex 3, sigma 2 subunit, putative
715	PBANKA_040860	SAC3/GNAP family-related protein, putative
716	PBANKA_070130	conserved Plasmodium protein, unknown function
717	PBANKA_090190	tubulin-tyrosine ligase, putative
718	PBANKA_112900	secreted ookinete protein, putative (PSOP6)
719	PBANKA_102130	mitochondrial ribosomal protein L21 precursor, putative
720	PBANKA_103740	conserved Plasmodium protein, unknown function

721	PBANKA_142900	conserved Plasmodium protein, unknown function
722	berg13:tRNA:rfamscan:116536-116639	unspecified product
723	PBANKA_090020	BIR protein
724	PBANKA_051940	conserved Plasmodium protein, unknown function
725	PBANKA_124290	conserved Plasmodium protein, unknown function
726	PBANKA_083380	mRNA processing protein, putative
727	PBANKA_082010	PPPDE peptidase, putative
728	PBANKA_082420	perforin like protein 3 (PPLP3)
729	PBANKA_143250	DNA-binding chaperone, putative
730	PBANKA_080020	Pb-fam-1 protein, pseudogene
731	PBANKA_111390	conserved Plasmodium protein, unknown function
732	PBANKA_146190	conserved Plasmodium protein, unknown function
733	PBANKA_070870	RNA polymerase II mediator complex protein MED7, putative
734	PBANKA_030790	conserved Plasmodium protein, unknown function
735	PBANKA_092940	conserved Plasmodium protein, unknown function
736	berg08:tRNA:rfamscan:218200-218272	unspecified product
737	PBANKA_091390	conserved Plasmodium protein, unknown function
738	PBANKA_093380	conserved Plasmodium protein, unknown function
739	PBANKA_142780	peptidase family C50, putative
740	PBANKA_102260	pantothenate kinase, putative
741	PBANKA_000900	BIR protein, pseudogene, fragment
742	PBANKA_020035	BIR protein, pseudogene, fragment
743	PBANKA_000830	BIR protein, pseudogene, fragment
744	PBANKA_101270	conserved Plasmodium protein, unknown function
745	PBANKA_011185	BIR protein, pseudogene, fragment
746	PBANKA_020160	early transcribed membrane protein (ETRAMP)
747	PBANKA_130150	conserved Plasmodium protein, unknown function
748	berg02:tRNA:rfamscan:569318-569389	unspecified product
749	PBANKA_110280	4-diphosphocytidyl-2c-methyl-D-erythritol kinase (CMK), putative
750	PBANKA_103080	conserved Plasmodium protein, unknown function;
751	PBANKA_031130	conserved Plasmodium protein, unknown function
752	PBANKA_113430	patatin-like phospholipase, putative
753	PBANKA_133590	DNA-directed RNA polymerase, alpha subunit, putative
754	PBANKA_102130	mitochondrial ribosomal protein L21 precursor, putative
755	PBANKA_103740	conserved Plasmodium protein, unknown function
756	PBANKA_142900	conserved Plasmodium protein, unknown function
757	berg13:tRNA:rfamscan:116536-116639	unspecified product
758	PBANKA_090020	BIR protein
759	PBANKA_051940	conserved Plasmodium protein, unknown function
760	PBANKA_124290	conserved Plasmodium protein, unknown function
761	PBANKA_083380	mRNA processing protein, putative
762	PBANKA_082010	PPPDE peptidase, putative
763	PBANKA_082420	perforin like protein 3 (PPLP3)
764	PBANKA_143250	DNA-binding chaperone, putative
765	PBANKA_080020	Pb-fam-1 protein, pseudogene
766	PBANKA_111390	conserved Plasmodium protein, unknown function
767	PBANKA_146190	conserved Plasmodium protein, unknown function
768	PBANKA_070870	RNA polymerase II mediator complex protein MED7, putative
769	PBANKA_030790	conserved Plasmodium protein, unknown function
770	PBANKA_092940	conserved Plasmodium protein, unknown function
771	berg08:tRNA:rfamscan:218200-218272	unspecified product

772	PBANKA_091390	conserved Plasmodium protein, unknown function
773	PBANKA_093380	conserved Plasmodium protein, unknown function
774	PBANKA_142780	peptidase family C50, putative
775	PBANKA_102260	pantothenate kinase, putative
776	PBANKA_000900	BIR protein, pseudogene, fragment
777	PBANKA_020035	BIR protein, pseudogene, fragment
778	PBANKA_000830	BIR protein, pseudogene, fragment
779	PBANKA_101270	conserved Plasmodium protein, unknown function
780	PBANKA_011185	BIR protein, pseudogene, fragment
781	PBANKA_144540	transport protein Sec13, putative
782	PBANKA_130150	conserved Plasmodium protein, unknown function
783	berg02:tRNA:rfamscan:569318-569389	unspecified product
784	PBANKA_110280	4-diphosphocytidyl-2c-methyl-D-erythritol kinase (CMK), putative
785	PBANKA_103080	conserved Plasmodium protein, unknown function
786	PBANKA_031130	conserved Plasmodium protein, unknown function
787	PBANKA_113430	patatin-like phospholipase, putative
788	PBANKA_133590	DNA-directed RNA polymerase, alpha subunit, putative
789	PBANKA_144630	pre-mRNA-splicing factor ATP-dependent RNA helicase PRP2, putative
790	PBANKA_000470	BIR protein, pseudogene
791	PBANKA_060380	UGA suppressor tRNA-associated antigenic protein, putative
792	PBANKA_060440	targeted glyoxalase II, putative
793	PBANKA_083140	conserved Plasmodium protein, unknown function
794	PBANKA_102670	conserved Plasmodium protein, unknown function
795	PBANKA_132220	conserved Plasmodium protein, unknown function
796	PBANKA_142070	conserved Plasmodium protein, unknown function
797	PBANKA_072080	conserved Plasmodium protein, unknwon function
798	PBANKA_110130	conserved rodent malaria protein, unknown function
799	PBANKA_101270	conserved Plasmodium protein, unknown function
800	PBANKA_011185	BIR protein, pseudogene, fragment
801	PBANKA_130150	conserved Plasmodium protein, unknown function
802	berg02:tRNA:rfamscan:569318-569389	unspecified product
803	PBANKA_110280	4-diphosphocytidyl-2c-methyl-D-erythritol kinase (CMK), putative
804	PBANKA_103080	conserved Plasmodium protein, unknown function
805	PBANKA_031130	conserved Plasmodium protein, unknown function
806	PBANKA_113430	patatin-like phospholipase, putative
807	PBANKA_133590	DNA-directed RNA polymerase, alpha subunit, putative
808	PBANKA_144630	pre-mRNA-splicing factor ATP-dependent RNA helicase PRP2, putative
809	PBANKA_000470	BIR protein, pseudogene
810	PBANKA_060380	UGA suppressor tRNA-associated antigenic protein, putative
811	PBANKA_060440	targeted glyoxalase II, putative
812	PBANKA_083140	conserved Plasmodium protein, unknown function
813	PBANKA_102670	conserved Plasmodium protein, unknown function
814	PBANKA_132220	conserved Plasmodium protein, unknown function
815	PBANKA_142070	conserved Plasmodium protein, unknown function
816	PBANKA_072080	conserved Plasmodium protein, unknwon function
817	PBANKA_110130	conserved rodent malaria protein, unknown function
818	PBANKA_132510	conserved Plasmodium protein, unknown function
819	berg04:ncRNA:rfamscan:288046-288130	unspecified product
820	PBANKA_020150	Plasmodium exported protein, unknown function
821	PBANKA_020490	conserved Plasmodium protein, unknown function

822	PBANKA_000910	BIR protein, pseudogene, fragment
823	PBANKA_000378	Plasmodium exported protein, unknown function
824	PBANKA_060910	conserved Plasmodium protein, unknown function
825	PBANKA_021040	DNA mismatch repair protein, putative
826	PBANKA_040690	conserved Plasmodium protein, unknown function
827	PBANKA_122540	conserved Plasmodium protein, unknown function
828	PBANKA_090150	Product:conserved Plasmodium protein, unknown function
829	PBANKA_091180	DnaJ protein, putative
830	PBANKA_136180	conserved Plasmodium protein, unknown function
831`	PBANKA_062080	conserved Plasmodium protein, unknown function
832	PBANKA_093540	coq4 homolog, putative
833	PBANKA_146070	dipeptidyl peptidase 2, putative (DPAP2)
834	PBANKA_050870	conserved Plasmodium protein, unknown function
835	PBANKA_052450	conserved rodent malaria protein, unknown function
836	PBANKA_124270	beta adaptin protein, putative
837	PBANKA_081360	conserved Plasmodium protein, unknown function
838	PBANKA_135250	conserved Plasmodium protein, unknown function
839	PBANKA_030460	iron-sulfur assembly protein, putative
840	PBANKA_132910	plasmepsin VIII, putative
841	PBANKA_113980	conserved Plasmodium protein, unknown function
842	PBANKA_070560	conserved Plasmodium protein, unknown function
843	PBANKA_123110	tRNApseudouridine synthase, putative
844	PBANKA_122660	tubulin gamma chain, putative
845	PBANKA_083630	cytoadherence linked asexual protein 9 (CLAG9)
846	PBANKA_072090	conserved Plasmodium protein, unknown function
847	PBANKA_146210	conserved Plasmodium protein, unknown function
848	PBANKA_121720	conserved Plasmodium protein, unknown function
849	PBANKA_101260	conserved Plasmodium protein, unknown function
850	PBANKA_071000	conserved Plasmodium protein, unknown function
851	PBANKA_113470	conserved Plasmodium protein, unknown function
852	PBANKA_144540	transport protein Sec13, putative
853	PBANKA_113230	conserved Plasmodium protein, unknown function
854	PBANKA_100910	conserved Plasmodium protein, unknown function
855	PBANKA_010340	glyoxalase I, putative (GILP)
856	PBANKA_061900	conserved Plasmodium protein, unknown function

Table 2 showing the list of down regulated genes in *Pb SSPELD* knock out

S.No	GeneID	Function
2-3fold		
1	berg05_28s	Unspecified product
2	berg10:ncRNA: rfamscan: 937162-937469	Signal recognition particle RNA
3	PBANKA_062130	Conserved *Plasmodium* protein, unknown function
4	PBANKA_083000	RNA-binding protein, putative
5	PBANKA_090340	GAF domain-related protein
6	PBANKA_123450	Conserved *Plasmodium* protein, unknown function
7	PBANKA_111740	Conserved *Plasmodium* protein, unknown function
8	PBANKA_144710	Conserved *Plasmodium* protein, unknown function
1-2 fold		
9	PBANKA_142340	Conserved *Plasmodium* protein, unknown function
10	PBANKA_080500	RAP protein, putative
11	PBANKA_081390	26S proteasome regulatory subunit, putative
12	PBANKA_093950	Rad51 homolog, putative
13	PBANKA_093910	transcription factor with AP2 domain(s), putative (ApiAP2)

14	PBANKA_072020	conserved *Plasmodium* protein, unknown function
15	PBANKA_103590	glycerophodiester phosphodiesterase, putative
16	PBANKA_133020	conserved *Plasmodium* protein, unknwon function
17	PBANKA_132430	conserved *Plasmodium* protein, unknown function
18	PBANKA_133780	DHHC-type zinc finger protein, putative
19	PBANKA_010590	uroporphyrinogen III decarboxylase, putative (UROD)
20	PBANKA_040980	conserved protein, unknown function
21	PBANKA_060530	eukaryotic translation initiation factor 5, putative
22	PBANKA_146200	conserved *Plasmodium* protein, unknown function
23	PBANKA_050660	pre-mRNA splicing factor, putative
24	PBANKA_081100	small nuclear ribonucleoprotein Sm D3, putative (SNRPD3)
25	PBANKA_081570	membrane transporter, putative
26	PBANKA_010780	citrate synthase-like protein, putative
27	PBANKA_041660	replication protein A1, small fragment
28	PBANKA_142380	ABC transporter, putative
29	PBANKA_136120	conserved *Plasmodium* protein
30	PBANKA_101000	conserved *Plasmodium* protein, unknown function
31	PBANKA_020600	conserved *Plasmodium* protein, unknown function
32	PBANKA_rRNA_14	unspecified product
33	PBANKA_136380	phosphatidylinositol transfer protein, putative
34	PBANKA_rRNA_15.1	unspecified product (SSUD)
35	PBANKA_041180	vesicle transport v-SNARE protein, putative
36	PBANKA_041430	conserved *Plasmodium* protein, unknown function
37	PBANKA_061440	conserved *Plasmodium* protein, unknown function
38	PBANKA_MIT0001	cytochrome c oxidase subunit 3
39	PBANKA_135950	conserved *Plasmodium* protein, unknown function
40	PBANKA_rRNA_1	unspecified product (rRNA1
41	PBANKA_123800	conserved *Plasmodium* protein, unknown function
42	PBANKA_061050	glutathione peroxidase, putative
43	PBANKA_rRNA_18	unspecified product (LSUD
44	PBANKA_052240	steroid dehydrogenase, putative
45	PBANKA_132980	transcription factor with AP2 domain(s) (ApiAP2
46	PBANKA_112810	phospholipase (PL)
47	PBANKA_041070	conserved *Plasmodium* protein, unknown function
48	PBANKA_120660	26S proteasome regulatory subunit 4, putative
49	PBANKA_rRNA_LSUG	unspecified product
50	PBANKA_141300	cop-coated vesicle membrane protein p24 precursor, putative
51	PBANKA_143940	chromatin assembly protein, putative
52	PBANKA_rRNA_SSUB	unspecified product
53	PBANKA_071290	high mobility group protein, putative (HMGB2)
54	PBANKA_136050	ethanolamine-phosphate cytidylyltransferase (ECT)
55	PBANKA_051780	Sec1 family protein, putative
56	PBANKA_133390	conserved Plasmodium protein, unknown function
57	PBANKA_rRNA_11	unspecified product (SSUA)
58	PBANKA_082090	long chain fatty acid elongation enzyme, putative
59	PBANKA_136390	conserved *Plasmodium* protein, unknown function
60	PBANKA_071460	vacuolar sorting protein, putative
61	PBANKA_080910	subunit of proteaseome activator complex, putative
62	PBANKA_136070	conserved *Plasmodium* protein, unknown function
63	PBANKA_rRNA_RNA7	unspecified product
64	PBANKA_134430	chromatin assembly factor 1 subunit
65	PBANKA_100300	sequestrin, putative
66	PBANKA_131210	conserved *Plasmodium* protein, unknown function
67	PBANKA_041110	conserved *Plasmodium* protein, unknown function
68	PBANKA_050810	chromodomain-helicase-DNA-binding protein 1, putative (CHD1
69	PBANKA_100230	conserved *Plasmodium* protein, unknown function

70	PBANKA_103610	conserved *Plasmodium* protein, unknown function
71	PBANKA_110110	*Plasmodium* exported protein, unknown function
72	PBANKA_132120	vacuolar protein sorting-associated protein 4, putative
73	PBANKA_091230	EBNA2 binding protein P100 homologue, putative
74	PBANKA_011040	eukaryotic translation initiation factor 3 subunit L, putative
75	PBANKA_020720	vacuolar ATP synthase subunit c, putative
76	PBANKA_040530	40S ribosomal protein S23, putative
77	PBANKA_052310	eukaryotic initiation factor, putative
78	PBANKA_100440	conserved *Plasmodium* protein, unknown function
79	PBANKA_103330	conserved *Plasmodium* protein, unknown function
80	PBANKA_141010	conserved *Plasmodium* protein, unknown function
81	PBANKA_111310	GTP-binding protein, putative
82	PBANKA_112150	conserved *Plasmodium* protein, unknown function
83	PBANKA_144990	CCR4-NOT transcription complex subunit 4, putative
84	PBANKA_133190	eukaryotic initiation factor 4a, putative
85	PBANKA_134890	chaperone binding protein, putative)
86	PBANKA_091210	casein kinase 1 (CK1)
87	PBANKA_041410	inorganic pyrophosphatase, putative
88	PBANKA_060050	XPA binding protein 1, putative
89	PBANKA_rRNA_17.1	unspecified product (LSUE)
90	PBANKA_rRNA_9.1	unspecified product (RNA2
100	PBANKA_134670	60S ribosomal protein L23, putative
101	PBANKA_102330	conserved *Plasmodium* protein, unknown function
102	PBANKA_103510	fibrillarin, putative (NOP1)
103	PBANKA_103660	ribonucleotide reductase small subunit, putative
104	PBANKA_062110	conserved *Plasmodium* protein, unknown function
105	PBANKA_130780	heat shock protein 90, putative
106	PBANKA_061180	N-acetyltransferase, putative
107	PBANKA_143730	endoplasmin homolog precursor
108	PBANKA_133910	conserved *Plasmodium* protein, unknown function
109	PBANKA_135640	DNA helicase, putative
110	PBANKA_122000	conserved *Plasmodium* protein, unknown function
111	PBANKA_122120	60S ribosomal protein L34a, putative
112	PBANKA_092270	conserved *Plasmodium* protein, unknown function
113	PBANKA_051540	conserved *Plasmodium* protein, unknown function
114	PBANKA_081130	Ran-binding protein, putative
115	PBANKA_051190	60S ribosomal protein L3, putative
116	PBANKA_111100	RNA pseudouridylate synthase, putative, fragment
117	PBANKA_114330	conserved *Plasmodium* protein, unknown function)
118	PBANKA_122810	transcription factor with AP2 domain(s), putative (ApiAP2)
119	PBANKA_rRNA_19	unspecified product (RNA8)
120	PBANKA_102580	prefoldin subunit 2, putative
121	PBANKA_091800	60S ribosomal protein, putative
122	PBANKA_020810	conserved *Plasmodium* protein, unknown function
123	PBANKA_051640	conserved *Plasmodium* protein, unknown function
124	PBANKA_070250	leucine - tRNA ligase, putative
125	PBANKA_144140	proliferating cell nuclear antigen 2, putative
126	PBANKA_101430	conserved *Plasmodium* protein, unknown function
127	PBANKA_123840	conserved *Plasmodium* protein, unknown function
128	PBANKA_060190	high mobility group protein, putative (HMGB1)
129	PBANKA_134880	conserved *Plasmodium* protein, unknown function
130	PBANKA_083310	aspartyl aminopeptidase, putative
131	PBANKA_135530	conserved *Plasmodium* protein, unknown function
132	PBANKA_135880	conserved *Plasmodium* protein, unknown function
133	PBANKA_120500	RNA-binding protein, putative
134	PBANKA_120900	eukaryotic translation initiation factor 2, beta, putative
135	PBANKA_082180	U4/U6 snRNA-associated-splicing factor, putative

136	PBANKA_rRNA_10.2	unspecified product (RNA3)
137	PBANKA_136240	conserved *Plasmodium* protein, unknown function
138	PBANKA_111790	conserved *Plasmodium* protein, unknown function
139	PBANKA_123250	eukaryotic translation initiation factor 3 subunit, putative
140	PBANKA_052280	40S ribosomal protein S19, putative
141	PBANKA_100020	Pb-fam-1 protein
142	PBANKA_102250	surface protein,putative
143	PBANKA_091830	transporter, putative
144	PBANKA_092750	conserved *Plasmodium* protein, unknown function
145	PBANKA_101950	60S ribosomal protein L5, putative
146	PBANKA_120190	40S ribosomal protein S20e, putative
147	PBANKA_120260	zinc finger, C3HC4 type, putative
148	PBANKA_120440	DNA/RNA-binding protein Alba 3, putative
149	PBANKA_132640	glyceraldehyde-3-phosphate dehydrogenase, putative
150	PBANKA_010170	conserved *Plasmodium* protein, unknown function
151	PBANKA_021210	eukaryotic translation initiation factor 2 alpha subunit, putative
152	PBANKA_060270	nucleosome assembly protein 1, putative
153	PBANKA_060480	eukaryotic translation initiation factor 3 subunit 8, putative
154	PBANKA_142990	phosphatidylinositol-glycan, putative
155	PBANKA_135510	40S ribosomal protein S6, putative
156	PBANKA_103390	40S ribosomal protein S8e, putative
157	PBANKA_121100	GMP synthetase, putative (GMPS)
158	PBANKA_083550	conserved *Plasmodium* protein, unknown function
159	PBANKA_090180	conserved *Plasmodium* protein, unknown function
160	PBANKA_093030	GTP-binding nuclear protein, putative
161	PBANKA_031160	conserved *Plasmodium* protein, unknown function
162	PBANKA_081300	inhibitor of cysteine proteases (ICP);
163	PBANKA_142350	60S ribosomal protein L13-2, putative
164	PBANKA_142610	conserved *Plasmodium* protein, unknown function
165	PBANKA_144700	cytochrome b5, putative
166	PBANKA_140740	mRNA-decapping enzyme 2, putative (DCP2)
167	PBANKA_140850	mitochondrial ATP synthase delta subunit, putative (OSCP)
168	PBANKA_110570	60S ribosomal subunit protein L24, putative
169	PBANKA_051740	myb2 transcription factor, putative (Myb2)
170	PBANKA_103970	conserved *Plasmodium* protein, unknown function
171	PBANKA_120230	conserved *Plasmodium* protein, unknown function
172	berg06:rRNA:rfamscan:875179-875314	unspecified product
173	PBANKA_040480	FAD-dependent glycerol-3-phosphate dehydrogenase, putative
174	PBANKA_040550	60S ribosomal protein L7, putative
175	PBANKA_051090	40S ribosomal protein S2B, putative
176	PBANKA_100350	conserved *Plasmodium* protein, unknown function
177	PBANKA_100690	conserved *Plasmodium* protein, unknown function
178	PBANKA_102350	conserved *Plasmodium* protein, unknown function
179	PBANKA_113120	60S ribosomal protein L7-2, putative
180	PBANKA_123170	60S ribosomal protein L8, putative
181	PBANKA_092960	pre-RNA processing ribonucleoprotein, putative
182	PBANKA_010950	transcription factor with AP2 domain(s), putative (ApiAP2)
183	PBANKA_133870	plasmepsin V, putative (PMV)
184	PBANKA_140710	conserved *Plasmodium* protein, unknown function
185	PBANKA_090310	nucleolarpreribosomal assembly protein, putative
186	PBANKA_090980	conserved *Plasmodium* protein, unknown function
187	PBANKA_040170	conserved *Plasmodium* protein, unknown function
188	PBANKA_140680	40S ribosomal protein S27, putative
189	PBANKA_122200	sin3 associated polypeptide p18 protein, putative
190	PBANKA_123480	40S ribosomal protein S9, putative

191	PBANKA_030110	conserved *Plasmodium* protein, unknown function
192	PBANKA_060570	small subunit rRNA processing factor, putative
193	PBANKA_061200	ATP-dependent Clp protease proteolytic subunit, putative
194	PBANKA_061860	conserved *Plasmodium* protein, unknown function
195	PBANKA_142360	40S ribosomal protein S16, putative
196	PBANKA_130460	adaptor complexes medium subunit family
197	PBANKA_090090	reticulocyte binding protein, putative, fragment (Pb235)
198	PBANKA_092210	40S ribosomal protein S18, putative
199	PBANKA_020520	conserved *Plasmodium* protein, unknown function
200	PBANKA_030560	acyl carrier protein, putative (ACP)
201	PBANKA_031450	40S ribosomal protein S26e, putative
202	PBANKA_041830	retrieval receptor for endoplasmic reticulum membrane proteins, putative
203	PBANKA_071010	2-oxoglutarate dehydrogenase e1, putative
204	PBANKA_100880	glucose-6-phosphate isomerase, putative
205	PBANKA_021130	cysteine desulfurase, putative (NFS)
206	PBANKA_040540	40S ribosomal protein S12, putative
207	PBANKA_041750	60S ribosomal protein L32, putative
208	PBANKA_145230	conserved *Plasmodium* protein, unknown function
209	PBANKA_140410	membrane integral peptidase, M50 family, putative
210	PBANKA_082020	thioredoxin, putative
211	PBANKA_041060	60S ribosomal protein L26, putative
212	PBANKA_050360	60S ribosomal protein L30e, putative
213	PBANKA_050640	conserved *Plasmodium* membrane protein, unknown function
214	PBANKA_061820	phosphoinositide-binding protein, putative
215	PBANKA_061980	zinc finger protein, putative
216	PBANKA_135630	conserved *Plasmodium* protein, unknown function
217	PBANKA_113990	conserved *Plasmodium* protein, unknown function
218	PBANKA_123510	U6 snRNA-associated sm-like protein lsm2, putative (LSM2)
219	PBANKA_123560	adenosylhomocysteinase, putative (SAHH)
220	PBANKA_124110	nucleolarJumonji domain interacting protein, putative
221	PBANKA_030860	GDP-fructose:GMP antiporter, putative
222	PBANKA_060730	conserved *Plasmodium* protein, unknown function
223	PBANKA_061090	HSP40, subfamily A, putative
224	PBANKA_071220	conserved *Plasmodium* protein, unknown function
225	PBANKA_071260	14-3-3 protein, putative
226	PBANKA_081420	elongation factor 1-beta, putative
227	PBANKA_144950	conserved *Plasmodium* protein, unknown function
228	PBANKA_110310	actin-depolymerizing factor 1 (ADF1)
229	PBANKA_113020	ER lumen protein retaining receptor, putative
230	PBANKA_122670	AAA family ATPase, putative
231	PBANKA_040490	conserved *Plasmodium* protein, unknown function
232	PBANKA_041050	transporter, putative
233	PBANKA_060680	mitochondrial ACP precursor, putative
234	PBANKA_141050	malonyl CoA-acyl carrier protein transacylase precursor, putative
235	PBANKA_141130	eukaryotic translation initation factor 4 gamma, putative
236	PBANKA_145280	cell cycle control protein, putative
237	PBANKA_112110	radical SAM protein, putative
238	PBANKA_121270	conserved *Plasmodium* protein, unknown function
239	PBANKA_091350	conserved *Plasmodium* protein, unknown function
240	PBANKA_050710	CDGSH iron-sulfur domain-containing protein, putative
241	PBANKA_134930	conserved *Plasmodium* protein, unknown function
242	PBANKA_120250	conserved *Plasmodium* protein, unknown function
243	PBANKA_120750	conserved *Plasmodium* protein, unknown function
244	PBANKA_120980	proteasome subunit beta type-5, putative
245	PBANKA_123100	40S ribosomal protein S14, putative

246	PBANKA_124150	conserved *Plasmodium* protein, unknown function
247	PBANKA_132140	large ribosomal subunit nuclear export factor, putative (UIS20)
248	PBANKA_060230	conserved *Plasmodium* protein, unknown function
249	PBANKA_141410	phosphatidylinositol synthase, putative (PIS)
250	PBANKA_144910	conserved *Plasmodium* protein, unknown function
251	PBANKA_144970	conserved *Plasmodium* protein, unknown function
252	PBANKA_101280	conserved *Plasmodium* protein, unknown function
253	PBANKA_121200	conserved *Plasmodium* protein, unknown function
254	PBANKA_041350	conserved *Plasmodium* protein, unknown function
255	PBANKA_041460	40S ribosomal protein S15A, putative
256	PBANKA_135100	1-deoxy-D-xylulose 5-phosphate synthase, putative
257	PBANKA_094320	casein kinase II beta chain, putative
258	PBANKA_113000	Ran-binding protein, putative
259	PBANKA_113330	elongation factor 1 alpha (EF-1alpha)
260	PBANKA_114100	conserved *Plasmodium* protein, unknown function
261	PBANKA_091790	26S protease subunit regulatory subunit 6a, putative
262	PBANKA_040520	T-complex protein beta subunit, putative
263	PBANKA_050920	formin 2, putative
264	PBANKA_142510	karyopherin alpha, putative (KARalpha
265	PBANKA_133860	60S ribosomal protein L23a, putative
266	PBANKA_136420	60S ribosomal protein L17, putative
267	PBANKA_114560	conserved *Plasmodium* protein, unknown function
268	PBANKA_120600	conserved *Plasmodium* protein, unknown function
269	PBANKA_121820	T-complex protein 1 epsilon subunit, putative
270	PBANKA_081890	heat shock protein 70, putative
271	PBANKA_135900	sec61 alpha subunit, putative
272	PBANKA_121020	QF122 antigen, putative
273	PBANKA_130500	conserved *Plasmodium* protein, unknown function
274	PBANKA_000280	reticulocyte binding protein, putative, fragment (Pb235)
275	PBANKA_031090	T-complex protein 1, putative
276	PBANKA_081350	conserved *Plasmodium* protein, unknown function
277	PBANKA_145260	calcyclin binding protein, putative
278	PBANKA_131740	co-chaperone p23, putative
279	PBANKA_122840	mannose-6-phosphate isomerase, putative
280	PBANKA_144110	hydrolase, putative
281	PBANKA_136030	DNA/RNA-binding protein Alba 4, putative
282	PBANKA_114170	60S ribosomal protein L40/UBI, putative
283	PBANKA_130620	tRNA binding protein, putative
284	PBANKA_132100	conserved *Plasmodium* protein, unknown function
285	PBANKA_083340	30S ribosomal protein S6, putative)
286	PBANKA_041100	conserved *Plasmodium* protein, unknown function
287	PBANKA_052290	pre-mRNA-splicing helicase BRR2, putative
288	PBANKA_080490	ubiquitin-protein ligase e3, putative
289	PBANKA_121420	ribonucleotide reductase small subunit, putative
290	PBANKA_130530	FACT complex subunit SSRP1, putative (FACT-S)
291	PBANKA_091440	heat shock protein hsp70 homologue, putative (UIS24)
292	PBANKA_093770	apicoplast ribosomal protein L36e precursor, putative
293	PBANKA_010850	mitochondrial ribosomal protein L19 precursor, putative
294	PBANKA_030700	60S ribosomal protein L37ae, putative
295	PBANKA_040770	60S acidic ribosomal protein P2, putative
296	PBANKA_051620	phosphatidyl inositol glycan, class A, putative
297	PBANKA_144690	dihydrolipoamide dehydrogenase, putative (mLipDH)
298	PBANKA_122920	60S ribosomal protein L19, putative
299	PBANKA_130330	ubiquinol-cytochrome c reductase, iron-sulfur subunit, putative
300	PBANKA_082720	monocarboxylase transporter, putative

301	PBANKA_090640	60S ribosomal protein L35ae, putative
302	PBANKA_091460	RNA (uracil-5-)methyltransferase, putative
303	PBANKA_091520	conserved *Plasmodium* protein, unknown function)
304	PBANKA_093720	asparagine-rich antigen, putative
305	PBANKA_010870	conserved *Plasmodium* protein, unknown function
306	PBANKA_031440	conserved *Plasmodium* protein, unknown function
307	PBANKA_141030	M1-family aminopeptidase, putative
308	PBANKA_135500	vacuolar ATP synthase subunit d, putative
309	PBANKA_141030	M1-family aminopeptidase, putative
310	PBANKA_101030	dynein-related AAA-type ATPase, putative
311	PBANKA_111700	histone H2A, putative (H2A
312	PBANKA_112170	leucyltRNA synthase, putative
313	PBANKA_114060	DNA-directed RNA polymerase II, putative
314	PBANKA_121310	prohibitin, putative
315	PBANKA_145610	40S ribosomal protein S17, putative
316	PBANKA_134390	conserved *Plasmodium* protein, unknown function
317	PBANKA_100100	conserved *Plasmodium* protein, unknown function
318	PBANKA_131080	40S ribosomal protein S2, putative
319	PBANKA_132270	ATP-dependent RNA helicase DBP5, putative
320	PBANKA_090670	conserved *Plasmodium* protein, unknown function
321	PBANKA_091010	beta-catenin-like protein 1, putative
322	PBANKA_092060	conserved *Plasmodium* protein, unknown function
323	PBANKA_092340	60S ribosomal protein L35, putative
324	PBANKA_071120	conserved *Plasmodium* protein, unknown function
325	PBANKA_071120	conserved *Plasmodium* protein, unknownfunction
326	PBANKA_146450	DEAD/DEAH helicase, putative
327	PBANKA_134120	conserved *Plasmodium* protein, unknown function
328	PBANKA_140440	conserved *Plasmodium* protein, unknown function
329	PBANKA_140760	60S ribosomal protein L24, putative
330	PBANKA_101860	60S ribosomal protein L21e, putative
331	PBANKA_122350	RNA helicase, putative
332	PBANKA_123420	40S ribosomal protein S24, putative
333	PBANKA_132310	conserved *Plasmodium* protein, unknown function
334	PBANKA_132440	60S ribosomal protein L27, putative
335	PBANKA_082880	cytochrome c oxidase, putative
336	PBANKA_092160	conserved *Plasmodium* protein, unknown function
337	PBANKA_080320	inositol-phosphate phosphatase, putative
338	PBANKA_135370	conserved *Plasmodium* protein, unknown function
339	PBANKA_101050	Hsp70/Hsp90 organizing protein, putative (HOP)
340	PBANKA_103760	U3 small nucleolar ribonucleoprotein, putative
341	PBANKA_113530	conserved *Plasmodium* protein, unknown function
342	PBANKA_122650	proteasome beta-subunit, putative
343	PBANKA_090470	60S ribosomal protein L41, putative
344	PBANKA_020870	4-hydroxy-3-methylbut-2-enyl diphosphate reductase, putative (LytB)
345	PBANKA_144410	t-complex protein 1 gamma subunit, putative
346	PBANKA_135170	conserved *Plasmodium* protein, unknown function
347	PBANKA_135920	DNA/RNA-binding protein Alba 2, putative
348	PBANKA_102480	conserved *Plasmodium* protein, unknown function
349	PBANKA_110900	RNA polymerase I, putative
350	PBANKA_111680	conserved *Plasmodium* protein, unknown function

2.4 Discussion

Malaria transmission to vertebrates occurs when female *Anopheles* mosquitoes introduces sporozoites into skin while probing for the blood meal [148]. Salivary gland sporozoites modulate their gene expression such that they achieve competence for infecting hepatocytes. Several lines of evidence indicate that the products of sporozoite specific genes are crucial in performing an arsenal of functions central to establishment of infection in the vertebrate host. For example, the selective arrest of sporozoites to target cell hepatocytes is a function of CSP [15, 149], while transmembrane proteins like TRAP [150], S6 [140], TRSP [151], TREP [152], SSP3 [141] SEP2 [153]are important for movement of sporozoites through gliding motility and others like *Pb* LCAT [12], SPECT [10], SPECT-2 [11] are necessary for tissue migration and host cell invasion. Other category of genes like UIS-3 [28], UIS-4 [27], P36p [29] a member of P48/45 family and members of 6-Cys family related proteins like sequestrin and B9 [154] have shown to be essential for completion of liver stage development. Thus, identifying the function of other novel sporozoite membrane proteins is important because they can be of therapeutic potential either to block attachment of sporozoite to hepatocytes, mitigate their traversal activity or to prevent the EEF transformation in the hepatocytes.

In the current study, we investigated the role of PBANKA_091090 [*Pb SSPELD*] in pre erythrocytic biology owing to its high transcription in salivary gland sporozoites in SAGE analysis [144]. We generated *Pb SSPELD* null mutants by replacing its ORF with a cassette coding GFP and malaria drug resistance marker hDHFR. The KO parasites were successfully cloned and investigated for their ability to complete the malaria life cycle. The KO parasites were not compromised in their ability to propagate asexually or transmit malaria to mosquitoes. Female *Anopheles* mosquitoes infected with *Pb SSPELD* KO parasites developed oocyst numbers comparable to that of WT and also showed identical sporulating pattern. The number of sporozoites that reached the salivary glands also were comparable to that of WT. Thus *Pb SSPELD* played no role in the mosquito stages of the *P.berghei* life cycle. However when *Pb SSPELD* mutant sporozoites were introduced by natural mosquito bite into C57BL/6 mice, they failed to cause blood stage infection. When high doses of mutant sporozoites were injected into mouse, an occasional break through infection was noted, with a significantly delayed prepatent period of day 8/9. To confirm the possibility of *Pb SSPELD* mutants being associated with a defect in EEF development, we studied its*in vitro* transformation in HepG2 cells by analyzing its growth during different times points. We observed that *Pb SSPELD* showed a defect during mid and later liver stage development.

Considering the significant role of *Pb SSPELD* in liver stage development, we generated mCherry transgenic of *Pb SSPELD* and studied the localization across all life cycle stages by visualization of the reporter expression. While no mCherry expression was found in the asexual blood stages, we noted the expression of reporter from D14 onwards, where it localized to the sporozoites within the oocyst, that became more prominent in the D18-20 salivary gland sporozoites. Our attempts to demonstrate the cellular distribution of *PbSSPELD* mCherry in sporozoite stages showed its association with plasma membrane, as confirmed with its colocalisationwith CSP, another major sporozoite surface protein [146]. The sporozoite membrane localization of *Pb SSPELD* was unexpected, given that there were no predicted membrane targeting or attachment motifs in its coding sequence. However, our localization data is consistent with a recent investigation that identified a sub subset of putative surface exposed sporozoite proteins revealed through biotin conjugated cross linking method. Interestingly, the orthologue of *Pb SSPELD* was reported in this study and was detected in the proteomics analysis of *P. yoelli*[Py: PY02432] and *P.falciparum* sporozoites (Pf: PF11_0545)[155]. Further, the mCherry also localized to the PVM membrane of EEF at 36 hours. The fact *Pb SSPELD*mCherry continues to express at 36 hours and localizes to PVM may reveal its critical role in the EEF development which accounted for the failure of *Pb SSPELD* KO to complete development at the hepatic stages. *Pb SSPELD* orthologue was also recovered in *P. vivax*sporozoite arrays and designated as *SCOT-2* [156]. Its occurrence across *Plasmodium* species of human and rodents may likely indicate its conserved role in the liver stage development.

To unravel the biological process and pathways that were affected following depletion of *Pb SSPELD*, we performed micro array analysis of WT and *Pb SSPELD* mutants at 36 hours time point. These studies revealed dramatic changes in the expression of several important functional clusters. The up regulated clusters included genes that governed nucleotide excision repair, ubiquitin mediated proteolysis gene, DNA repair genes, purine metabolism pathway and mRNA splicing pathway. Up regulation of these genes may likely point to the needs of the developing EEFs in establishing infection within hepatocytes. The functional clusters pertaining to ribosome genes, general transcription by RNA polymerase 1, glycolysis/gluconeogenesis, cell cycle pathway, oxidative phosphorylation, proteasome and ribosome pathway were down regulated in *Pb SSPELD* KO. A group of putative genes like enolase (PBANKA_121430), receptor for activated c kinase (RACK)(PBANKA_070390), proteindisulphideisomerase(PBANKA_070280), HSP110c (PBANKA_121930), endoplasmin(GRP94)(PBANKA_143730), and biotin carboxylase subunit of acetyl CoA

carboxylase (PBANKA_133280) that was shown to be induced in the late liver stages of *P. yoelii* in the transcriptomic analysis [128] were all down regulated in *Pb SSPELD* mutants. In the absence of any information about *Pb SSPELD* as a probable signaling protein that can modulate extensively the global gene expression, we hypothesise that much of these changes may not be a direct consequence of *Pb SSPELD* depletion, but rather a secondary effect, induced owing to the developmental defect of the mid liver stage parasites in the absence of *Pb*SSPELD. In preparation for liver stage schizogony it is expected that there could be in increased demand for synthesis of new proteins and lipids. Down regulation of genes central to these processes in *Pb SSPELD* KO may be a consequence of premature termination of the liver stage development. Concurrent with such assumption, some of the well characterized late liver stage genes like UIS-4 [27], LIPS2 [157], EXP-1 [18], and FABL [94] and SERA4 [25] were down regulated. Considering the lack EEF maturation in *Pb SSPELD* mutants together with the likely localisation to the PVM membrane, a speculative role of *Pb SSPELD* in membrane biogenensis required for formation of liver stage merozoites [18], nutrient acquisition and protein export [158, 159] or egress may not be excluded and merits further investigation.

Protective immunity generated by developmentally arrested liver stage parasites forms the basis for resistance against infectious challenge. Owing to the defect of *Pb SSPELD* mutants in completion of liver stage development, we analysed its potential to generate pre-erythrocytic immunity. A prime boost regimen with $2X10^4$ *Pb SSPELD* mutants in C57BL6 mice resulted in protective immunity whose efficacy was nearly 50%. Analysis of corelates of protection revealed significantly more CD4+ T cells as compared to CD8+ T cells. Cross presentation of antigens by liver resident professional antigen presenting cells have been shown following acquisition of infected hepatocytes harbouring aborted EEFs [160] and in other infectious models[161, 162]. This may account for the observed activation of CD4+ and CD8+ T cells following immunization with *Pb SSPELD* mutants.

The top two groups of genes classified in the SAGE transcriptomic analysis [144] were based on the abundance of the SAGE tags recovered and included candidates essential for gliding motility, cell traversal activity and sporozoite or liver stage development. The group 1 included genes that were independently discovered through other methods of gene expression and included UIS-4, UIS-7, [80], TRAP [131, 134]and S23 [131]. Group 2 included genes like S13/SPECT, S21/Pb TRSP, S12, [131], UIS10 [80]. Other group 2 genes included ECP1, a cysteine protease required for egress of sporozoites from oocyst [163] and Pbs36p

[29], a member of P45/48 family of surface proteins shown to be important for completion of liver stage development. Thus the role of *Pb* SSPELD in liver stages development is not surprising given that in the SAGE analysis of sporozoite transcriptome, it clusters with well characterized transcripts like UIS-4 [27] and Pbs36p [29] whose essential role in liver stage development has been demonstrated through gene KO experiments. In conclusion we argue that with dual attributes of being associated with sporozoite plasma membrane and having an essential role in the liver stage development*, Pb*SSPELD can be exploited either to generate a recombinant subunit vaccine capable of eliciting sporozoite neutralizing antibodies, or alternatively *Pb SSPELD* mutants can be additional candidates of choice if multiple attenuation of *Plasmodium* parasites are desired to ensure a safer whole organism vaccine. Having strong orthologues in other human species of *Plasmodium*[155, 156], *SSPELD* can be a good choice for obtaining attenuated liver stages of human malaria parasites. In conclusion, our studies highlight the importance of *Pb* SSPELD in completion of liver stage development and these mutants as a complement of pre-erythrocytic immunogens capable of eliciting protective immunity.

CHAPTER 3

Functional characterization of *P. berghei SCOT3* by reverse genetics reveals its role in egress of liver stage parasites

3.1 Introduction

Malaria infects nearly 300 million people every year world wide and approximately 1.5-2 million people die following exposure to this disease. Approximately 40% of the world population living in poor countries is at risk of getting infected with *Plasmodium* species. Of all *Plasmodium* species that infect humans, *P. falciparum* has been the model of emphasis and priority and studied extensively because of the severe clinical manifestation associated with this human species, even though *P. vivax* remains the most geographically wide spread species with infection rates around 80-250 million each year [164]. This scenario is because of the notion that *P. vivax* infections are relatively infrequent, benign, and can be treated easily as compared to *P. falciparum*. However, several recent lines of evidence suggest that *P. vivax* may cause equally adverse symptoms, as *P. falciparum* [165-167]. A fundamental biological difference between *P. falciparum* and *P. vivax* is the ability of the latter to form dormant liver stages called as hypnozoites. These forms are extremely resistant to schizonticidal drugs that are effective against asexual blood stages. The reasons behind occurrence of hypnozoite stages in *P. vivax* is not known, though it is believed that these dormants forms facilitates the persistence of parasites, especially in those areas where mosquito populations are appear seasonally. Not much is known as what parameters triggers relapse of *P. vivax*, although it occurs at varying frequencies in different strains of *P. vivax* and some studies point to the role of latitude in reverting the *P. vivax* latency [168]. In the absence of any information on the biology or metabolism of the hypnozoites, there has been a lapse in devising any drugs that could specifically target these stages. The only known drug that is effective against these stages is the 8-aminoquinoline drug-primaquine, but its mode of action is not completely understood. The growing drug resistance and lack of effective vaccines have greatly hindered the control of *P. vivax* infections.

Though considerable investigation in the field of liver stage biology has been done in rodent species in recent past [128, 169], neither *P. yoelli* nor *P. berghei* can form hyponozoites, thus precluding the possibility of any insight into these unique stages. One possible option to study the hypnozoite biology is to use the *P. cynomolgi* species that infects monkeys or alternatively, setting up *P. vivax in vitro* cultures obtained from blood samples harvested from infected humans or vectors that harbor mosquito stages of this species. Because of these technical limitations, genetic manipulations of *P. vivax* have been less frequently attempted [170]. While reverse genetics of *P. falciparum* has accelerated greatly the understanding of gene

specific functions, only comparative genomics is likely to offer an insight into the probable gene functions in *P. vivax* in the absence of routine genetic manipulations. Profiling of gene expression in *P. falciparum* [125, 129] and *P. yoelli* [171], across stages that occur in mammalian host and in the *Anopheles* vector, and *P. vivax* [172, 173] in blood stages have provided to some extent a glimpse of the how gene functions could be predicted based on the expression patterns throughout the development of *Plasmodium*.

To characterize the transcriptome of *P. vivax* in stages that occur in mammals and in *Anopheles* species, Westernberger SJ et al., [156] used a systems biology approach. By using a high density tiling custom arrays, a diverse set of gene expression data was obtained from human and mosquito stages that included gametes, zygotes, ookinetes and sporozoites and *in vivo* asexual blood stages from subjects of Pruvian Amazon [172]. Comparison of *P. vivax* data sets with that of *P. falciparum* and *P. yoelli* revealed novel insight into the metabolic activity of the parasites growing in human subjects. There were several important highlights of this paper. Primarily, analysis of 5,419 genes revealed extensive changes in the transcriptome as the parasites passes from human to mosquitoes. Several genes that govern one biological process or encode for components of molecular machinery were co-expressed. Co-ordinated transcription was also a function of several genes encoding for exported proteins and members of multigene families. The proteins encoded by these stage specifically regulated genes may be novel targets for therapeutic intervention and vaccines.

Interestingly, the sporozoite specific genes recovered from the *P. vivax* sporozoite transcriptome also seemed to be conserved in the sporozoite transcriptome of *P. yoelli* [171] and *P. falciparum* [174] with a positively correlated expression of abundantly expressed genes [r=0.5]. These findings suggest that very minor transcriptional regulation may account for the formation of dormant hynozoites in *P. vivax*. Some of these well characterized transcripts included candidates like UIS-1, UIS-2 discovered in SSH of midgut sporozoites versus salivary gland sporozoites [80], transcripts like CS and AMA1, that are prime candidates for pre-erythrocytic vaccine development and other genes like UIS-3 [28], UIS-4 [80, 27], P52 [29], whose depletion lead to the generation of genetically attenuated sporozoites. A set of genes that were upregulated across all species of sporozoites and that were not annotated yet were designated as SCOT genes [Sporozoite Conserved Orthologous Transcripts]. We selected for our study one of these genes referred to as *Pv SCOT3* and having known that it has orthologue in *P. berghei,* we resorted to functionally characterise this gene by reverse genetics approach. *Pv* SCOT3 ranked 23 amongst other sporozoite upregulated genes reported in this

study where as SCOT1 and SCOT2 ranked number 1 and 3 respectively. The orthologue of *Pv SCOT2* in *P. berghei* is *SSPELD* that was functionally characterized in chapter 2 of this thesis and shown to be important for *Plasmodium* liver stages development.

In the current chapter we provide evidence for the role of *Pb SCOT3* in egress completion of *Plasmodium* liver stages. *Pb SCOT3* KO parasites were successfully generated and investigated for their ability to propagate in mammalian host as well as in the *Anopheles* mosquitoes. While the *Pb SCOT3* KO parasites were indistinguishable from WT parasites in their ability to propagate asexually, or transmit malaria to mosquito and complete their life cycle, they however, failed to produce a timely blood stage infection when *Pb SCOT3* sporozoites were delivered through natural mosquito bite. Occasionally however, the mutants gave rise to a break through infection, with a significant delay in the prepatent period. *In vitro* analysis of EEF growth at different time points at 12h, 36h and 62 hours revealed that the mutants did not differ from WT EEFs at 12 and 36 hours. Surprisingly however, the *SCOT3* mutants exhibited better EEF growth than WT at 62 hours. The fact that *Pb SCOT3* mutants developed completely in HepG2 cells and were unable to initiate blood stage infection or occasionally its ability to give rise to a delayed prepatent period [D9], suggested a defect in the egress of the mature EEFs. These findings point to the role of *Pb SCOT-3* in late liver stages and is consistent with its enhanced expression in the sporozoites stage in the transcriptomic analysis [156].

3.2 Materials and Methods

All methods used in functional characterization of *Pb SCOT3* KO have also been described in great detail in generation and functional characterization of *Pb SSPELD* in chapter 2. Since many of the methods are common, to avoid redundancy, the description of methods in this chapter have been made very brief.

3.2.1 Retrieval of target genes sequences:

Two public domain databases namely Plasmo DB (http://www.plasmodb.org/ plasmo) and Sanger gene data base (http://www.genedb.org/Homepage/Pberghei) were used to retrieve the 5' untranslated region, the ORF and the 3' untranslated regions of *Pb SCOT3*.

3.2.2 Construction of the transfection /knockout vector and transfection of WT parasites

Construction of the transfection vector involved cloning of approximately 500bp of 5' and 3' DNA fragments that flanked the *Pb SCOT3* (PBANKA_101470) locus. The 5' fragment was amplified by using forward primer, FP1-5'AGTCTCGAGATGGGTTATCCACTTTCTTA3'), where Xho1 site underlined and reverse primer, RP1-5'CGTATCGATTGAGTTTAATTGTCTAGCTAT3', where Cla1 site underlined. The 3' fragment was amplified using forward primer, FP2-5'ATAGCGGCCGCAATAGCAAGCATCGAATAG3', where Not1 site underlined and reverse primer, RP2-5'GTAGGCGCGCCATCCTTCAAATAATAGTCA3' where Asc1 site underlined. PCR amplification was performed for 35 cycles at following conditions, 94°C for 2 minutes, 94°C for 30sec, 56°C for 30sec and 72°C for 1 minute and final extension at 74°C for 10 minutes. The PCR products were cloned in pTZ57R/T vector and following sequence confirmation, the cloned product were released and subcloned into transfection vector pBC-GFP-hDHFR. A maxi prep of the transfection vector was made and following release of the targeting DNA fragment and its purification, 5-10μg DNA was used for electroporation of schizonts purified over 60% nicodenz gradient.

3.2.3 Drug selection

Selection of successful transfectants was done by treating mouse with an antimalarial drug, pyrimethamine provided in drinking water. The stable transfectanats were confirmed for expression of GFP and the correct site specific integration was confirmed by PCR using primer with in the targeting cassette and sites beyond recombination in both the 5' and 3' regions. Two clones were obtained form two independent transfections. While both clones were studied for the phenotypic characteristion of the *Pb SCOT3* KO, that gave identical phenotype, the results of one the clones is reported below.

3.2.4 Confirmation of targeted gene knockout by site specific integration PCR

To confirm the site specific integration of the targeting cassette, PCR was performed using genomic DNA as a template. Diagnostic primers were designed, such that the forward primer, FP3-5'ATGGGTTATCCACTTTCTTA3' flanked upstream of the 5' recombined fragment and the reverse primer, RP3-5'TTCCGCAATTTGTTGTACATA3' was with in the GFP cassette. A single amplified product of 738bp in PCR confirmed the stable 5' integration

at the gene locus. Similarly, a second set of diagnostic primers were designed where the forward primer, FP4-5'GTTGTCTCTTCAATGATTCATAAATAG3' had sequence within the hDHFR cassette and reverse primer, RP4-5ATCCTTCAAATAATAGTCA3' was a sequence beyond of the site of 3' fragment integration. A single amplified product of 719bp in PCR confirmed the correct 3' integration at the gene locus. Following limiting dilution and obtaining a clonal line of the *Pb SCOT3* KO, genomic DNA was isolated and used as a template to perform PCR using forward primer, FP5-5'TGTTTAATTATACATTTACCA3' and reverse primer, RP5-5'TGCATCATCATTTGGTAAG3' from within the target gene ORF. The PCR gave a product of 506bp from WT genomic DNA while complete absence of the product in the KO line confirmed successful cloning.

3.2.5 Maintenance of *Anopheles stephensi* colony and transmission of *Pb SCOT-3* KO to mosquitoes

To generate the mosquito stages of *P. berghei*, a colony of *Anopheles stephensi* was continuously maintained. Eggs were obtained from mated female *Anopheles* mosquitoes after obtaining two consecutive blood meals from anesthetized rabbit. The eggs were placed in environmental chamber maintained at 27°C and 80% RH that allowed their transformation in larva and pupa. The pupa were manually collected and placed in water bowls within clothed cage cloths to facilitate emergence. The female mosquitoes were collected by vacuum suction and were placed in separate cage. These mosquitoes were allowed to obtain blood meal from mouse harboring gametocytes stages of either WT or *Pb SCOT3* KO. Following two successive feeding with infective blood meal, the mosquito cages were placed in environmental chamber maintained at 23°C and 80% RH. The mosquitoes were dissected on D14 to observe the midgut infectivity and on day 18-20 for analysing the salivary gland infectivity. For obtaining salivary glands sporozoite, the glands were dissected and crushed to release free sporozoites. These sporozoites were counted under haemocytometer and $2X10^4$ were added to HepG2 cultures to study the exo-erythrocytic development.

3.2.6 Transmission of *Pb SCOT3* KO sporozoites to mice through natural mosquito bite

To study the prepatent period following delivery of *Pb SCOT3* sporozoites, we allowed transmission of malaria through natural mosquito bite, Towards this end, we collected 12-15 infected mosquitoes in each cage, that were allowed to take blood meal from

anesthesia C57BL/6 mice. Three independent experiments were done, with 3 mice in each experiment. As control, pre patent period was also monitored for mice that received WT sporozoites, through bite in two independent experiments (3 mice in each experiments). All infected mosquitoes that obtained blood meal were subjected to salivary gland dissections to confirm the presence of GFP expressing WT and *Pb SCOT3* KO sporozoites, which was used as a correlate of successful malaria transmission to mice.

3.2.7 *In vitro* development of EEF and IFA to reveal to growth of EEFs

HepG2 cultures were maintained in complete Dulbeco's Modified Eagle Medium (DMEM) containing 2mM L-glutamine and 4.5 g/liter glucose supplemented with 10% FCS. After the addition of sporozoites, the cultures was fixed at 12h, 36h and 62h with 4% PFA. The cultures were stained using antibody against UIS-4. Anti-mouse secondary antibody conjugated to Alexa Fluor 594 was used to localize the UIS4 immuno-reactivity. DAPI was used to localize the host and the parasite nuclei. Nikon (Ni-E AR) upright fluorescent microscope was used to observe processed slides.

3.2.8 RNA isolation from all *P. berghei* life cycle stages to study expression of *Pb SCOT3*

To study expression of *Pb SCOT3*, RNA was obtained from all life cycle stages. In brief, mice were infected with WT *P. berghei* asexual blood stages and after obtaining 10-12% parasitaemia, the blood was harvested by cardiac puncture. The blood was lysed using 0.5% saponin and pelleted at 15,000 rpm at 4°C. Following 3-4 washes with sterile RNAse free PBS, the pellet was used for RNA extraction. The midguts and salivary glands were obtained on D14 and on D18 respectively following dissection of infected *Anopheles stephensi* mosquitoes. Different stages of developing liver stages or EEFs were harvested from HepG2 culture, following trypsinisation. The cells were washed 3-4 times with sterile RNAse free PBS and pellet was used for RNA extraction. The samples obtained from different stages were subjected to RNA extraction using a micro to midi RNA isolation kit as described above.

3.2.9 cDNA synthesis

For cDNA synthesis, 2µg of RNA was reverse transcribed in a reaction mixture containing 1X PCR buffer, 2.5mM dNTPs, 5mM Mg Cl2, 1.5U RNAse inhibitor, 2.5 mM random hexamers and 1.5U reverse transcriptase. The thermal cycling conditions were 25°C for 10 min, 42°C for 20 min and 98°C for 5 min.

3.2.10 Expression analysis of *Pb SCOT3* by quantitative real time PCR

Pb SCOT3 gene expression was quantified by absolute method of real time PCR. Towards this end, a 175 bp fragment of *Pb SCOT3* was amplified using forward primer, RTFP-5'AATGTCGATGATTTAGGTGAT3' reverse primer, RTRP-5'TTACTTGTTCATAATAATTTGT3' and the PCR product was cloned into a TA vector (pTZ57R/T). The clone was expanded by transformation and following purification of the plasmid by mini-prep method, a log dilution of the plasmid was generated to be used as gene specific standard with a dynamic range that covered from 10^2 copies/µl to 10^8 copies /µl. Similarly, a standard was generated for *Pb 18S* rRNA that was used as internal control. For performing real time PCR, cDNA obtained from various stages of *P. berghei* was used as template, that was added to SYBR green (Biorad) master mix along with 0.25µM concentration of forward and reverse primer corresponding to either *Pb SCOT3* or *Pb 18S rRNA*. The samples were run alongside with both *Pb SCOT3* and *Pb 18S rRNA* standards. The data normalisation was done by obtaining ratio of copy numbers of *Pb SCOT3* and *Pb 18S rRNA* for each sample.

3.3. Results

3.3.1 *Pb SCOT3* is conserved amongst other *Plasmodium* species

Alignment of amino acid sequence of SCOT3 from various rodent and human species revealed nearly 40% identity in the sequence (Fig 29).

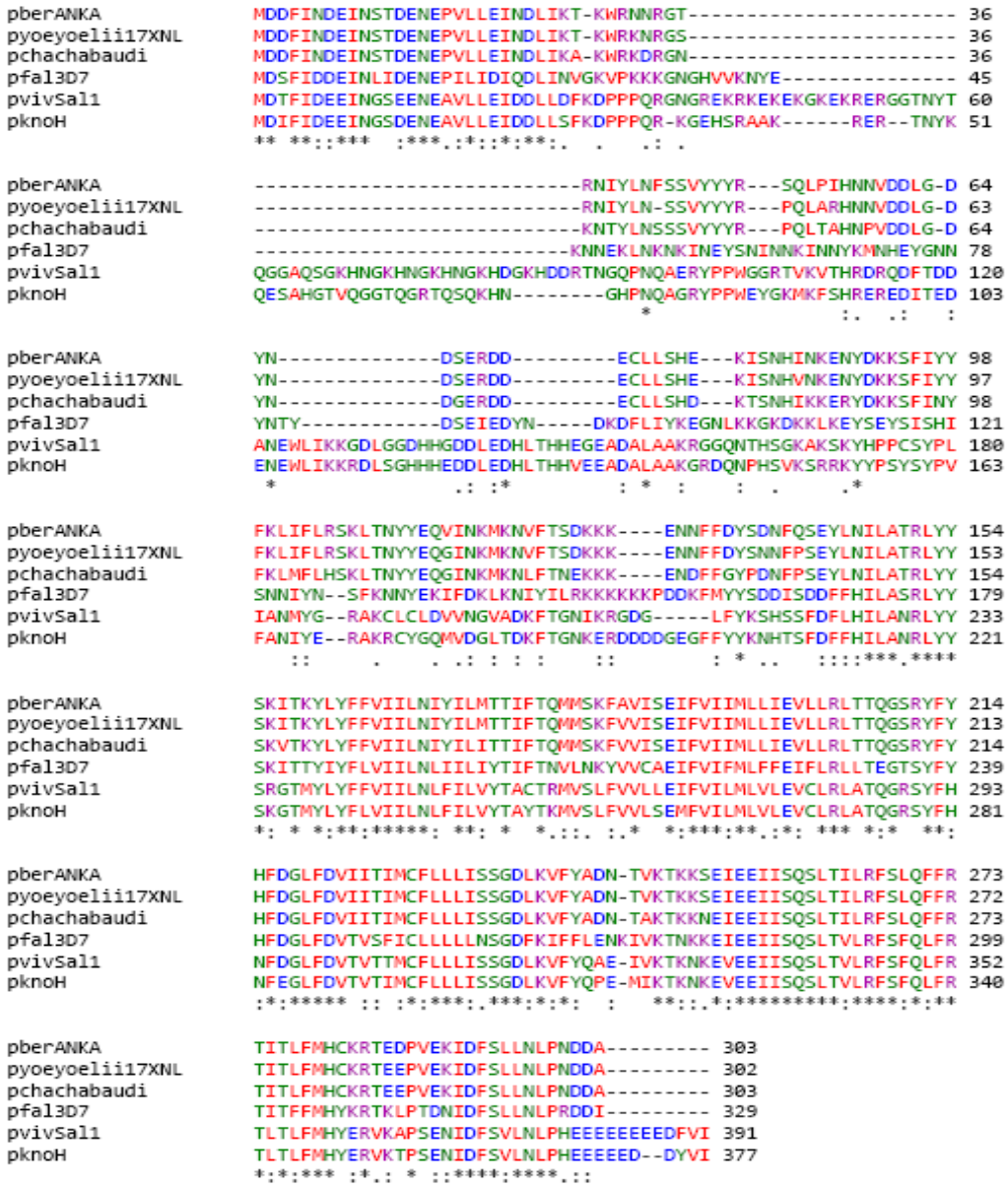

Fig 29. Amino acid sequence alignment of orthologues of *Pb SCOT-3* amongst *Plasmodium* species. pberANKA: *P.berghei ANKA*, pyoeyoelli17XNL: *P. yoelli yoelli 17XNL* strain, pchachabaudi: *P. chaubaudi*, pfal3D7: *P. falciparum,* pkno: *P. knowlsii*.

3.3.2 Gene expression analysis by quantitative real time PCR revealed maximal expression of *Pb SCOT3* in midgut sporozoite stages and late liver stages

In order to quantify the gene expression of *Pb SCOT3*, gene specific standards were generated for *SCOT3* and *Pb 18S* rRNA and the stage specific DNA samples were run along side with standards. Gene expression was revealed as absolute copy numbers. Data normalization was done by obtaining a ratio of *Pb SCOT3* versus *Pb 18S* rRNA.. The normalised data revealed highest expression of *Pb SCOT3* in midgut oocyst stages and in late liver stages at 50h (Fig 30).

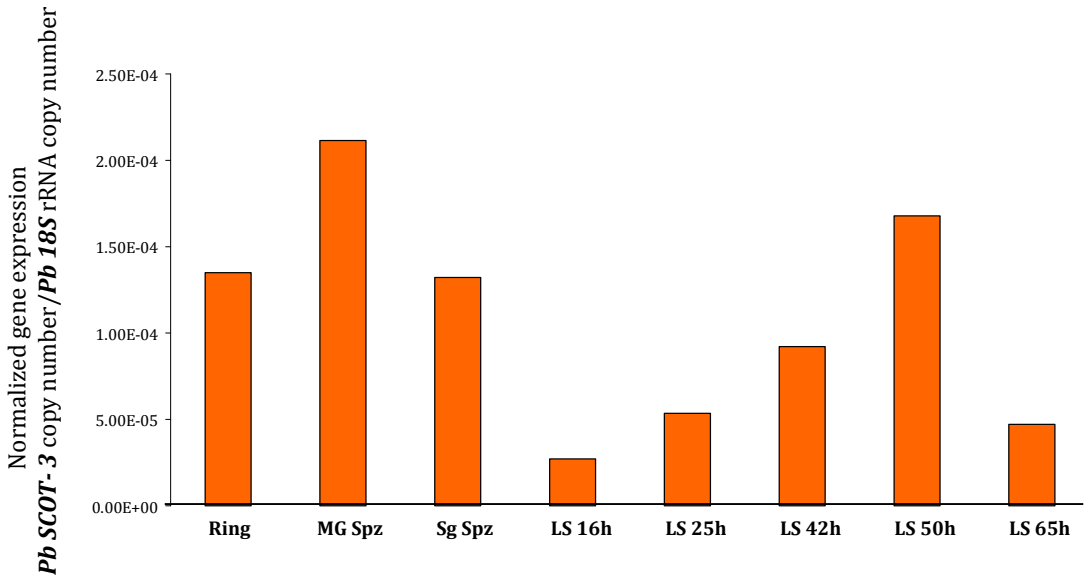

Fig 30. Normalized gene expression for *Pb SCOT-3* across *Plasmodium berghie* life cycle stages. Analysis of gene expression by quantitative real time PCR revealed highest gene expression in the midgut sporozoite stages and 50h liver stages (LS50H). The normalized data was expressed as a ratio of absolute copy numbers of *Pb SCOT3* versus *Pb 18S rRNA* (internal control) for each stage of the *Plasmodium* life cycle. Ring: Ring stages, MG Spz: Midgut sporozoite stage, SgSpz: salivary gland sporozoites, LS16H: Liver stage 16h, LS25H: Liver stage 25h, LS42H: Liver stage 42h, LS50H: Liver stage 50h, LS65H: Liver stage 65h.

3.3.3 Successful replacement of *Pb SCOT3* locus by GFP-hDHFR cassette by double homologous recombination method

The organisation of the *Pb SCOT3* locus is shown Fig 31A. To achieve a successful double homologous recombination for replacement of the *Pb SCOT3* locus with *GFP-hDHFR* cassette, the 5' fragment and 3' fragments were cloned on either ends of the *GFP-hDHFR* cassette (Fig 31B). The organization of the genomic locus of *Pb SCOT3* following its replacement is shown in Fig 31C. The 5' and 3' fragments of *Pb SCOT3* amplified by PCR and resolved on 1% agarose gel are shown in Fig 31D and 31E. Following cloning of these

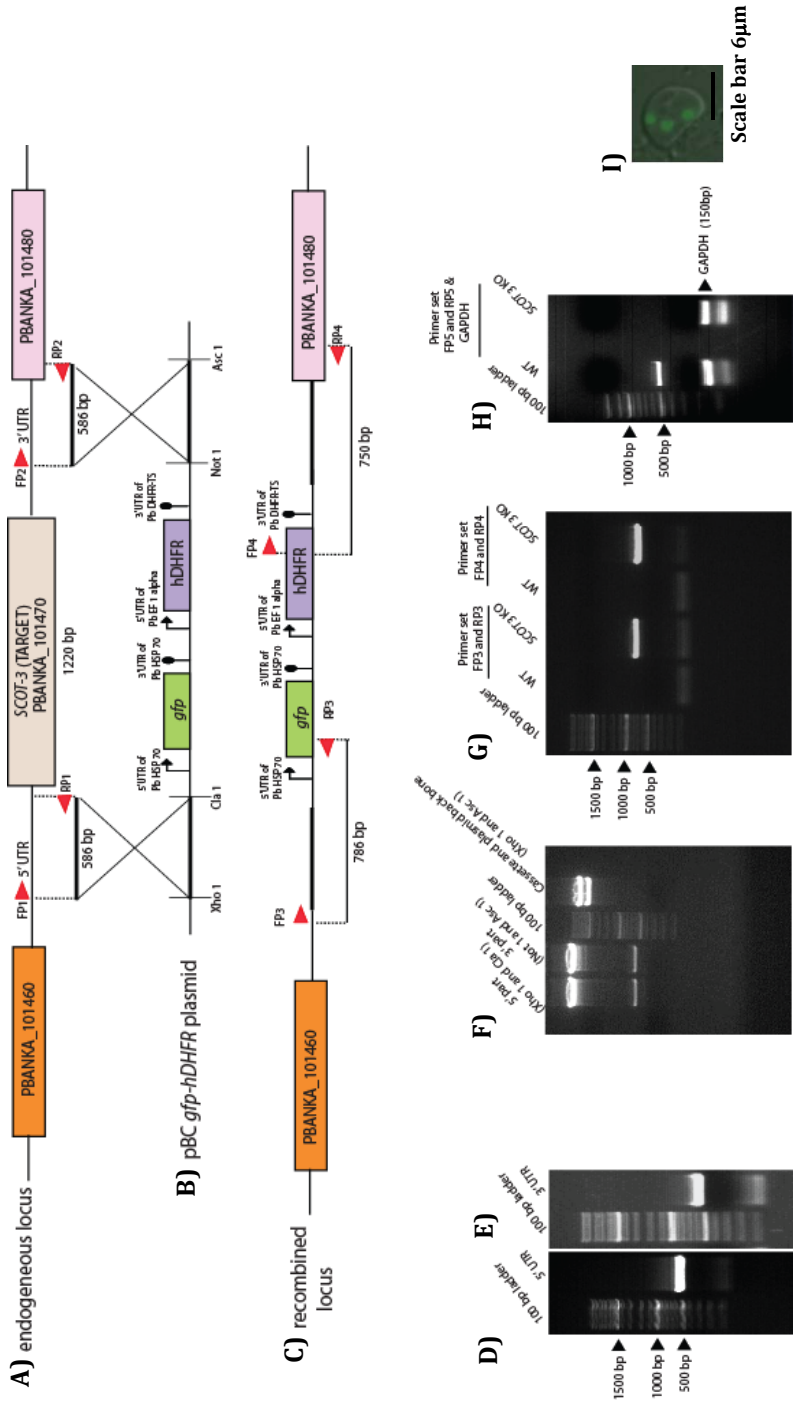

Fig 31. Generation of *Pb SCOT-3* KO parasite line. A) Genomic locus of *Pb SCOT-3* (PBANKA_101470) showing 5' and 3' UTRs. B) Elements of the targeting vector showing pBC-GFP-hDHFR. A 586 bp 5' fragment of *Pb SCOT-3* was cloned in XhoI/ClaI site of the targeting vector. A 586 bp of 3' fragment was cloned into NotI/AscI site of the targeting vector. C) Recombined locus following successful double cross over recombination resulting in replacement of target gene, *Pb SCOT-3* by GFP-DHFR cassette. A 1% agarose gel showing the PCR product of : D) 5' and E) 3' UTRs. The 5' UTR fragment was amplified with primers FP1 and RP1. The 3' UTR fragment was amplified with primers FP2 and RP2. F) Release of 5' UTR fragment from transfection vector using restriction enzymes XhoI/ClaI and release of 3'UTR fragment from transfection vector using restriction enzymes NotI/AscI. Release of targeting cassette (5' UTR fragment+GFP-DHFR cassette+3' UTR fragment) and vector backbone using restriction enzymes XhoI/AscI. G) Diagnostic PCR using primers within the targeting cassette and beyond sites of recombination revealing the correct site specific integration. A PCR product with primers FP3 and RP3 indicated a correct 5' integration and a PCR product with primers FP4 and RP4 indicated a correct 3' integration. H) Genomic DNA isolated from cloned *Pb SCOT-3* KO parasites does not amplify a PCR product from the ORF whereas WT parasites amplify a product of 527bp with primer set FP5 and RP5 H) A merged DIC image showing a GFP expressing *Pb SCOT-3* KO parasite inside RBC.

fragments into the targeting vector, these fragments were further reconfirmed by release of the 5' fragment by using restriction enzymes Xho1 and Cla1, the 3' fragment by using restriction enzymes Not1 and Asc1, and targeting vector was release from the plasmid back bone using restriction enzymes Xho1 and Asc1 (Fig 31F). The linearized *Pb SSPELD* KO targeting construct was electroporated into *P. berghei ANKA* schizonts using U-033 program in Amaxa nucleofector device and injected intravenously into mice. The mice were kept under pyrimethamine drug pressure and parasitemia was monitored daily by Giemsa stained blood smears. Genomic DNA was isolated from drug resistant parasites and site specific 5' and 3' integration was confirmed by primers designed at beyond sites of recombination, that indicated correct integration (Fig 31G). Limiting dilution was performed to obtain clonal population of *Pb SCOT3* KO parasites. *Pb SCOT3* ORF specific primers were used to confirm the deletion of *Pb SCOT3* locus, that gave a PCR product only with WT *P. berghei* genomic DNA and not with *Pb SCOT3* KO genomic DNA (Fig 31H). The cloned line of *Pb SCOT3* KO expressed GFP constitutively (Fig 31I).

3.3.4 Pb SCOT3 is not essential for asexual blood stages

To monitor, if *Pb SCOT3* depletion affected asexual blood stage propagation, two groups of BALB/c mice (3 mice per group) were intravenously injected with $1X10^3$ iRBC (infected RBC) of either WT or *Pb SCOT3* KO and the asexual blood stage replication was monitored for 7 days by making Giemsa stained blood smears. The identical propagation of *Pb SCOT3* KO as that of WT parasites and presence of all stages of asexual forms in *Pb SCOT3* KO revealed its non essential role in asexual blood stages (Fig 32).

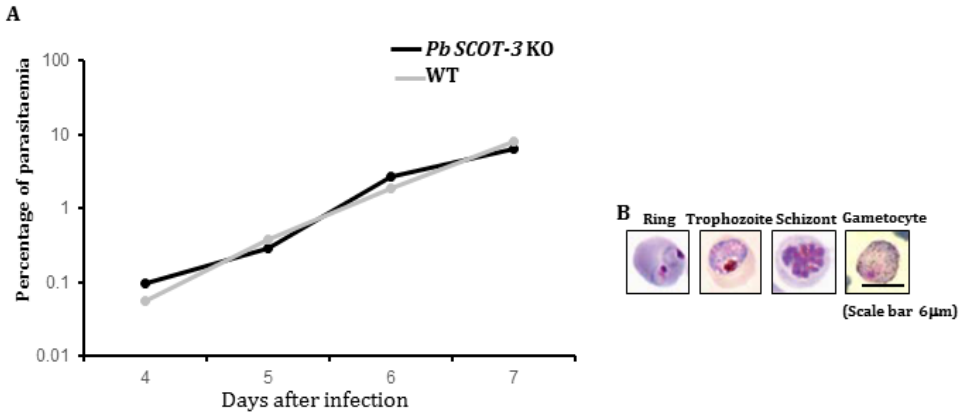

Fig 32. *Pb SCOT-3* KO asexual parasites propagate identically as WT parasites. A) $1X10^3$ infected RBC of either WT or *Pb SCOT-3* KO were intravenously injected in two groups of mouse (3 mouse/group) and monitored for propagation of the parasites daily for 7 days by making Giemsa stained smears. B) Representative pictures showing asexual blood stages obtained from Rathore et al., [147]

3.3.5 *Pb SCOT3* is not essential for mosquito stages

Transmission of *Pb SCOT3* KO parasites to mosquitoes resulted in formation of oocysts, whose numbers were comparable to the oocysts derived from the WT parasites (Fig. 33A and B). The sporulation pattern inside oocyst (Fig 33C and D) and the ability of the egressed sporozoites to reach salivary gland (Fig 33E and F) also were comparable to that of WT parasites suggesting that *Pb SCOT3* KO manifested no defect in the mosquito stages of *P. berghei*.

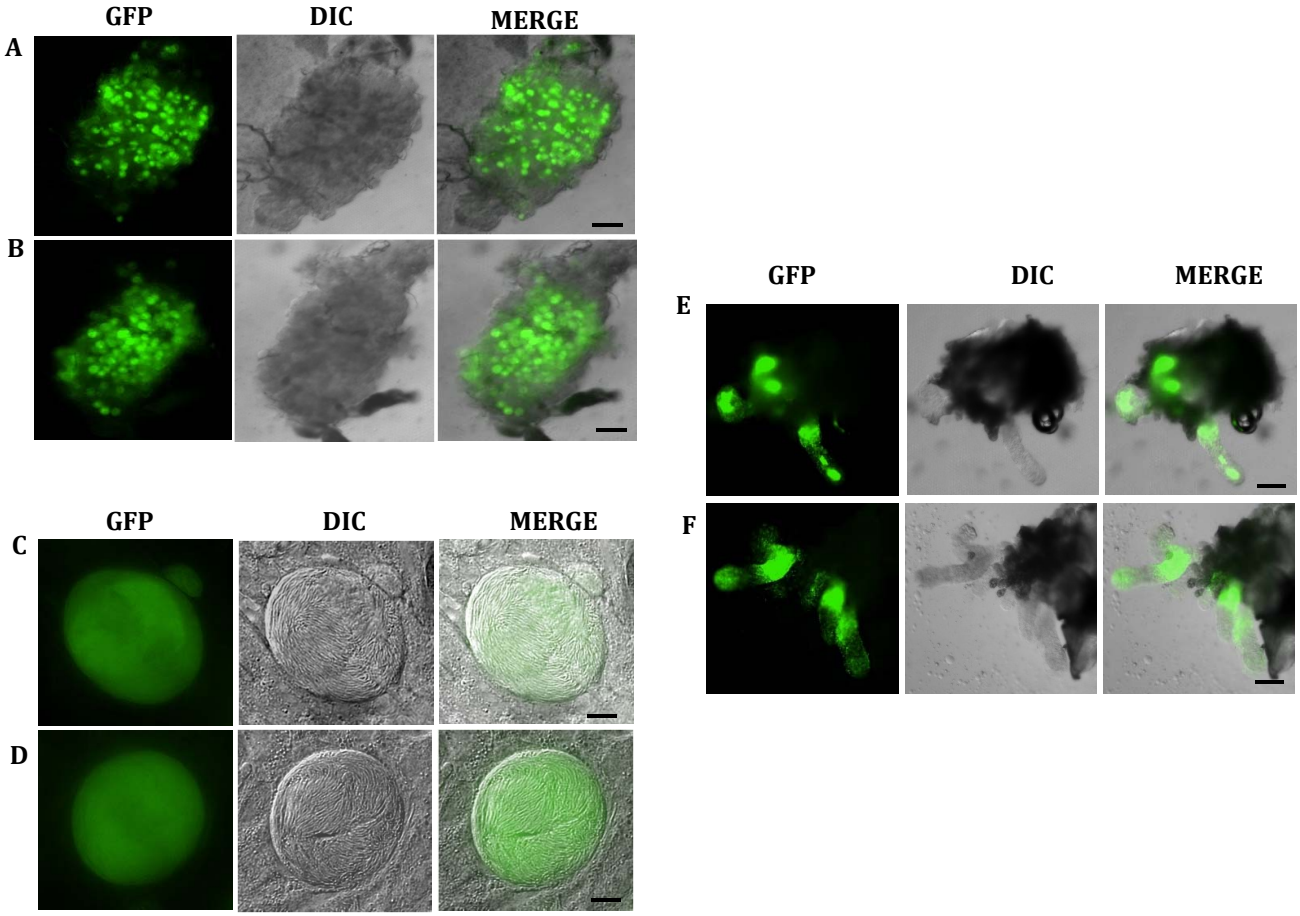

Fig 33. Mosquito stages of *Pb SCOT-3* KO do not show any defect in oocyst development and sporulation. Malaria was transmitted to female *Anopheles* mosquitoes from mouse harboring gametocyte stages of either WT or *Pb SCOT-3* KO. Midguts showing oocyst derived from WT parasites (A) and *Pb SCOT-3* KO parasites (B), scale bar 200µm. A single magnified oocyst from WT (C) and *Pb SCOT-3* KO (D), scale bar 10µm. Dissected salivary glands showing similar loads of WT sporozoites (E) and *Pb SCOT-3* KO sporozoites (F), scale bar 10µm.

3.3.6 *Pb SCOT3* sporozoites fail to initiate blood stage infection when malaria is transmitted though natural mosquito bite

Inoculation of *Pb SCOT3* KO sporozoites through natural mosquito bite did not initiate blood stage infection in 2 out of three independent experiments, where 3 mice were used per experiment. However, there was a break through infection in one of the experiments where 1 out of three mice became positive for blood stage infection. However, there was a significant delay in the pre patent period of this mouse that became positive on D9. All blood meal positive mosquitoes that were used for transmission were dissected and majority of them had high loads of sporozoites in the salivary glands. Thus lack of break through infection was not due to absence of salivary gland sporozoites in the batch of mosquitoes used for transmission experiments (Fig 34 and Table E).

3.3.7 *Pb SCOT3* KO exhibit better growth than WT EEFs at 62h time points

Pb SCOT3 KO EEF's developing in HepG2 cells were indistinguishable from WT EEF's at 12h (Fig 35A and D) and 36h (Fig 35B and E) time points. However, at 62h time point, the *Pb SCOT3* KO EEF's were significantly larger in size as compared to WT EEFs (Fig 35C and F), likely suggesting that *Pb SCOT3* KO EEF's exhibited better growth than WT EEF's. These observations likely point to the role of *Pb* SCOT 3 in egress of the merozoites following completion of liver stage schizogony.

Table E

Parasite Strain	Expt no.	Number of animals used for bite	Number of animals positive for blood stage infection	∗Pre-patent period
WT	I	3	3/3	D4
	II	3	3/3	D4
Pb SCOT-3 KO	I	3	0/3	ND
	II	3	1♣/3	D9
	III	3	0/3	ND
	IV	3	0/3	ND

Fig 34. Transmission of *Pb SCOT-3* KO sporozoites to mouse by natural mosquito bite induces an occasional blood stage infection with delayed pre patent period. A) 12-15 mosquitoes infected with WT or *Pb SCOT-3* KO were placed in a small container and covered with mosquito net. Anesthesized C57BL/6 mice were placed on the top of cage and the mosquitoes were allowed to obtain a blood meal for 15 minutes. During the process of uptake of blood meal, salivary gland sporozoites are injected into the dermis of the mouse leading to successful malaria transmission to mouse. All blood meal positive mosquitoes following bite experiment were dissected to collect salivary glands to confirm the presence of GFP expressing sporozoites (WT or ***Pb SCOT-3* KO**) under fluorescent microscope

Table E. Showing the kinetics of the mosquito bite experiment, the details of number of experiments performed, number of animals used in each experiment, the number of animals that became positive for blood stage infection and the pre patent period (∗ defined as the time required for the appearance of blood stage infection following infection with sporozoites). ND: not detected. A pre patent period of D9 indicated a highly compromised egress of the *Pb SCOT-3* KO liver stages. ♣The occasional break through infection in mouse following *Pb SCOT3* sporozoite injection gave a delayed pre patent period

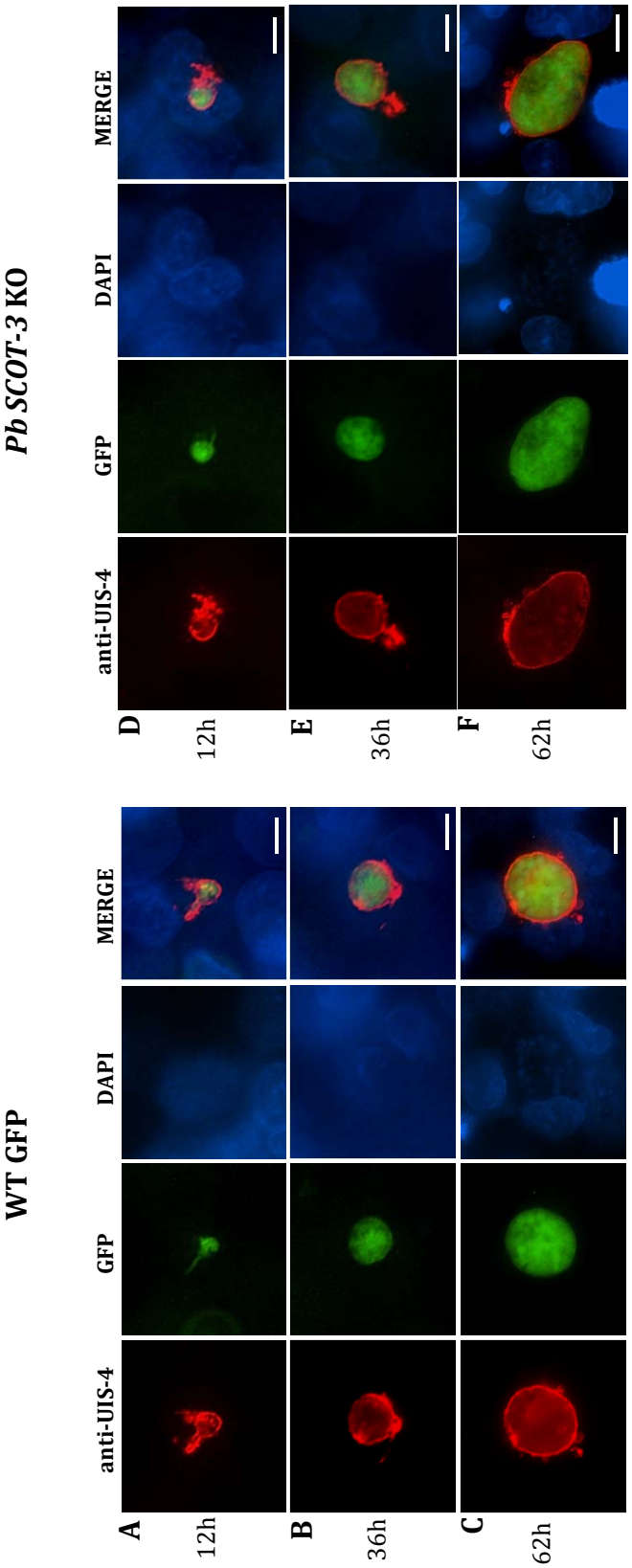

Fig 35. The Exo Erythrocytic Forms (EEF's) of *Pb SCOT-3* KO reveals better growth at late stages of *in vitro* development (62h). Salivary glands sporozoites were isolated by dissection and $2X10^4$ sporozoites of either WT or *Pb SCOT-3* KO were added to HepG2 cultures, that supported the complete development of the *P. berghei* EEF's. The cultures were fixed at different time points: 12h, 36h and 62h. The cultures were stained with anti-UIS-4 antibody that reacts with the parasitophorous vacuolar membrane (PVM) of EEF and DAPI (4', 6' diamidino-2 phenyl indole) for visualization of HepG2 and parasite nuclei. EEF's derived from *Pb SCOT-3* KO sporozoites at 12h (D) and 36h (E) were comparable to that of the WT EEF's at 12h (A) and 36h (B). EEF's derived from *Pb SCOT-3* KO sporozoites at 62h (F) was significantly larger as compared to WT EEF's at the same time point (C). Scale bar 10μm.

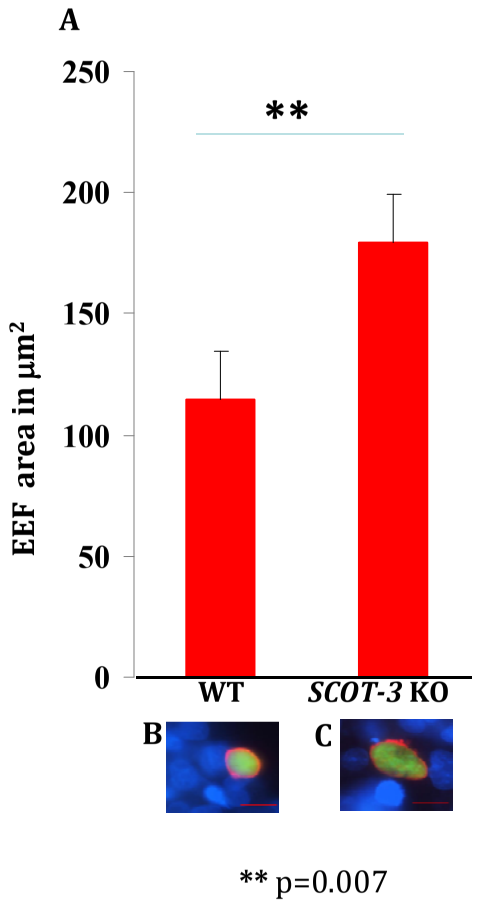

Table F

S.NO	WT	*SCOT-3*KO
1	132.78	100.86
2	94.12	357.15
3	168.61	266.31
4	134.27	144.47
5	131.7	212.29
6	102.57	189.05
7	89.34	131.49
8	137.3	84.19
9	124.5	90.13
10	84.17	100.92
11	80.76	130.3
12	143.3	214.19
13	76.87	252.01
14	78.56	149.02
15	144.47	269.79
Average area in microns	124.888	179.478

Fig 36. Measurement of EEF area at 62h reveals better growth in *Pb SCOT-3* KO. A) Average area of the 62H EEF is indicated in the bar graph. P value =0.007. B) and C) are representative pictures of EEF's derived from WT and *Pb SCOT-3* KO respectively.
Table C. Values corresponding to the area measurement of 15 individual EEF's derived from WT and *Pb SCOT-3* KO.

3.4 Discussion

Sporozoites that have been attenuated genetically have gained prominence in the recent past as live attenuated vaccines, able to elicit protective pre-erythrocytic immunity [27-29, 154]. In an urge to gain a better understanding of the sporozoite biology pertaining to aspects of invasion, motility and intra hepatic development, several transcriptomic studies have been carried out using different platforms. Independent of the methods of transcriptomic analysis, grossly, the same pattern of sporozoite gene expression was observed for several rodent and human species of malaria. Surprisingly, even species like *P. vivax*, that have a unique tendency to form hypnozoites, a dormant EEF stage, tends to exhibit the same pattern of gene expression as *P. falciparum* or *P. yoelli*, suggesting that minor, and not global transcriptional changes are sufficient for manifestation of this dormancy.

P. vivax is the most neglected human species of *Plasmodium*. Owing to its benign nature, a lack of interest in detailed exploration of its genetics, together with its limitation of maintaining in continuous culture, has imposed tremendous limitations in understanding the biology *P. vivax*. By using systems biology approach, Westerberger et al [156] have resorted to study the transcriptome of this parasite in mosquito stages and in asexual blood stages. An interesting aspect of this study was the discovery of several hypothetical genes that were upregulated in *P. vivax* and in other human and rodent species, but have not been annotated yet. These genes were referred to as Sporozoite Conserved Orthologous Transcripts (SCOT). SCOT candidates can be excellent vaccine or drug targets, provided their functional role on the pre-erythrocytic stages is known.

Towards this end, we have selected one of the candidates described as *Pv SCOT3* (PVX_85040), whose orthologue was also present in *P. berghei* (PBANKA_101470). Because, the *P. berghei* are genetically more tractable, compared to other human *Plasmodium* species, we took a genetic approach to validate the function of *Pb SCOT3* in parasite life cycle. We readily obtained a KO of *Pb SCOT3*, following replacement of the gene locus with GFP-hDHFR cassette, suggesting that the gene was dispensible in the blood stages. After obtaining a clonal line of *Pb SCOT3* mutant, we assessed its ability to transmit malaria to mosquitoes. We found that *Pb SCOT3* mutant were not compromised either to form oocyst, to sporulate or to reach the salivary glands. However, when *Pb* SCOT3 mutants were delivered to C57BL6 mouse by natural mosquito bite, they failed to produce blood stage infection. However an occasional

break through infection was noted with significant delay in the prepatent period (D9). In order to possibly explain the inability of *Pb* SCOT3 mutants to initiate blood stage, we studied the development of the EEF's in HepG2 cells at different time points. We found that the EEF's were indistinguishable from WT at 12 and 36 hours, but at 62 hours, interesting the *SCOT3* KO exhibited a better growth of EEF than WT. The inability of *Pb SCOT3* mutants to initiate a timely break through infection, in spite of complete development of EEFs likely points to a defect in the egress of the merozoites from the hepatic schizonts.

Disruption of parasite plasma membrane and PVM seems to the mode of release of merozoites in both erythrocytes and hepatocytes and there are several known mechanisms to achieve this process [70]. Cysteine protease activity is essential for PVM rupture and treatment with a cysteine protease inhibitor, E64 blocked the rupture of PVM [20]. Serine repeat antigen [SERA] family is a group of cysteine proteases expressed during schizogonic cycle involved in PVM rupture in asexual blood stages [175, 176]. In rodent *Plasmodium* strains, five SERA proteins are identified amongst which four SERA proteins were upregulated during late liver stage development [175]. During merozoite formation SERA2 and SERA3 proteins are released in the hepatocyte cytoplasm [25].

Very few proteases other than SERA were identified that participate in merozoite egress from hepatic schizonts. For example, the subtilisin like protease [SUB1] is a serine protease that is essential for the merozoite egress from liver stages. Role of SUB1 was first identified in merozoite release from infected RBC [177], where it role was documented in maturation of SERA proteins essential for egress of merozoites from infected RBC [177]. Later *SUB1* conditional mutagenesis unraveled its role in liver stages. *SUB1* conditional KO parasites failed to initiate blood stage infection confirming the role of SUB1 in hepatic merozoite release [26].

Signaling molecules like cGMP dependent protein kinase [PKG] that mediate the cGMP [3'-5'-cyclic guanosine monophosphate] signal transduction plays an important role throughout *Plasmodium* life cycle [178]. PKG mediates the blood stage schizogony as well as gametogenesis [179, 180]. Conditional mutants of PKG revealed its role in the egress of merozoites from the infected hepatocyte [24]. Conditional mutants of PKG were defective in merosome formation, merozoite release and subsequent blood stage infection. Interestingly, injection of PKG conditional knockout sporozoites elicited protective immune response in mice [24].

More recently, a *Plasmodium* phospholipase has been shown to be involved in disruption of PVM membrane [181] as well as in the egress of the sporozoites from oocyst. While the role this phospholipase was earlier shown to associated with sporozoite plasma membrane [12], facilitating the migration of sporozoites through cells before invasion of hepatocytes, this new study further confirmed its localization to PVM, through generation of a GFP transgenic under a liver stage specific promotor *lisp2* [PBANKA_100300]. The phospholipase mutants showed a defect in PVM disruption, as evident by its normal completion of EEF development, but highly compromised merozoite egress.

Our own unpublished data [Togiri J and Kumar KA] where a mutant of *Plasmodium S23* was generated by reverse genetics and studied for its probable function across all life cycle stages has yielded information on its function at late liver stages, specifically in egress of hepatic merozoites. Infection of *Pb S23* mutants rarely gave a break through infection, with delayed pre patent period. Infact a phenotype, identical to *PbS23* was reported earlier where depletion of a gene that encodes for Liver specific protein-1 [LISP-1] was shown to generate merozoites in the late liver stages that delayed significantly the initiation of blood stage infection, owing to a defect in the egress [96].

In our study, *Pb SCOT3* KO parasites also exhibited a similar phenotype as above mentioned gene knockouts having a role in the egress of merozoites from liver stages. *Pb SCOT3* KO parasites behaved identically as WT parasites during their asexual propagation and during their development in the mosquito, except that they were not able to egress out of the hepatocytes, following completion of EEF development. An occasional breakthrough infection of *Pb SCOT3* mutants may indicate that, other parasite molecules, likely described above but not limited to, may have over lapping functions with *Pb SCOT3* and may substitute for its loss of function, albeit less efficiently. The possibility of a mechanical disruption of the EEF membrane also cannot be ruled out owing the strategic positioning of the mature EEFs in the vicinity of the sinusoidal lumen, for efficient release of merozomes [181] into the blood circulation. Interestingly, other *Plasmodium* mutants lacking LISP1 [96] and perforin like PPLP2 [182, 183] also did not result in complete "non-egress" phenotype. This likely suggests that egress of intracellular parasites may be mediate by different effector proteins and multiple mechanisms may exist, which may have partially overlapping or synergistic functions. Therefore, depletion of any one effector protein like *Pb* SCOT3, may only lead to a partial defect in egress.

The fact that *Pb SCOT3* parasites exhibit better growth characteristics during late liver

stage development, may also have implications for its ability to expose antigens to the immune system likely eliciting a cross stage immunity [blood stage specific], in addition to pre-erythrocytic immunity. However, the moderate phenotype of *Pb SCOT3* where, occasional break through infections was observed may not be by itself, an ideal mutant to achieve sterile protection. In line with this, generation of a double mutant where, any of the afore mentioned parasite proteins can be depleted in combination with *Pb SCOT3* may offer a robust egress defective phenotype. Investigation of protective immunity of such doubly attenuated could facilitate the generation of genetically attenuated whole organism vaccines with potential for cross stage immunity.

SUMMARY

Summary

The focus of the present thesis was to functionally characterize the genes that are up regulated in salivary gland sporozoite stages of *Plasmodium*. In this context, two candidates, *Pb SSPELD* (PBANKA_091090) reported in the SAGE analysis of *P. berghei* salivary gland sporozoites [144] and P. *berghei* orthologue (PBANKA_101470) of *Pv SCOT3* (PVX_085040) reported in the microarrays of *P vivax* [155] were selected and by reverse genetics approach their functional role was investigated.

Pb SSPELD played an important role in the completion of the liver stage development as *Pb SSPELD* mutants were arrested in the mid-liver stage development. The transcriptomic analysis of 36h liver stage cultures showed down regulation of several late liver stage transcripts. Consistent with the role of *Pb SSPELD* in completion of EEF development, *Pb SSPELD* mCherry transgenics showed maximal expression beginning from stages of sporulating oocyst, in salivary glands sporozoites and continued to express in the 36h EEF's. *Pb SSPELD* mCherry colocalised with CSP, a major sporozoite surface protein, and also localized to the PVM membrane in 36h EEF's. *Pb SSPELD* mutants were unable to initiate blood stage infection following transmission of malaria through natural mosquito bite. However occasional break through infection was noted when high doses of sporozoite were delivered through the intravenous route. A prime boost regiment with $2X10^4$ *Pb SSPELD* mutants, yielded protection whose efficacy was 50% and the co-relates of protection were mediated by anti-sporozoite antibodies and parasite specific T cells. Taken together, we propose the role of *Pb SSPELD* in completion of liver stage development and these mutants as a complement of pre-erythrocytic antigens, capable of eliciting protective immunity.

P. vivax sporozoites occasionally enter into a state of dormancy in the hepatocytes and these stages are referred to as hynozoites. The molecular mechanism underlying the formation of these arrested stages are not known. In order to gain insight into the transcriptome of salivary gland sporozoite stages, a system approach was taken, where using microarrays, the transcription of all stages of *P. vivax* were studied [ref]. Analysis of salivary gland sporozoite transcriptome yielded information on the upregulation of several genes that have already been extensively studied in the human and rodent models. Surprisingly, inspite of its ability to form hypnozoites, *P. vivax* differed only minimally, in terms of sporozoite gene expression when compared to human and rodent species. This study however, uncovered several other sporozoite specific genes that have not been annotated yet but were found to be consistently expressed in other species of *Plasmodium* and hence were referred to as SCOT

genes. We selected one such gene, *SCOT3* from *P. vivax* sporozoite transcriptomic studies and using a genetically tractable *P. berghei* model, explored the functional role of the *P. berghei* orthologue of *Pv SCOT3*. Investigation of the gene function by reverse genetics approach revealed the dispensible role of *Pb SCOT3* in asexual blood stage propagation and in the mosquito stages. However, we found the role *Pb SCOT3* in egress of the liver stage parasites as 62h EEFs that successfully completed development failed to initiate blood stage infection in a timely manner. While we noted an occastional break through infection following malaria transmission through natural mosquito bite, yet, the appearance of blood stage infection with a delayed prepatent period clearly reflected the role of *Pb SCOT3* in egress of hepatic merozoites. While this study highlights the importance of *Pb SCOT3* in initiation of blood stage infection following completion of EEF development, we also bring to forefront the possibility of using *P. berghei* models to study and address the functional role of several yet to be characterized *P. vivax* SCOT genes, that offer limitations to study owing to the technical challenges associated with maintaining the *P. vivax* stages. Our study demonstrates the feasibility to unravel the function of liver stage specific genes of *P. vivax* by using rodent models to gain functional insights.

REFERENCES

References

1. World malria report 2013.
2. Miller, Louis H, and Brian Greenwood. 2002. "Malaria--a Shadow over Africa." *Science (New York, N.Y.)* 298 (5591): 121–22.
3. Worrall, Eve, Suprotik Basu, and Kara Hanson. 2005. "Is Malaria a Disease of Poverty? A Review of the Literature." *Tropical Medicine & International Health* 10 (10): 1047–59.
4. Alonso, Pedro L, and Marcel Tanner. 2013. "Public Health Challenges and Prospects for Malaria Control and Elimination." *Nature Medicine* 19 (2): 150–55.
5. Cowman, Alan F, Drew Berry, and Jake Baum. 2012. "The Cellular and Molecular Basis for Malaria Parasite Invasion of the Human Red Blood Cell." *The Journal of Cell Biology* 198 (6): 961–71.
6. King, C A. 1981. "Cell Surface Interaction of the Protozoan Gregarina with Concanavalin A Beads - Implications for Models of Gregarine Gliding." *Cell Biology International Reports* 5 (3): 297–305.
7. Russell, D G, and R E Sinden. 1981. "The Role of the Cytoskeleton in the Motility of Coccidian Sporozoites." *Journal of Cell Science* 50 (August): 345–59.
8. Vanderberg, J P. 1974. "Studies on the Motility of *Plasmodium* Sporozoites." *The Journal of Protozoology* 21 (4): 527–37.
9. Mota, M M, G Pradel, J P Vanderberg, J C Hafalla, U Frevert, R S Nussenzweig, V Nussenzweig, and A Rodríguez. 2001. "Migration of *Plasmodium* Sporozoites through Cells before Infection." *Science (New York, N.Y.)* 291 (5501): 141–44.
10. Ishino, Tomoko, Kazuhiko Yano, YasuoChinzei, and Masao Yuda. 2004. "Cell-Passage Activity Is Required for the Malarial Parasite to Cross the Liver Sinusoidal Cell Layer." *PLoS Biology* 2 (1): E4.
11. Ishino, Tomoko, YasuoChinzei, and Masao Yuda. 2005. "A *Plasmodium* Sporozoite Protein with a Membrane Attack Complex Domain Is Required for Breaching the Liver Sinusoidal Cell Layer prior to Hepatocyte Infection." *Cellular Microbiology* 7 (2): 199–208.
12. Bhanot, Purnima, Kristine Schauer, Isabelle Coppens, and Victor Nussenzweig. 2005. "A Surface Phospholipase Is Involved in the Migration of *Plasmodium* Sporozoites through Cells." *The Journal of Biological Chemistry* 280 (8): 6752–60.
13. Amino, Rogerio, Donatella Giovannini, Sabine Thiberge, Pascale Gueirard, Bertrand Boisson, Jean-François Dubremetz, Marie-Christine Prévost, Tomoko Ishino, Masao

Yuda, and Robert Ménard. 2008. "Host Cell Traversal Is Important for Progression of the Malaria Parasite through the Dermis to the Liver." *Cell Host & Microbe* 3 (2): 88–96.

14. Pradel, Gabriele, ShivaniGarapaty, and Ute Frevert. 2002. "Proteoglycans Mediate Malaria Sporozoite Targeting to the Liver." *Molecular Microbiology* 45 (3): 637–51.
15. Coppi, Alida, Rita Tewari, Joseph R Bishop, Brandy L Bennett, Roger Lawrence, Jeffrey D Esko, Oliver Billker, and PhotiniSinnis. 2007. "Heparan Sulfate Proteoglycans Provide a Signal to *Plasmodium* Sporozoites to Stop Migrating and Productively Invade Host Cells." *Cell Host & Microbe* 2 (5): 316–27.
16. Prudêncio, Miguel, Ana Rodriguez, and Maria M Mota. 2006. "The Silent Path to Thousands of Merozoites: The *Plasmodium* Liver Stage." *Nature Reviews. Microbiology* 4 (11): 849–56.
17. Tarun, Alice S, Kerstin Baer, Ronald F Dumpit, Sean Gray, Nicholas Lejarcegui, Ute Frevert, and Stefan H I Kappe. 2006. "Quantitative Isolation and in Vivo Imaging of Malaria Parasite Liver Stages." *International Journal for Parasitology* 36 (12): 1283–93.
18. Graewe, Stefanie, Kathleen E. Rankin, Christine Lehmann, Christina Deschermeier, Leonie Hecht, Ulrike Froehlke, Rebecca R. Stanway, and Volker Heussler. 2011. "Hostile Takeover by *Plasmodium*: Reorganization of Parasite and Host Cell Membranes during Liver Stage Egress." Edited by Boris Striepen. *PLoS Pathogens* 7 (9): e1002224.
19. Sturm, Angelika, Rogerio Amino, Claudia van de Sand, Tommy Regen, SilkeRetzlaff, Annika Rennenberg, Andreas Krueger, Jörg-Matthias Pollok, Robert Menard, and Volker T Heussler. 2006. "Manipulation of Host Hepatocytes by the Malaria Parasite for Delivery into Liver Sinusoids." *Science (New York, N.Y.)* 313 (5791): 1287–90.
20. Blackman, Michael J. 2008. "Malarial Proteases and Host Cell Egress: An 'Emerging' Cascade." *Cellular Microbiology* 10 (10): 1925–34.
21. Agarwal, Shalini, Maneesh Kumar Singh, Swati Garg, Chetan E Chitnis, and Shailja Singh. 2013. "Ca(2+) -Mediated Exocytosis of Subtilisin-like Protease 1: A Key Step in Egress of *Plasmodium falciparum* Merozoites." *Cellular Microbiology* 15 (6): 910–21.
22. Tawk, Lina, Céline Lacroix, Pascale Gueirard, Robyn Kent, Olivier Gorgette, Sabine Thiberge, OdileMercereau-Puijalon, Robert Ménard, and Jean-Christophe Barale. 2013. "A Key Role for *Plasmodium* Subtilisin-like SUB1 Protease in Egress of Malaria Parasites from Host Hepatocytes." *The Journal of Biological Chemistry* 288 (46): 33336–46.

23. Collins, Christine R, Fiona Hackett, Malcolm Strath, Maria Penzo, Chrislaine Withers-Martinez, David A Baker, and Michael J Blackman. 2013. "Malaria Parasite cGMP-Dependent Protein Kinase Regulates Blood Stage Merozoite Secretory Organelle Discharge and Egress." *PLoS Pathogens* 9 (5)
24. Falae, Adebola, Audrey Combe, AnburajAmaladoss, Teresa Carvalho, Robert Menard, and PurnimaBhanot. 2010. "Role of *Plasmodium berghei* cGMP-Dependent Protein Kinase in Late Liver Stage Development." *The Journal of Biological Chemistry* 285 (5): 3282–88.
25. Schmidt-Christensen, Anja, Angelika Sturm, Sebastian Horstmann, and Volker T Heussler. 2008. "Expression and Processing of *Plasmodium berghei* SERA3 during Liver Stages." *Cellular Microbiology* 10 (8): 1723–34.
26. Suarez, Catherine, Katrin Volkmann, Ana Rita Gomes, Oliver Billker, and Michael J Blackman. 2013. "The Malarial Serine Protease SUB1 Plays an Essential Role in Parasite Liver Stage Development." *PLoS Pathogens* 9 (12): e1003811.
27. Mueller, Ann-Kristin, Nelly Camargo, Karine Kaiser, Cathy Andorfer, Ute Frevert, Kai Matuschewski, and Stefan H I Kappe. 2005. "*Plasmodium* Liver Stage Developmental Arrest by Depletion of a Protein at the Parasite-Host Interface." *Proceedings of the National Academy of Sciences of the United States of America* 102 (8): 3022–27.
28. Mueller, Ann-Kristin, Mehdi Labaied, Stefan H I Kappe, and Kai Matuschewski. 2005. "Genetically Modified *Plasmodium* Parasites as a Protective Experimental Malaria Vaccine." *Nature* 433 (7022): 164–67.
29. Van Dijk, Melissa R, Bruno Douradinha, BlandineFranke-Fayard, Volker Heussler, Maaike W van Dooren, Ben van Schaijk, Geert-Jan van Gemert, et al. 2005. "Genetically Attenuated, P36p-Deficient Malarial Sporozoites Induce Protective Immunity and Apoptosis of Infected Liver Cells." *Proceedings of the National Academy of Sciences of the United States of America* 102 (34): 12194–99.
30. Matuschewski, K. 2007. "Hitting Malaria before It Hurts: Attenuated *Plasmodium* Liver Stages." *Cellular and Molecular Life Sciences* 64 (23): 3007–11.
31. Cowman, Alan F, and Brendan S Crabb. 2006. "Invasion of Red Blood Cells by Malaria Parasites." *Cell* 124 (4): 755–66.
32. Goel, Vikas K, Xuerong Li, Huiqing Chen, Shih-Chun Liu, Athar H Chishti, and Steven S Oh. 2003. "Band 3 Is a Host Receptor Binding Merozoite Surface Protein 1

during the *Plasmodium falciparum* Invasion of Erythrocytes." *Proceedings of the National Academy of Sciences of the United States of America* 100 (9): 5164–69.

33. Sim, B K, P AOrlandi, J D Haynes, F W Klotz, J M Carter, D Camus, M E Zegans, and J D Chulay. 1990. "Primary Structure of the 175K *Plasmodium falciparum* Erythrocyte Binding Antigen and Identification of a Peptide Which Elicits Antibodies That Inhibit Malaria Merozoite Invasion." *The Journal of Cell Biology* 111 (5 Pt 1): 1877–84.
34. Rayner, J C, M R Galinski, P Ingravallo, and J W Barnwell. 2000. "Two *Plasmodium falciparum* Genes Express Merozoite Proteins That Are Related to *Plasmodium vivax* and *Plasmodium yoelii* Adhesive Proteins Involved in Host Cell Selection and Invasion." *Proceedings of the National Academy of Sciences of the United States of America* 97 (17): 9648–53.
35. Triglia, T, J Thompson, S R Caruana, M Delorenzi, T Speed, and A F Cowman. 2001. "Identification of Proteins from *Plasmodium falciparum* That Are Homologous to Reticulocyte Binding Proteins in *Plasmodium vivax*." *Infection and Immunity* 69 (2): 1084–92.
36. Duraisingh, Manoj T, Tony Triglia, Stuart A Ralph, Julian C Rayner, John W Barnwell, Geoffrey I McFadden, and Alan F Cowman. 2003. "Phenotypic Variation of *Plasmodium falciparum* Merozoite Proteins Directs Receptor Targeting for Invasion of Human Erythrocytes." *The EMBO Journal* 22 (5): 1047–57.
37. Mitchell, G H, A W Thomas, G Margos, A R Dluzewski, and L H Bannister. 2004. "Apical Membrane Antigen 1, a Major Malaria Vaccine Candidate, Mediates the Close Attachment of Invasive Merozoites to Host Red Blood Cells." *Infection and Immunity* 72 (1): 154–58.
38. Pinder, J C, R E Fowler, A R Dluzewski, L H Bannister, F M Lavin, G H Mitchell, R J Wilson, and W B Gratzer. 1998. "Actomyosin Motor in the Merozoite of the Malaria Parasite, *Plasmodium falciparum*: Implications for Red Cell Invasion." *Journal of Cell Science* 111 (Pt 1 (July): 1831–39.
39. Jewett, Travis J, and L David Sibley. 2003. "Aldolase Forms a Bridge between Cell Surface Adhesins and the Actin Cytoskeleton in Apicomplexan Parasites." *Molecular Cell* 11 (4): 885–94.
40. Baum, Jake, Dave Richard, Julie Healer, Melanie Rug, ZitaKrnajski, Tim-Wolf Gilberger, Judith L Green, Anthony A Holder, and Alan F Cowman. 2006. "A Conserved Molecular Motor Drives Cell Invasion and Gliding Motility across Malaria

Life Cycle Stages and Other Apicomplexan Parasites." *The Journal of Biological Chemistry* 281 (8): 5197–5208.

41. Douse, Christopher H, Judith L Green, Paula S Salgado, Peter J Simpson, Jemima C Thomas, Gordon Langsley, Anthony A Holder, Edward W Tate, and Ernesto Cota. 2012. "Regulation of the *Plasmodium* Motor Complex: Phosphorylation of Myosin A Tail-Interacting Protein (MTIP) Loosens Its Grip on MyoA." *The Journal of Biological Chemistry* 287 (44): 36968–77. doi:10.1074/jbc.M112.379842.
42. Saliba, K J, H A Horner, and K Kirk. 1998. "Transport and Metabolism of the Essential Vitamin Pantothenic Acid in Human Erythrocytes Infected with the Malaria Parasite *Plasmodium falciparum*." *The Journal of Biological Chemistry* 273 (17): 10190–95.
43. Egan, Timothy J. 2014. "Recent Advances in Understanding the Mechanism of Hemozoin (malaria Pigment) Formation." *Journal of Inorganic Biochemistry* 102 (5-6): 1288–99.
44. Roberts, D J, A G Craig, A R Berendt, R Pinches, G Nash, K Marsh, and C I Newbold. 1992. "Rapid Switching to Multiple Antigenic and Adhesive Phenotypes in Malaria." *Nature* 357 (6380): 689–92.
45. Smith, J D, C E Chitnis, A G Craig, D J Roberts, D E Hudson-Taylor, D S Peterson, R Pinches, C I Newbold, and L H Miller. 1995. "Switches in Expression of *Plasmodium falciparum* Var Genes Correlate with Changes in Antigenic and Cytoadherent Phenotypes of Infected Erythrocytes." *Cell* 82 (1): 101–10.
46. Baruch, D I, B L Pasloske, H B Singh, X Bi, X C Ma, M Feldman, T F Taraschi, and R J Howard. 1995. "Cloning the P. *falciparum* Gene Encoding PfEMP1, a Malarial Variant Antigen and Adherence Receptor on the Surface of Parasitized Human Erythrocytes." *Cell* 82 (1): 77–87.
47. Su, X Z, V M Heatwole, S P Wertheimer, F Guinet, J A Herrfeldt, D S Peterson, J A Ravetch, and T E Wellems. 1995. "The Large Diverse Gene Family Var Encodes Proteins Involved in Cytoadherence and Antigenic Variation of *Plasmodium falciparum*-Infected Erythrocytes." *Cell* 82 (1): 89–100.
48. Adams, Yvonne, PongsakKuhnrae, Matthew K Higgins, AshfaqGhumra, and J Alexandra Rowe. 2014. "Rosetting *Plasmodium falciparum*-Infected Erythrocytes Bind to Human Brain Microvascular Endothelial Cells in Vitro, Demonstrating a Dual Adhesion Phenotype Mediated by Distinct P. *falciparum* Erythrocyte Membrane Protein 1 Domains." *Infection and Immunity* 82 (3): 949–59.

49. Abdi, Abdirahman I, Gregory Fegan, Michelle Muthui, Esther Kiragu, Jennifer N Musyoki, Michael Opiyo, Kevin Marsh, George M Warimwe, and Peter C Bull. 2014. "*Plasmodium falciparum* Antigenic Variation: Relationships between Widespread Endothelial Activation, Parasite PfEMP1 Expression and Severe Malaria." *BMC Infectious Diseases* 14 (1): 170.
50. Ampomah, Paulina, Liz Stevenson, Michael F Ofori, Lea Barfod, and Lars Hviid. 2014. "B-Cell Responses to Pregnancy-Restricted and -Unrestricted *Plasmodium falciparum* Erythrocyte Membrane Protein 1 Antigens in Ghanaian Women Naturally Exposed to Malaria Parasites." *Infection and Immunity* 82 (5): 1860–71.
51. Gitau, Evelyn N, James Tuju, Henry Karanja, Liz Stevenson, PilarRequena, Eva Kimani, Ally Olotu, et al. 2014. "CD4+ T Cell Responses to the *Plasmodium falciparum* Erythrocyte Membrane Protein 1 in Children with Mild Malaria." *Journal of Immunology* 192 (4): 1753–61.
52. Boddey, Justin A, Robert L Moritz, Richard J Simpson, and Alan F Cowman. 2009. "Role of the *Plasmodium* Export Element in Trafficking Parasite Proteins to the Infected Erythrocyte." *Traffic (Copenhagen, Denmark)* 10 (3): 285–99.
53. Goldberg, Daniel E, and Alan F Cowman. 2010. "Moving in and Renovating: Exporting Proteins from *Plasmodium* into Host Erythrocytes." *Nature Reviews. Microbiology* 8 (9): 617–21.
54. Marti, Matthias, Robert T Good, Melanie Rug, Ellen Knuepfer, and Alan F Cowman. 2004. "Targeting Malaria Virulence and Remodeling Proteins to the Host Erythrocyte." *Science (New York, N.Y.)* 306 (5703): 1930–33.
55. Sargeant, Tobias J, Matthias Marti, ElisabetCaler, Jane M Carlton, Ken Simpson, Terence P Speed, and Alan F Cowman. 2006. "Lineage-Specific Expansion of Proteins Exported to Erythrocytes in Malaria Parasites." *Genome Biology* 7 (2): R12.
56. Bruce, M C, P Alano, S Duthie, and R Carter. 1990. "Commitment of the Malaria Parasite *Plasmodium falciparum* to Sexual and Asexual Development." *Parasitology* 100 Pt 2 (April): 191–200.
57. Smith, T G, P Lourenço, R Carter, D Walliker, and L C Ranford-Cartwright. 2000. "Commitment to Sexual Differentiation in the Human Malaria Parasite, *Plasmodium falciparum*." *Parasitology* 121 (Pt. 2 (August): 127–33.
58. Billker, O, V Lindo, M Panico, A E Etienne, T Paxton, A Dell, M Rogers, R E Sinden, and H R Morris. 1998. "Identification of Xanthurenic Acid as the Putative Inducer of Malaria Development in the Mosquito." *Nature* 392 (6673): 289–92.

59. Arai, M, O Billker, H R Morris, M Panico, M Delcroix, D Dixon, S V Ley, and R E Sinden. 2001. "Both Mosquito-Derived Xanthurenic Acid and a Host Blood-Derived Factor Regulate Gametogenesis of *Plasmodium* in the Midgut of the Mosquito." *Molecular and Biochemical Parasitology* 116 (1): 17–24.
60. Billker, Oliver, Sandrine Dechamps, Rita Tewari, Gerald Wenig, BlandineFranke-Fayard, and Volker Brinkmann. 2004. "Calcium and a Calcium-Dependent Protein Kinase Regulate Gamete Formation and Mosquito Transmission in a Malaria Parasite." *Cell* 117 (4): 503–14.
61. Hirai, Makoto, Meiji Arai, Toshiyuki Mori, Shin-YaMiyagishima, Satoru Kawai, Kiyoshi Kita, TsuneyoshiKuroiwa, OlleTerenius, and Hiroyuki Matsuoka. 2008. "Male Fertility of Malaria Parasites Is Determined by GCS1, a Plant-Type Reproduction Factor." *Current Biology* 18 (8): 607–13.
62. Liu, Yanjie, Rita Tewari, JueNing, Andrew M Blagborough, Sara Garbom, Jimin Pei, Nick V Grishin, et al. 2008. "The Conserved Plant Sterility Gene HAP2 Functions after Attachment of Fusogenic Membranes in Chlamydomonas and *Plasmodium* Gametes." *Genes & Development* 22 (8): 1051–68.
63. Tewari, Rita, Ursula Straschil, Alex Bateman, Ulrike Böhme, Inna Cherevach, Peng Gong, Arnab Pain, and Oliver Billker. 2010. "The Systematic Functional Analysis of *Plasmodium* Protein Kinases Identifies Essential Regulators of Mosquito Transmission." *Cell Host & Microbe* 8 (4): 377–87.
64. Tewari, Rita, Dominique Dorin, Robert Moon, Christian Doerig, and Oliver Billker. 2005. "An Atypical Mitogen-Activated Protein Kinase Controls Cytokinesis and Flagellar Motility during Male Gamete Formation in a Malaria Parasite." *Molecular Microbiology* 58 (5): 1253–63.
65. Reininger, Luc, Oliver Billker, Rita Tewari, ArunimaMukhopadhyay, Clare Fennell, Dominique Dorin-Semblat, Caroline Doerig, et al. 2005. "A NIMA-Related Protein Kinase Is Essential for Completion of the Sexual Cycle of Malaria Parasites." *The Journal of Biological Chemistry* 280 (36): 31957–64.
66. Reininger, Luc, Rita Tewari, Clare Fennell, Zoe Holland, Dean Goldring, Lisa Ranford-Cartwright, Oliver Billker, and Christian Doerig. 2009. "An Essential Role for the *Plasmodium* Nek-2 Nima-Related Protein Kinase in the Sexual Development of Malaria Parasites." *The Journal of Biological Chemistry* 284 (31): 20858–68.
67. Silva-Neto, Mário A C, Geórgia C Atella, and Mohammed Shahabuddin. 2002. "Inhibition of Ca2+/calmodulin-Dependent Protein Kinase Blocks Morphological

Differentiation of *Plasmodium* Gallinaceum Zygotes to Ookinetes." *The Journal of Biological Chemistry* 277 (16): 14085–91.

68. Huber, M, E Cabib, and L H Miller. 1991. "Malaria Parasite Chitinase and Penetration of the Mosquito Peritrophic Membrane." *Proceedings of the National Academy of Sciences of the United States of America* 88 (7): 2807–10.
69. Shahabuddin, M, T Toyoshima, M Aikawa, and D C Kaslow. 1993. "Transmission-Blocking Activity of a Chitinase Inhibitor and Activation of Malarial Parasite Chitinase by Mosquito Protease." *Proceedings of the National Academy of Sciences of the United States of America* 90 (9): 4266–70.
70. Tomas, A M, G Margos, G Dimopoulos, L H van Lin, T F de Koning-Ward, R Sinha, P Lupetti, et al. 2001. "P25 and P28 Proteins of the Malaria Ookinete Surface Have Multiple and Partially Redundant Functions." *The EMBO Journal* 20 (15): 3975–83.
71. Mair, Gunnar R, Joanna A M Braks, Lindsey S Garver, Joop C A G Wiegant, Neil Hall, Roeland W Dirks, Shahid M Khan, George Dimopoulos, Chris J Janse, and Andrew P Waters. 2006. "Regulation of Sexual Development of *Plasmodium* by Translational Repression." *Science (New York, N.Y.)* 313 (5787): 667–69.
72. Mair G, Braks J, Garver L, Dimopoulos G, Hall N, Wiegant J, Dirks R, Khan S, Janse C, Waters A. 2006 Translational repression is essential for *Plasmodium* sexual development and mediated by DDX6-type RNA helicase. Science. 313:667–9.
73. Hillyer, Julián F, Catherine Barreau, and Kenneth D Vernick. 2007. "Efficiency of Salivary Gland Invasion by Malaria Sporozoites Is Controlled by Rapid Sporozoite Destruction in the Mosquito Haemocoel." *International Journal for Parasitology* 37 (6): 673–81.
74. Canning, E U, and R E Sinden. 1973. "The Organization of the Ookinete and Observations on Nuclear Division in Oocysts of *Plasmodium berghei*." *Parasitology* 67 (1): 29–40.
75. Angrisano, Fiona, Yan-Hong Tan, Angelika Sturm, Geoffrey I McFadden, and Jake Baum. 2012. "Malaria Parasite Colonisation of the Mosquito Midgut--Placing the *Plasmodium* Ookinete Centre Stage." *International Journal for Parasitology* 42 (6): 519–27.
76. Ménard, R, A A Sultan, C Cortes, R Altszuler, M R van Dijk, C J Janse, A P Waters, R S Nussenzweig, and V Nussenzweig. 1997. "Circumsporozoite Protein Is Required for Development of Malaria Sporozoites in Mosquitoes." *Nature* 385 (6614): 336–40.
77. Posthuma, G, J F Meis, J P Verhave, M R Hollingdale, T Ponnudurai, J H Meuwissen, and H J Geuze. 1988. "Immunogold Localization of Circumsporozoite Protein of the

Malaria Parasite *Plasmodium falciparum* during Sporogony in Anopheles StephensiMidguts." *European Journal of Cell Biology* 46 (1): 18–24.

78. Wang, Qian, Hisashi Fujioka, and Victor Nussenzweig. 2005. "Exit of *Plasmodium* Sporozoites from Oocysts Is an Active Process That Involves the Circumsporozoite Protein." *PLoS Pathogens* 1 (1):
79. Matuschewski, Kai, Alvaro C Nunes, Victor Nussenzweig, and Robert Ménard. 2002. "*Plasmodium* Sporozoite Invasion into Insect and Mammalian Cells Is Directed by the Same Dual Binding System." *The EMBO Journal* 21 (7): 1597–1606.
80. Matuschewski, Kai, Jessica Ross, Stuart M Brown, Karine Kaiser, Victor Nussenzweig, and Stefan H I Kappe. 2002. "Infectivity-Associated Changes in the Transcriptional Repertoire of the Malaria Parasite Sporozoite Stage." *The Journal of Biological Chemistry* 277 (44): 41948–53.
81. Mikolajczak, Sebastian A, Hilda Silva-Rivera, XinxiaPeng, Alice S Tarun, Nelly Camargo, Vanessa Jacobs-Lorena, Thomas M Daly, et al. 2008. "Distinct Malaria Parasite Sporozoites Reveal Transcriptional Changes That Cause Differential Tissue Infection Competence in the Mosquito Vector and Mammalian Host." *Molecular and Cellular Biology* 28 (20): 6196–6207.
82. Aly, Ahmed S I, Sebastian A Mikolajczak, Hilda Silva Rivera, Nelly Camargo, Vanessa Jacobs-Lorena, Mehdi Labaied, Isabelle Coppens, and Stefan H I Kappe. 2008. "Targeted Deletion of SAP1 Abolishes the Expression of Infectivity Factors Necessary for Successful Malaria Parasite Liver Infection." *Molecular Microbiology* 69 (1): 152–63.
83. Aly, Ahmed S I, Scott E Lindner, Drew C MacKellar, XinxiaPeng, and Stefan H I Kappe. 2011. "SAP1 Is a Critical Post-Transcriptional Regulator of Infectivity in Malaria Parasite Sporozoite Stages." *Molecular Microbiology* 79 (4): 929–39
84. Müller, Katja, Kai Matuschewski, and Olivier Silvie. 2011. "The Puf-Family RNA-Binding Protein Puf2 Controls Sporozoite Conversion to Liver Stages in the Malaria Parasite." *PloS One* 6 (5): e19860.
85. Gomes-Santos, Carina S S, Joanna Braks, Miguel Prudêncio, Céline Carret, Ana Rita Gomes, Arnab Pain, Theresa Feltwell, et al. 2011. "Transition of *Plasmodium* Sporozoites into Liver Stage-like Forms Is Regulated by the RNA Binding Protein Pumilio." *PLoS Pathogens* 7 (5): e1002046.
86. Lindner, Scott E, Sebastian A Mikolajczak, Ashley M Vaughan, Wonjong Moon, Brad R Joyce, William J Sullivan, and Stefan H I Kappe. 2013. "Perturbations of *Plasmodium*

Puf2 Expression and RNA-Seq of Puf2-Deficient Sporozoites Reveal a Critical Role in Maintaining RNA Homeostasis and Parasite Transmissibility." *Cellular Microbiology* 15 (7): 1266–83.

87. Kumar, Kota Arun, Peter Baxter, Alice S Tarun, Stefan H I Kappe, and Victor Nussenzweig. 2009. "Conserved Protective Mechanisms in Radiation and Genetically Attenuated uis3(-) and uis4(-) *Plasmodium* Sporozoites." *PloS One* 4 (2): e4480.
88. Sedegah, M, R Hedstrom, P Hobart, and S L Hoffman. 1994. "Protection against Malaria by Immunization with Plasmid DNA Encoding Circumsporozoite Protein." *Proceedings of the National Academy of Sciences of the United States of America* 91 (21): 9866–70.
89. Dunachie, Susanna J, Michael Walther, Jenni M Vuola, Daniel P Webster, Sheila M Keating, Tamara Berthoud, Laura Andrews, et al. 2006. "A Clinical Trial of Prime-Boost Immunisation with the Candidate Malaria Vaccines RTS,S/AS02A and MVA-CS." *Vaccine* 24 (15): 2850–59.
90. Dunachie, S J, M Walther, J E Epstein, S Keating, T Berthoud, L Andrews, R F Andersen, et al. 2006. "A DNA Prime-Modified Vaccinia Virus Ankara Boost Vaccine Encoding Thrombospondin-Related Adhesion Protein but Not Circumsporozoite Protein Partially Protects Healthy Malaria-Naive Adults against *Plasmodium falciparum* Sporozoite Challenge." *Infection and Immunity* 74 (10): 5933–42.
91. Reyes-Sandoval, Arturo, Tamara Berthoud, Nicola Alder, LoredanaSiani, Sarah C Gilbert, Alfredo Nicosia, Stefano Colloca, Riccardo Cortese, and Adrian V S Hill. 2010. "Prime-Boost Immunization with Adenoviral and Modified Vaccinia Virus Ankara Vectors Enhances the Durability and Polyfunctionality of Protective Malaria CD8+ T-Cell Responses." *Infection and Immunity* 78 (1): 145–53.
92. Hodgson, Susanne H, Katie J Ewer, Carly M Bliss, Nick J Edwards, Thomas Rampling, Nicholas A Anagnostou, Eoghan de Barra, et al. 2014. "Evaluation of the Efficacy of ChAd63-MVA Vectored Vaccines Expressing Circumsporozoite Protein and ME-TRAP Against Controlled Human Malaria Infection in Malaria-Naive Individuals." *The Journal of Infectious Diseases*, October.
93. Mueller, Ann-Kristin, Martina Deckert, Kirsten Heiss, Kristin Goetz, Kai Matuschewski, and Dirk Schlüter. 2007. "Genetically Attenuated *Plasmodium berghei* Liver Stages Persist and Elicit Sterile Protection Primarily via CD8 T Cells." *The American Journal of Pathology* 171 (1): 107–15.

94. Yu, Min, T R Santha Kumar, Louis J Nkrumah, AlidaCoppi, SilkeRetzlaff, Celeste D Li, Brendan J Kelly, et al. 2008. "The Fatty Acid Biosynthesis Enzyme FabI Plays a Key Role in the Development of Liver-Stage Malarial Parasites." *Cell Host & Microbe* 4 (6): 567–78.

95. Haussig, Joana M, Kai Matuschewski, and Taco W A Kooij. 2011. "Inactivation of a *Plasmodium* Apicoplast Protein Attenuates Formation of Liver Merozoites." *Molecular Microbiology* 81 (6): 1511–25.

96. Ishino, Tomoko, Bertrand Boisson, Yuki Orito, Céline Lacroix, Emmanuel Bischoff, Céline Loussert, Chris Janse, Robert Ménard, Masao Yuda, and Patricia Baldacci. 2009. "LISP1 Is Important for the Egress of *Plasmodium berghei* Parasites from Liver Cells." *Cellular Microbiology* 11 (9): 1329–39.

97. Dahl, Erica L, and Philip J Rosenthal. 2007. "Multiple Antibiotics Exert Delayed Effects against the *Plasmodium falciparum* Apicoplast." *Antimicrobial Agents and Chemotherapy* 51 (10): 3485–90.

98. Xue, Jian, Bin Jiang, Cong-Shan Liu, Jun Sun, and Shu-Hua Xiao. 2013. "Comparative Observation on Inhibition of Hemozoin Formation and Their in Vitro and in Vivo Anti-Schistosome Activity Displayed by 7 Antimalarial Drugs." *ZhongguoJi Sheng Chong Xue Yu Ji Sheng Chong Bing ZaZhi = Chinese Journal of Parasitology & Parasitic Diseases* 31 (3): 161–69.

99. Watsierah, Carren A, and Collins Ouma. 2014. "Access to Artemisinin-Based Combination Therapy (ACT) and Quinine in Malaria Holoendemic Regions of Western Kenya." *Malaria Journal* 13 (January): 290.

100. Carter, R. 2001. "Transmission Blocking Malaria Vaccines." *Vaccine* 19 (17-19): 2309–14.

101. Ferrari, V, and D J Cutler. 1990. "Uptake of Chloroquine by Human Erythrocytes." *Biochemical Pharmacology* 39 (4): 753–62.

102. Ferrari, V, and D J Cutler. 1991. "Simulation of Kinetic Data on the Influx and Efflux of Chloroquine by Erythrocytes Infected with *Plasmodium falciparum*. Evidence for a Drug-Importer in Chloroquine-Sensitive Strains." *Biochemical Pharmacology* 42 Suppl (December): S167–79.

103. Sanchez, Cecilia P, Petra Rohrbach, Jeremy E McLean, David A Fidock, Wilfred D Stein, and Michael Lanzer. 2007. "Differences in Trans-Stimulated Chloroquine Efflux Kinetics Are Linked to PfCRT in *Plasmodium falciparum*." *Molecular Microbiology* 64 (2): 407–20.

104. Imwong, M, S Pukrittakayamee, S Looareesuwan, G Pasvol, J Poirreiz, N J White, and G Snounou. 2001. "Association of Genetic Mutations in *Plasmodium vivax*Dhfr with Resistance to Sulfadoxine-Pyrimethamine: Geographical and Clinical Correlates." *Antimicrobial Agents and Chemotherapy* 45 (11): 3122–27.

105. Bwijo, B, A Kaneko, M Takechi, I L Zungu, Y Moriyama, J K Lum, T Tsukahara, et al. 2003. "High Prevalence of Quintuple Mutant Dhps/dhfr Genes in *Plasmodium falciparum* Infections Seven Years after Introduction of Sulfadoxine and Pyrimethamine as First Line Treatment in Malawi." *ActaTropica* 85 (3): 363–73.

106. Noedl, Harald, Youry Se, Kurt Schaecher, Bryan L Smith, Duong Socheat, and Mark M Fukuda. 2008. "Evidence of Artemisinin-Resistant Malaria in Western Cambodia." *The New England Journal of Medicine* 359 (24): 2619–20..

107. Krishna, Sanjeev, ed. 2014. "Efficacy and Safety of the RTS,S/AS01 Malaria Vaccine during 18 Months after Vaccination: A Phase 3 Randomized, Controlled Trial in Children and Young Infants at 11 African Sites." *PLoS Medicine* 11 (7): e1001685.

108. Sun, Peifang, Robert Schwenk, Katherine White, Jose A Stoute, Joe Cohen, W Ripley Ballou, Gerald Voss, Kent E Kester, D Gray Heppner, and UrszulaKrzych. 2003. "Protective Immunity Induced with Malaria Vaccine, RTS,S, Is Linked to *Plasmodium falciparum* Circumsporozoite Protein-Specific CD4+ and CD8+ T Cells Producing IFN-Gamma." *Journal of Immunology* 171 (12): 6961–67.

109. Van Schaijk, Ben C L, Chris J Janse, Geert-Jan van Gemert, Melissa R van Dijk, Audrey Gego, Jean-Francois Franetich, Marga van de Vegte-Bolmer, et al. 2008. "Gene Disruption of *Plasmodium falciparum* p52 Results in Attenuation of Malaria Liver Stage Development in Cultured Primary Human Hepatocytes." *PloS One* 3 (10): e3549.

110. Vaughan, Ashley M, and Stefan H I Kappe. 2013. "Vaccination Using Radiation- or Genetically Attenuated Live Sporozoites." *Methods in Molecular Biology (Clifton, N.J.)* 923 (January): 549–66.

111. Mikolajczak, Sebastian A, ViswanathanLakshmanan, Matthew Fishbaugher, Nelly Camargo, AnkeHarupa, Alexis Kaushansky, Alyse N Douglass, et al. 2014. "A next-Generation Genetically Attenuated *Plasmodium falciparum* Parasite Created by Triple Gene Deletion." *Molecular Therapy* 22 (9): 1707–15.

112. VanBuskirk, Kelley M, Matthew T O'Neill, Patricia De La Vega, Alexander G Maier, UrszulaKrzych, Jack Williams, Megan G Dowler, et al. 2009. "Preerythrocytic, Live-Attenuated *Plasmodium falciparum* Vaccine Candidates by Design." *Proceedings of the National Academy of Sciences of the United States of America* 106 (31): 13004–9.

113. Beeson, James G, Jo-Anne Chan, and Freya J I Fowkes. 2013. "PfEMP1 as a Target of Human Immunity and a Vaccine Candidate against Malaria." *Expert Review of Vaccines* 12 (2): 105–8.

114. Shimp, Richard L, Christopher Rowe, Karine Reiter, Beth Chen, Vu Nguyen, Joan Aebig, Kelly M Rausch, et al. 2013. "Development of a Pfs25-EPA Malaria Transmission Blocking Vaccine as a Chemically Conjugated Nanoparticle." *Vaccine* 31 (28): 2954–62.

115. Vincke IH and Lips M. 1948. Un nouveau *Plasmodium* d' unrongeursauvage du congo, *Plasmodium berghei* n sp. Ann SocBelge Med Trop; 28: 97-104.

116. Ménard, R, and C Janse. 1997. "Gene Targeting in Malaria Parasites." *Methods (San Diego, Calif.)* 13 (2): 148–57.

117. Van Dijk, M R, C J Janse, J Thompson, A P Waters, J ABraks, H J Dodemont, H G Stunnenberg, G J van Gemert, R W Sauerwein, and W Eling. 2001. "A Central Role for P48/45 in Malaria Parasite Male Gamete Fertility." *Cell* 104 (1): 153–64.

118. Crabb, B S, B M Cooke, J C Reeder, R F Waller, S R Caruana, K M Davern, M E Wickham, G V Brown, R L Coppel, and A F Cowman. 1997. "Targeted Gene Disruption Shows That Knobs Enable Malaria-Infected Red Cells to Cytoadhere under Physiological Shear Stress." *Cell* 89 (2): 287–96.

119. Lobo, C A, H Fujioka, M Aikawa, and N Kumar. 1999. "Disruption of the Pfg27 Locus by Homologous Recombination Leads to Loss of the Sexual Phenotype in P. *falciparum*." *Molecular Cell* 3 (6): 793–98.

120. Carvalho, Teresa Gil, Sabine Thiberge, Hiroshi Sakamoto, and Robert Ménard. 2004. "Conditional Mutagenesis Using Site-Specific Recombination in *Plasmodium berghei*." *Proceedings of the National Academy of Sciences of the United States of America* 101 (41): 14931–36.

121. Natarajan, R, V Thathy, M MMota, J C Hafalla, R Ménard, and K D Vernick. 2001. "Fluorescent *Plasmodium berghei* Sporozoites and Pre-Erythrocytic Stages: A New Tool to Study Mosquito and Mammalian Host Interactions with Malaria Parasites." *Cellular Microbiology* 3 (6): 371–79.

122. Sturm, Angelika, Stefanie Graewe, BlandineFranke-Fayard, SilkeRetzlaff, Stefanie Bolte, Bernhard Roppenser, Martin Aepfelbacher, Chris Janse, and Volker Heussler. 2009. "Alteration of the Parasite Plasma Membrane and the Parasitophorous Vacuole Membrane during Exo-Erythrocytic Development of Malaria Parasites." *Protist* 160 (1): 51–63.

123. Graewe, Stefanie, SilkeRetzlaff, Nicole Struck, Chris J Janse, and Volker T Heussler. 2009. "Going Live: A Comparative Analysis of the Suitability of the RFP Derivatives RedStar, mCherry and tdTomato for Intravital and in Vitro Live Imaging of *Plasmodium* Parasites." *Biotechnology Journal* 4 (6): 895–902.

124. .De Koning-Ward, T F, M ASperança, A P Waters, and C J Janse. 1999. "Analysis of Stage Specificity of Promoters in *Plasmodium berghei* Using Luciferase as a Reporter." *Molecular and Biochemical Parasitology* 100 (1): 141–46.

125. Le Roch, Karine G, Yingyao Zhou, Peter L Blair, Muni Grainger, J Kathleen Moch, J David Haynes, Patricia De La Vega, et al. 2003. "Discovery of Gene Function by Expression Profiling of the Malaria Parasite Life Cycle." *Science (New York, N.Y.)* 301 (5639): 1503–8.

126. Hall, N. 2005. "A Comprehensive Survey of the *Plasmodium* Life Cycle by Genomic, Transcriptomic, and Proteomic Analyses." *Science* 307 (5706): 82–86.

127. Wang, Qian, Stuart Brown, David S Roos, Victor Nussenzweig, and PurnimaBhanot. 2004. "Transcriptome of Axenic Liver Stages of *Plasmodium yoelii*." *Molecular and Biochemical Parasitology* 137 (1): 161–68.

128. Tarun, Alice S, XinxiaPeng, Ronald F Dumpit, Yuko Ogata, Hilda Silva-Rivera, Nelly Camargo, Thomas M Daly, Lawrence W Bergman, and Stefan H I Kappe. 2008. "A Combined Transcriptome and Proteome Survey of Malaria Parasite Liver Stages." *Proceedings of the National Academy of Sciences of the United States of America* 105 (1): 305–10.

129. Bozdech, Zbynek, Manuel Llinás, Brian Lee Pulliam, Edith D Wong, Jingchun Zhu, and Joseph L DeRisi. 2003. "The Transcriptome of the Intraerythrocytic Developmental Cycle of *Plasmodium falciparum*." *PLoS Biology* 1 (1): E5.

130. Otto, Thomas D, Daniel Wilinski, Sammy Assefa, Thomas M Keane, Louis R Sarry, Ulrike Böhme, Jacob Lemieux, et al. 2010. "New Insights into the Blood-Stage Transcriptome of *Plasmodium falciparum* Using RNA-Seq." *Molecular Microbiology* 76 (1): 12–24.

131. Kaiser, Karine, Kai Matuschewski, Nelly Camargo, Jessica Ross, and Stefan H I Kappe. 2004. "Differential Transcriptome Profiling Identifies *Plasmodium* Genes Encoding Pre-Erythrocytic Stage-Specific Proteins." *Molecular Microbiology* 51 (5): 1221–32.

132. Srinivasan, Prakash, Eappen G Abraham, Anil K Ghosh, Jesus Valenzuela, Jose M C Ribeiro, George Dimopoulos, Fotis C Kafatos, John H Adams, Hisashi

Fujioka, and Marcelo Jacobs-Lorena. 2004. "Analysis of the *Plasmodium* and Anopheles Transcriptomes during Oocyst Differentiation." *The Journal of Biological Chemistry* 279 (7): 5581–87.

133. Matuschewski, Kai. 2006. "Getting Infectious: Formation and Maturation of *Plasmodium* Sporozoites in the Anopheles Vector." *Cellular Microbiology* 8 (10): 1547–56.

134. Kappe, S H, M J Gardner, S M Brown, J Ross, K Matuschewski, J M Ribeiro, J H Adams, et al. 2001. "Exploring the Transcriptome of the Malaria Sporozoite Stage." *Proceedings of the National Academy of Sciences of the United States of America* 98 (17): 9895–9900.

135. Roberts, F, C W Roberts, J J Johnson, D E Kyle, T Krell, J R Coggins, G H Coombs, et al. 1998. "Evidence for the Shikimate Pathway in Apicomplexan Parasites." *Nature* 393 (6687): 801–5.

136. Kappe, S H, A R Noe, T S Fraser, P L Blair, and J H Adams. 1998. "A Family of Chimeric Erythrocyte Binding Proteins of Malaria Parasites." *Proceedings of the National Academy of Sciences of the United States of America* 95 (3): 1230–35.

137. Gantt, S M, P Clavijo, X Bai, J D Esko, and P Sinnis. 1997. "Cell Adhesion to a Motif Shared by the Malaria Circumsporozoite Protein and Thrombospondin Is Mediated by Its Glycosaminoglycan-Binding Region and Not by CSVTCG." *The Journal of Biological Chemistry* 272 (31): 19205–13.

138. Sinnis, P. 1996. "The Malaria Sporozoite's Journey into the Liver." *Infectious Agents and Disease* 5 (3): 182–89.

139. Kappe, S, T Bruderer, S Gantt, H Fujioka, V Nussenzweig, and R Ménard. 1999. "Conservation of a Gliding Motility and Cell Invasion Machinery in Apicomplexan Parasites." *The Journal of Cell Biology* 147 (5): 937–44.

140. Steinbuechel, Marion, and Kai Matuschewski. 2009. "Role for the *Plasmodium* Sporozoite-Specific Transmembrane Protein S6 in Parasite Motility and Efficient Malaria Transmission." *Cellular Microbiology* 11 (2): 279–88.

141. Harupa, Anke, Brandon K Sack, ViswanathanLakshmanan, Nadia Arang, Alyse N Douglass, Brian G Oliver, Andrew B Stuart, et al. 2014. "SSP3 Is a Novel *Plasmodium yoelii* Sporozoite Surface Protein with a Role in Gliding Motility." *Infection and Immunity* 82 (11): 4643–53.

142. Kronstad, James W. 2006. "Serial Analysis of Gene Expression in Eukaryotic Pathogens." *Infectious Disorders Drug Targets* 6 (3): 281–97.

143. Munasinghe, A, S Patankar, B P Cook, S L Madden, R K Martin, D E Kyle, A Shoaibi, L M Cummings, and D F Wirth. 2001. "Serial Analysis of Gene Expression (SAGE) in *Plasmodium falciparum*: Application of the Technique to A-T Rich Genomes." *Molecular and Biochemical Parasitology* 113 (1): 23–34.

144. Rosinski-Chupin, Isabelle, Thomas Chertemps, Bertrand Boisson, Sylvie Perrot, Emmanuel Bischoff, JérômeBriolay, Pierre Couble, Robert Ménard, Paul Brey, and Patricia Baldacci. 2007. "Serial Analysis of Gene Expression in *Plasmodium berghei* Salivary Gland Sporozoites." *BMC Genomics* 8 (January): 466.

145. Janse, Chris J, Jai Ramesar, and Andrew P Waters. 2006. "High-Efficiency Transfection and Drug Selection of Genetically Transformed Blood Stages of the Rodent Malaria Parasite *Plasmodium berghei*." *Nature Protocols* 1 (1): 346–56.

146. Yoshida, N, R S Nussenzweig, P Potocnjak, V Nussenzweig, and M Aikawa. 1980. "Hybridoma Produces Protective Antibodies Directed against the Sporozoite Stage of Malaria Parasite." *Science (New York, N.Y.)* 207 (4426): 71–73.

147. Rathore, Sumit, DiptoSinha, MohdAsad, Thomas Böttcher, Farhat Afrin, Virander S Chauhan, Dinesh Gupta, Stephan A Sieber, and Asif Mohmmed. 2010. "A Cyanobacterial Serine Protease of *Plasmodium falciparum* Is Targeted to the Apicoplast and Plays an Important Role in Its Growth and Development." *Molecular Microbiology* 77(4):873-90.

148. Sinnis, Photini, and Fidel Zavala. 2008. "The Skin Stage of Malaria Infection: Biology and Relevance to the Malaria Vaccine Effort." *Future Microbiology* 3 (3): 275–78.

149. Coppi, Alida, RamyaNatarajan, Gabriele Pradel, Brandy L Bennett, Eric R James, Mario A Roggero, GiampietroCorradin, CathrinePersson, Rita Tewari, and PhotiniSinnis. 2011. "The Malaria Circumsporozoite Protein Has Two Functional Domains, Each with Distinct Roles as Sporozoites Journey from Mosquito to Mammalian Host." *The Journal of Experimental Medicine* 208 (2): 341–56.

150. Sultan, AA, V Thathy, U Frevert, K J Robson, A Crisanti, V Nussenzweig, R S Nussenzweig, and R Ménard. 1997. "TRAP Is Necessary for Gliding Motility and Infectivity of *Plasmodium* Sporozoites." *Cell* 90 (3): 511–22.

151. Labaied, Mehdi, Nelly Camargo, and Stefan H I Kappe. 2007. "Depletion of the *Plasmodium berghei* Thrombospondin-Related Sporozoite Protein Reveals a Role in Host Cell Entry by Sporozoites." *Molecular and Biochemical Parasitology* 153 (2): 158–66.

152. Combe, Audrey, Cristina Moreira, Susan Ackerman, Sabine Thiberge, Thomas J Templeton, and Robert Ménard. 2009. "TREP, a Novel Protein Necessary for Gliding Motility of the Malaria Sporozoite." *International Journal for Parasitology* 39 (4): 489–96.

153. Currà, Chiara, Marco Di Luca, Leonardo Picci, Carina de Sousa Silva Gomes dos Santos, Inga Siden-Kiamos, Tomasino Pace, and Marta Ponzi. 2013. "The ETRAMP Family Member SEP2 Is Expressed throughout *Plasmodium berghei* Life Cycle and Is Released during Sporozoite Gliding Motility." *PloS One* 8 (6): e67238.

154. Annoura, Takeshi, Ben C L van Schaijk, Ivo H J Ploemen, Mohammed Sajid, Jing-wen Lin, Martijn W Vos, Avinash G Dinmohamed, et al. 2014. "Two *Plasmodium* 6-Cys Family-Related Proteins Have Distinct and Critical Roles in Liver-Stage Development." *FASEB Journal* 28 (5): 2158–70. doi:10.1096/fj.13-241570.

155. Lindner, S. E., K. E. Swearingen, A. Harupa, A. M. Vaughan, P. Sinnis, R. L. Moritz, and S. H. I. Kappe. 2013. "Total and Putative Surface Proteomics of Malaria Parasite Salivary Gland Sporozoites." *Molecular & Cellular Proteomics* 12 (5): 1127–43.

156. Westenberger, Scott J, Colleen M McClean, RanaChattopadhyay, Neekesh V Dharia, Jane M Carlton, John W Barnwell, William E Collins, et al. 2010. "A Systems-Based Analysis of *Plasmodium vivax* Lifecycle Transcription from Human to Mosquito." *PLoS Neglected Tropical Diseases* 4 (4): e653.

157. Orito, Yuki, Tomoko Ishino, ShirohIwanaga, Izumi Kaneko, Tomomi Kato, Robert Menard, YasuoChinzei, and Masao Yuda. 2013. "Liver-Specific Protein 2: A *Plasmodium* Protein Exported to the Hepatocyte Cytoplasm and Required for Merozoite Formation." *Molecular Microbiology* 87 (1): 66–79.

158. Lingelbach, K, and K A Joiner. 1998. "The Parasitophorous Vacuole Membrane Surrounding *Plasmodium* and Toxoplasma: An Unusual Compartment in Infected Cells." *Journal of Cell Science* 111 (Pt 1 (June): 1467–75.

159. Spielmann, Tobias, Georgina N Montagna, Leonie Hecht, and Kai Matuschewski. 2012. "Molecular Make-up of the *Plasmodium* Parasitophorous Vacuolar Membrane." *International Journal of Medical Microbiology* 302 (4-5): 179–86.

160. Leiriao, Patricia, Maria M Mota, and Ana Rodriguez. 2005. "Apoptotic *Plasmodium*-Infected Hepatocytes Provide Antigens to Liver Dendritic Cells." *The Journal of Infectious Diseases* 191 (10): 1576–81.

161. Albert, Matthew L. 2004. "Death-Defying Immunity: Do Apoptotic Cells Influence Antigen Processing and Presentation?" *Nature Reviews. Immunology* 4 (3): 223–31. doi:10.1038/nri11308.

162. Fonteneau, Jean François, Marie Larsson, and Nina Bhardwaj. 2002. "Interactions between Dead Cells and Dendritic Cells in the Induction of Antiviral CTL Responses." *Current Opinion in Immunology* 14 (4): 471–77.

163. Aly, A. S. I., &Matuschewski, K. (2005). A malarial cysteine protease is necessary for *Plasmodium* sporozoite egress from oocysts. *The Journal of Experimental Medicine*, *202*(2), 225–30.

164. Mueller, Ivo, Mary R Galinski, J Kevin Baird, Jane M Carlton, Dhanpat K Kochar, Pedro L Alonso, and Hernando A del Portillo. 2009. "Key Gaps in the Knowledge of *Plasmodium vivax*, a Neglected Human Malaria Parasite." *The Lancet. Infectious Diseases* 9 (9): 555–66.

165. Rogerson, Stephen J, and Richard Carter. 2008. "Severe *vivax* Malaria: Newly Recognised or Rediscovered." *PLoS Medicine* 5 (6): e136.

166. Price, Ric N, Nicholas M Douglas, and Nicholas M Anstey. 2009. "New Developments in *Plasmodium vivax* Malaria: Severe Disease and the Rise of Chloroquine Resistance." *Current Opinion in Infectious Diseases* 22 (5): 430–35.

167. Tjitra, Emiliana, Nicholas M. Anstey, Paulus Sugiarto, Noah Warikar, EnnyKenangalem, Muhammad Karyana, Daniel A. Lampah, and Ric N. Price. 2008. "Multidrug-Resistant *Plasmodium vivax* Associated with Severe and Fatal Malaria: A Prospective Study in Papua, Indonesia." Edited by Stephen Rogerson. *PLoS Medicine* 5 (6): e128

168. Contacos, P G, W E Collins, G M Jeffery, W A Krotoski, and W A Howard. 1972. "Studies on the Characterization of *Plasmodium vivax* Strains from Central America." *The American Journal of Tropical Medicine and Hygiene* 21 (5): 707–12.

169. Sacci, John B, Jose M C Ribeiro, Fengying Huang, UzmaAlam, Joshua A Russell, Peter L Blair, Adam Witney, Daniel J Carucci, Abdu F Azad, and Joao C Aguiar. 2005. "Transcriptional Analysis of in Vivo *Plasmodium yoelii* Liver Stage Gene Expression." *Molecular and Biochemical Parasitology* 142 (2): 177–83.

170. Pfahler, Judith M, Mary R Galinski, John W Barnwell, and Michael Lanzer. 2006. "Transient Transfection of *Plasmodium vivax* Blood Stage Parasites." *Molecular and Biochemical Parasitology* 149 (1): 99–101.

171. Zhou, Yingyao, VandanaRamachandran, Kota Arun Kumar, Scott Westenberger, PhillippeRefour, Bin Zhou, Fengwu Li, et al. 2008. "Evidence-Based Annotation of the Malaria Parasite's Genome Using Comparative Expression Profiling." *PloS One* 3 (2): e1570.

172. Bozdech, Zbynek, SachelMok, Guangan Hu, MallikaImwong, AnchaleeJaidee, Bruce Russell, Hagai Ginsburg, et al. 2008. "The Transcriptome of *Plasmodium vivax* Reveals Divergence and Diversity of Transcriptional Regulation in Malaria Parasites." *Proceedings of the National Academy of Sciences of the United States of America* 105 (42): 16290–95.

173. Cui, Liwang, Qi Fan, Yi Hu, Svetlana A Karamycheva, John Quackenbush, BenjawanKhuntirat, JetsumonSattabongkot, and Jane M Carlton. 2005. "Gene Discovery in *Plasmodium vivax* through Sequencing of ESTs from Mixed Blood Stages." *Molecular and Biochemical Parasitology* 144 (1): 1–9.

174. Le Roch, Karine G, Jeffrey R Johnson, Laurence Florens, Yingyao Zhou, AndreySantrosyan, Munira Grainger, S Frank Yan, et al. 2004. "Global Analysis of Transcript and Protein Levels across the *Plasmodium falciparum* Life Cycle." *Genome Research* 14 (11): 2308–18.

175. Arisue, Nobuko, Makoto Hirai, Meiji Arai, Hiroyuki Matsuoka, and Toshihiro Horii. 2007. "Phylogeny and Evolution of the SERA Multigene Family in the Genus *Plasmodium*." *Journal of Molecular Evolution* 65 (1): 82–91. doi:10.1007/s00239-006-0253-1.

176. Hodder, Anthony N, Damien R Drew, V ChandanaEpa, Mauro Delorenzi, Richard Bourgon, Susanne K Miller, Robert L Moritz, et al. 2003. "Enzymic, Phylogenetic, and Structural Characterization of the Unusual Papain-like Protease Domain of *Plasmodium falciparum* SERA5." *The Journal of Biological Chemistry* 278 (48): 48169–77

177. Yeoh, Sharon, Rebecca A O'Donnell, KonstantinosKoussis, Anton R Dluzewski, Keith H Ansell, Simon A Osborne, Fiona Hackett, et al. 2007. "Subcellular Discharge of a Serine Protease Mediates Release of Invasive Malaria Parasites from Host Erythrocytes." *Cell* 131 (6): 1072–83.

178. Hopp, Christine S, Paul W Bowyer, and David A Baker. 2012. "The Role of cGMP Signalling in Regulating Life Cycle Progression of *Plasmodium*." *Microbes and Infection / Institut Pasteur* 14 (10): 831–37.

179. Taylor, Cathy J, Louisa McRobert, and David A Baker. 2008. "Disruption of a *Plasmodium falciparum* Cyclic Nucleotide Phosphodiesterase Gene Causes Aberrant Gametogenesis." *Molecular Microbiology* 69 (1): 110–18.

180. Taylor, Helen M, Louisa McRobert, Munira Grainger, Audrey Sicard, Anton R Dluzewski, Christine S Hopp, Anthony A Holder, and David A Baker. 2010. "The Malaria Parasite Cyclic GMP-Dependent Protein Kinase Plays a Central Role in Blood-Stage Schizogony." *Eukaryotic Cell* 9 (1): 37–45.

181. Burda, Paul-Christian, Matthias A Roelli, Marco Schaffner, Shahid M Khan, Chris J Janse, and Volker T Heussler. 2015. "A *Plasmodium* Phospholipase Is Involved in Disruption of the Liver Stage Parasitophorous Vacuole Membrane." *PLoS Pathogens* 11 (3): e1004760.

182. Deligianni, Elena, Rhiannon N Morgan, Lucia Bertuccini, Christine C Wirth, Natalie C Silmon de Monerri, LefterisSpanos, Michael J Blackman, Christos Louis, Gabriele Pradel, and Inga Siden-Kiamos. 2013. "A Perforin-like Protein Mediates Disruption of the Erythrocyte Membrane during Egress of *Plasmodium berghei* Male Gametocytes." *Cellular Microbiology* 15 (8): 1438–55.

183. Wirth, Christine C, Svetlana Glushakova, Matthias Scheuermayer, UrskaRepnik, Swati Garg, DominikSchaack, Marika M Kachman, et al. 2014. "Perforin-like Protein PPLP2 Permeabilizes the Red Blood Cell Membrane during Egress of *Plasmodium falciparum* Gametocytes." *Cellular Microbiology* 16 (5): 709–33

Anti-Plagiarism Certificate

Reverse Genetics Reveals The Critical Role of Sporozoite Specific Genes Pbsspeld and Pbscot3

ORIGINALITY REPORT

17%	12%	12%	7%
SIMILARITY INDEX	INTERNET SOURCES	PUBLICATIONS	STUDENT PAPERS

PRIMARY SOURCES

1	www.ncbi.nlm.nih.gov Internet Source	1%
2	iai.asm.org Internet Source	1%
3	Submitted to University of Pune Student Paper	1%
4	Submitted to University of Dehli Student Paper	<1%
5	lib.bioinfo.pl Internet Source	<1%
6	Submitted to Indian Institute of Science, Bangalore Student Paper	<1%
7	carrier.gnf.org Internet Source	<1%
8	Submitted to Mahidol University Student Paper	<1%

	Publication	
270	diss-epsilon.slu.se Internet Source	<1%
271	Submitted to Rhodes College Student Paper	<1%

EXCLUDE QUOTES	ON	EXCLUDE MATCHES	< 5 WORDS
EXCLUDE BIBLIOGRAPHY	ON		